SIMULATION OF IN-HOUSE DRYING OF CHICKEN EXCRETA

Thesis for the Degree of Ph. D.
MICHIGAN STATE UNIVERSITY
GRANT DEWITT WELLS
1972

MICHIGAN STATE UNIVERSITY LIBRARIES
3 1293 01070 3241

LIBRARY
Michigan
University

This is to certify that the

thesis entitled

SIMULATION OF IN-HOUSE DRYING OF CHICKEN EXCRETA

presented by

GRANT DEWITT WELLS

has been accepted towards fulfillment
of the requirements for

Ph. D. degree in Agri. Engr.

Merle L Esmay
Major professor

Date 7/7/72

O-7639

ABSTRACT

SIMULATION OF IN-HOUSE DRYING OF CHICKEN EXCRETA

by Grant DeWitt Wells

Fresh chicken excreta contains 88 percent moisture on the wet weight basis. Partial drying of chicken excreta within a few hours after deposit reduces odor production considerably. Handling characteristics are also improved by partial drying. The ventilation air exchange through a poultry house evaporates moisture from the exposed wet surfaces of the droppings. Improved ventilation patterns and supplemental heat sources within the excreta deposit area increase the rate of drying. Basic information concerning water movement within the material and over-all drying rates are needed for economical design of in-house drying systems and for systems analysis of poultry house environments.

This study was undertaken to develop drying rate equations for deposited chicken excreta. Laboratory drying tests were made with uniform samples (10 cm wide by 10 cm long) of three thicknesses (0.32, 0.64 and 0.96 cm). Environmental conditions similar to those found in windowless poultry laying houses were simulated. Supplemental energy was supplied in the form of electrically heated floor panels.

Two drying rate periods were observed. As long as surfaces remained saturated, constant rate drying took place.

The constant rate period was followed by an extended period of falling rate drying.

It was found that the constant drying rate was a function of free stream velocity, wet-bulb depression and ambient air temperature as it effects vapor pressure at the saturated surfaces. Process variables of increased surface area and conducted heat source also increased the drying rate. The constant drying rate was predicted on the basis of surface film resistance and concentration gradient terms.

More than half of the removable moisture was evaporated from the body surface at a constant rate. Because the rate of shrinkage was not measured, the end of the constant rate period could not be accurately defined, but break points were estimated for each sample tested.

The rate of change in moisture during the falling rate drying period was roughly proportional to the removable moisture remaining. The proportionality constant was estimated as a function of the constant drying rate and the sample thickness. The free stream conditions were found to be of major importance throughout both the constant and falling rate drying periods. Indications are that most of the non-hygroscopic water moves to the surface in liquid form and is evaporated there.

The experimental drying rates were compared to some in-house drying data and were shown to predict the in-house

drying rates if a measure of the mean boundary layer thickness and area of wet surface was approximated.

Approved Merle L Esmay
Major Professor

Approved B A Stout
Department Chairman

SIMULATION OF IN-HOUSE DRYING OF CHICKEN EXCRETA

By

Grant DeWitt Wells

A THESIS

Submitted to
Michigan State University
in partial fulfillment of the requirements
for the degree of

DOCTOR OF PHILOSOPHY

Department of Agricultural Engineering

1972

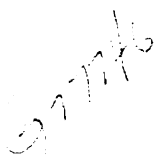

To Pixie

ACKNOWLEDGMENTS

The author wishes to express his appreciation and thanks to:

Dr. M. L. Esmay for serving as committee chairman and for his guidance, encouragement and patience;

Dr. F. W. Bakker-Arkema for his extra help and encouragement;

Drs. A. M. Dhanak and R. Hamelink for their help and support;

and the Agricultural Engineering Department for support that aided in the completion of this study.

TABLE OF CONTENTS

LIST OF TABLES

LIST OF FIGURES

LIST OF APPENDICES

LIST OF SYMBOLS

Symbol	Meaning	Units
A	Intercept of linear regression eq. 6.1	--
A_s	Exposed surface area of sample	cm^2
a	Sample dimension	cm
b	Sample dimension	cm
C_f	Skin friction coefficient	--
cc	Cubic centimeters	cm^3
c_p	Specific heat at constant pressure	cal/gm-^oC
D_c	Characteristic length, flow path length of air over sample	cm
D_e	Diffusion coefficient	cm^2/min
d	Nominal thickness of sample	cm
d_e	Effective depth (Vol/A_s)	cm
$d()/d\theta$	Time derivative	--
EMC	Equilibrium moisture content wet basis	%
exp	Exponential	--
F	Shape factor ($a^{-2} + b^{-2} + d^{-2}$)	cm^2
H	Absolute humidity	gm/gm
h_c	Convective heat transfer coefficient	cal/hr-cm^2-^oC
h_d	Convective mass transfer coefficient	gm/cm^2-hr
h_D	Convective mass transfer coefficient	cm/min
$h_{D,L}$	Laminar convective mass transfer coeff.	cm/min
h_{fg}	Heat of evaporation	cal/gm
h_r	Radiation heat transfer coefficient	cal/hr-cm^2-^oC
IMC	Initial moisture content percent wet basis	%

Symbol	Meaning	Units
j	Colburn j factors	--
K	Drying constant	1/hr
k	Thermal conductivity	cal/hr-cm-^{o}C
M	Moisture content ratio $(m - m_e)/(m_o - m_e)$	--
MC	Moisture content percent wet basis	%
m	Moisture content	gm
m_i	Total initial weight $(m_o + m_s)$	gm
m_o	Initial moisture content	gm
m_s	Dry weight of solids	gm
$\dot{m}$	Drying rate	gm/hr
$\dot{m}''$	Drying rate per unit area	gm/hr-cm^2
Nu	Nusselt number	--
n	Power coefficient of equation 6.3	--
P	Barometric pressure	atm
Pr	Prandtl number $(C_p\mu/k)$	--
p_s	Saturater vapor pressure	atm
p_v	Partial vapor pressure of air	atm
Q	Heat flow per unit area	cal/hr-cm^2
q	Heat flow rate	cal/hr
R	Gas constant for water vapor (4.55)	atm-cc/gm-mole-^{o}K
Re	Reynolds number	--
rH	Relative humidity	%
Sc	Schmidt number $(\mu/\rho D_e)$	--
T	Absolute temperature (273 + t)	^{o}K
t	Temperature	^{o}C

Symbol	Meaning	Units
U	Heat utilization factor	cal/kgm
U_{eff}	Heat utilization efficiency	%
u	Local boundary layer velocity	cm/sec
V	Mean free stream velocity	cm/sec
Vol	Volume	cm^3
wb	Wet basis	--

Greek Symbols

α	Coefficient of linear shrinkage	1/gm
γ	Specific volume	cc/gm
δ	Boundary layer thickness	cm
Δ	Difference	--
ϵ	Emissivity	--
η	Constant of equation 2.19	--
θ	Time	hours
μ	Viscosity	gm/cm-sec
ν	Kinematic viscosity	cm^2/min
ρ	Density	gm/cc

Subscripts

a	Air
b	Body, bulk
c	Constant rate, convection, characteristic
cr	Critical
d	Position distance from surface
dp	Dew point
e	Equilibrium

Subscripts

f	Falling rate
h	Supplemental heat
i	Initial
l	Lower
o	Initial, free stream
r	Radiation
s	Solids, surface, saturated
v	Vapor
u	Upper
wb	Wet bulb
x	At position x

Superscripts and Overscores

'	Falling rate
''	Flux
.	Rate
$\overline{\quad}$	Mean
$\wedge$	Estimated

1. INTRODUCTION

1.1 General Remarks

A common practice in poultry production systems is to let the chicken excrement drop directly to the floor or pit where it remains until removed. Frequency of removal depends on the type of facilities. After removal, further handling and conditioning operations are necessary before the material is finally disposed of, the exact nature depending on the overall operating facilities and the desired end product.

Water is a major component of fresh excreta and in most operations, outside those specifically designed for liquid processes, it is a hindrance. Any amount removed from the droppings, even if it is only a small percentage of the initial volume, is desirable in reducing volume and weight of material to be handled. Partial drying of poultry excreta minimizes odor production and air pollution. Still another advantage of moisture removal is that it results in overall improvement of handling characteristics.

The situation is favorable for partial excreta drying at the dropping site within the poultry house. The volume of ventilation air exchange provides sensible heat energy for evaporation, and its ability to absorbe moisture also provides the carrier by which moisture can be removed after evaporation.

The random deposition of poultry droppings both in time and space provides surface areas for heat and mass exchange. Supplemental energy inputs may be desirable to enhance the drying situation. Such inputs might include electrical energy in the form of heat (conductive or radiative), mechanical energy in the form of stirring and mixing the droppings to increase exposure, and/or electrical current to expell water from the droppings by the electro-osmosis phenomena as investigated by Cross (1966).

Preliminary research reports have shown that the use of electrical energy input in floor panels under the collection area in combination with bed stirring can economically reduce the moisture content of the droppings to such a degree that it is seriously being considered as a recommended management practice (Bressler, 1958; Esmay and Sheppard, 1971). However, due to a lack of basic information concerning water movement within the material and over-all drying rates, the optimum solution to each situation must be developed more or less by trial and error.

Phillips (1969) found this lack of basic knowledge to be one difficulty in his systems analysis of summer environment for laying hens. Free moisture evaporation from the droppings had to be estimated more or less arbitrarily. He recommended for future research that the actual mass transfer coefficient for evaporation of moisture from the surface of the droppings be determined.

1.2 Objectives

It was the purpose of this research to determine quantitatively the rate of drying of chicken excreta under the influence of moderate environments such as those found in poultry houses. Complete drying involves several phases or periods of drying as different mechanisms of drying dominate at different moisture contents. Although some sample material was completely dried, the emphasis of this research was on the initial drying phases.

Specifically, the objectives were to:

(1) Obtain sufficient experimental data to determine drying rates for the initial drying phases.

(2) Evaluate drying rates as influenced by environmental, geometrical and excreta conditions.

(3) Determine the duration of time in which each rate holds and how much water is removed during each period.

(4) Develop a semi-empirical mathematical model to predict drying rates in the initial phases.

1.3 Some Properties of Chicken Manure

The properties of chicken excreta can be classified as physical, chemical and biological. Each class has some effect on drying characteristics of the material. The following discussion is quite general with emphasis on those properties believed to have the most influence on drying.

Unlike most animals, urine and feces formed in the digestive processes of the bird are voided into the cloaca and passed from the rectum in a conglomerate mass. Excrement

leaves the body at body temperature (41.9°C, 107.5°F), but quickly cools to room temperature due to relatively high thermal conductance values, moisture contents and surface to volume ratios. The percentage of water depends on the type and breed of chicken, feed quality and quantity of intake, health of the bird and environmental factors.

Environmental factors are important in determining feed and water intake requirements. Fecal water output per pound of feed consumed is directly related to ambient air temperature resulting in excreta of higher moisture content (Esmay, 1969). The range of moisture content has been reported to be from 72 to 80 percent wet basis by weight. Seventy-five percent was the average value used by Sobel (1966). Although reported to be fresh values, it would appear that the samples were collected after some exposure to the atmosphere. Similar values were obtained by such methods of collecting samples for this research project. However, Esmay and Sheppard (1971) and Dixon (1958), report values of 88 percent moisture by collecting samples in oil covered pans.

The physical and chemical properties of chicken excreta are known to be affected by the physiology of the bird, the feed ration and the environment. The digestibility of the feed ration, the protein and fiber content and the nature of the other feed elements affect the composition of the excreta, which basically consists of undigested protein, fat, nitrogen free extract, minerals and crude protein. Sturkie (1965)

states that a high percent of fecal matter will be cellulose, lignin and other fiberous materials because chickens can digest but very little of these substances. In confinement housing, the waste found in the collection area will also contain feed and water spilled, egg shells and contents from broken eggs, feathers and other ingredients in addition to excreta passed by the chicken.

According to Sturkie (1965), the urine of birds contains thick muciod material, and is abundant in uric acid (approximately one part per 100). A number of other complex molecular substances are also present. Sturkie also states that the pH of chicken urine ranges from 6.22 to 6.7, decreasing with increasing consistency, and that the specific gravity is 1.0025. Dixon (1958) reports that urine contains between 95 and 96 percent water. Therefore, the liquid portion of the excreta is often referred to as water and its gaseous state as vapor.

Microbiological organisms that actively digest, metabolize and grow in the sub-environment of heat, oxygen, nutrients and water are always present in the excreta collection areas. The oxidation processes are involved and complex. Heat and moisture is produced as a result of this activity, whether the process is aerobic or anaerobic. Exact quantitative values can be determined only by experiment as they will vary depending upon the specific environment.

Chicken excreta is composed of discrete organic and biological particles bound together by water in a semi-solid state.

The term semi-solid is a consistancy term used to indicate that the material does not flow under the force of gravity but at the same time does not exhibit elastic properties of a solid. Excreta with moisture contents of 80 percent or more, approach a semi-liquid state where some flowability can be observed.

Sobel (1966) found the particle size of fresh chicken excreta to range from 2.34 mm to minuscule dissolved solids. Approximately 50 percent of the solids were found to pass a 200 mesh screen. This included dissolved solids. The average particle density ranged from 1.75 to 1.85 grams per cc.** Sobel also reported that bulk density varies from 65 to 67 pounds per cubic food (1.04 to 1.07 grams per cc) with the variation of moisture content from 75 to 80 percent. A quick calculation shows that for these values, fresh excreta contains from two to eight percent void space by volume. Thus, there are three basic components of the material: voids, water and solids. Build-up and settling in the collection pits will reduce the void space and increase the density if little or no water is removed by evaporation.

1.4 Typical Environments Encountered in Poultry Enterprises

Successful poultry housing systems provide optimum environmental control at minimum housing cost per production

---

**Verified by this author.

unit. The trend is to the windowless house with mechanical ventilation systems. The birds may be confined to cages, small pens or allowed free movement within the confines of the house. The bottom of the confinement space is usually made of woven wire so that excreta droppings fall through to a storage area below. The storage area may be shallow or deep pits depending on the planned frequency of cleaning.

Optimum ambient temperature control is obtained mainly by regulating the ventilation rate. Fifty-five degrees fahrenheit (13°C) is considered optimum housing temperature for cold weather (Esmay, 1966). Ventilation rates are kept to a minimum to reduce heat losses. However, rates of approximately 1/4 cfm (1/2 m^3/hr) are recommended by Esmay (1966) to keep moisture from condensing within the structure and to keep down accumulations of dust and odors. Under these conditions, air velocities over the droppings will be very low, approaching static conditions. Relative humidities may be as high as 80 to 85 percent.

Summer conditions present different environmental control problems. House temperatures will be approximately those of outside temperatures. However, 2 to 5 degrees of heating are not uncommon. House temperatures that exceed 80°F (27°C) affect production considerably. Temperatures of 100°F (38°C) or above may be lethal (Esmay, 1966). Hot weather ventilation rates are greatly increased to minimize house temperature increases above outside values. From 4 to 6 cfm (6-10 m^3/hr) per bird are recommended by Esmay (1966). Lilleng (1969)

found that with similar ventilation conditions, the air velocities above the droppings are of the order of 30-60 feet per minute (15-30 cm/sec). Relative humidities are approximately equal to outside conditions with little change in bulk air values within the building. Research by Esmay, et al. (1966) indicates that the psychrometric change of ventilation tends to follow lines of constant relative humidity. The absolute humidity will increase as the ambient air temperature increases. In Michigan, summer climatic relative humidities vary roughly from 50 to 80 percent.

Deep pits offer the opportunity for increasing the ventilation rate over the droppings independently of the house proper. In such a case, Bressler (1968) utilized air velocities up to 750 feet per minute (380 cm/sec) in the pit area.

Electrical energy input through heating cables or panels placed in the floor of the dropping pits are another source of energy input used specifically to speed up in-house excreta drying rates. Energy input rates up to 40 watts per square feet (37 cal/hr-cm^2) have been used by Bressler (1968). This high rate was applied only to areas where extra moisture was apt to collect, such as beneath the waterers. Esmay and Sheppard (1971) used heating panels with energy input rates of eight and sixteen watts per square foot (7.4 and 14.8 cal/hr-cm^2) in a cage housing situation.

Increased drying rates can be obtained by exposing more surface area to the air. Temporary retention of droppings on a fine mesh wire screen suspended between the cages and pit

has been used. Thus, the droppings are completely immersed in the drying fluid. The screens must be cleaned at least once daily to avoid build-up which quickly reduces drying efficiency. Droppings from the screens may be moved directly from the house or simply allowed to fall into the pit area. Stirring the droppings in the pit increases the total surface area exposed at one time by roughing the surface and more importantly it exposes previously covered material. Manually, stirring is usually done once a day, but with automation it could be done as frequently as thought desirable. The simplest form of stirring is by pulling some sort of toothed implement through the droppings. Research by Esmay and Sheppard (1971) indicated that once a day stirring accounted for up to 20 percent increase in water removed by natural ventilation.

1.5 Rate of Excreta Production

The magnitude of the drying problem depends on the rate of excreta production. As summarized by Loehr (1969), wet excreta production in pounds per day has been found to vary from 0.03 to 0.08 pounds per pound of live weight or in terms of each 4-5 pound chicken, 0.12 to 0.40 pounds (54-180 gms). Population densities are approaching 1/2 square foot (465 cm^2) of floor area per chicken over the excreta collection area. This means that up to 0.8 pounds (360 gms) of excrement is deposited on each square foot (929 cm^2) of pit area each day.

This amount of excreta contains more than 1/2 pound (225 gms) of moisture that can be removed by drying. Eight tenths pound of excreta spread uniformly over one square foot would have a mat thickness of approximately 0.144 inches (0.366 cm).

Because of the semi-solid state of chicken excrement, the bed thickness will not be uniform under typical housing conditions. The degree of surface roughness depends on the initial moisture content of the droppings, the amount of drying in the pit area, the time since the area was last cleaned and the system of chicken confinement. Cones of droppings have been observed to reach the height of two feet in certain cage operations with good distribution of ventilating air. These cones increase the drying rate because of the increase in dropping surface area exposed to the air stream.

Excrement is deposited intermitently throughout the day. It would be helpful to know the average volumetric size of each separate deposition, the frequency of deposition, the randomness of location where dropped and the average surface area exposed to air after being dropped. Perhaps this type of information sounds rather superficial, but as will be noted later, relatively large amounts of water can be removed in periods of hours rather than days. In addition, it is a well known fact that the thinner the material to be dried, the greater the drying efficiency. It would seem that optimum drying efficiency would be obtained if each new deposition were dried to the desired moisture content before being covered by a subsequent one.

2. REVIEW OF LITERATURE: HEAT AND MASS TRANSFER

2.1 Introduction

The phenomena involved in drying biological, porous systems are inherently dynamic and complex. However, by reducing the problem to components, it is found that although still complex, some aspects of the problem can be handled with relatively simple physical and mathematic analysis.

Drying a moist body always involves the movement of a quantity of water away from that body. For purposes of analysis this process involves two successive phenomena of: (1) migration of water within the moist body to the surfaces in the form of liquid and/or vapor, and (2) conveyance of the vaporized water away from the body surfaces. The factors that control the rate of transfer of vapor from the body to its surroundings are determined by the characteristics of the environment and not by the conditions within the body. On the other hand, the rate of moisture movement within the body can be regarded as independent of the external conditions to the extent that boundary values are known or assumed.

Some of the important external factors are: ambient air temperature (t_a), absolute humidity or concentration (H_o), atmospheric pressure (P), mean free stream velocity (V_o) and a scale of turbulent intensity. Internal factors are less

easily separated and defined. Moisture content (m), porosity, density (ρ), thickness (d), body temperature (t_b), and equilibrium moisture content (m_e) are a few of importance. These variables are not necessarily completely independent of each other. For example, ambient air temperature affects the body temperature and density is related to porosity.

Analytically, the phenomena of surface evaporation and internal moisture movement are quite different in terms of controlling factors and complexity. In this chapter, the surface phenomena will be reviewed, in the main, independently of the drying material. Chapter 3 will be devoted to the phenomena of internal moisture movement with emphasis on hygroscopic, biological materials and specifically with reference to chicken excreta.

The rate of transfer of any substance or energy depends on the driving force or potential and the conductance of the media to that substance or energy through which it must pass. In the words of Ohm's law: rate equals conductance times potential. Thus for heat energy

$$Q = h_c(t_1 - t_2) \tag{2.1}$$

where h_c is the conductance coefficient and the temperature difference is the driving potential. A similar expression for mass transfer is

$$\dot{m}'' = h_d(H_1 - H_2) \tag{2.2}$$

where the absolute humidity difference is the driving potential.

Kays (1966) states that the transfer coefficients are essentially aerodynamic properties of the system, whereas the terms within the parenthesis, the potential differences, are essentially thermodynamic properties.

2.2 Boundary Layer Concept and the Convective Transport Coefficients

The hydrodynamic boundary layer theory as extended to include heat and concentration boundary layers is well documented by Eckert and Drake (1959), among others. The transport coefficients depend on the characteristics and interactions of these boundary layers. Mean transfer coefficients may be obtained by exact analysis when the flow over a simple geometric surface is laminar. The nature of turbulent flow caused by higher velocities and rough or blunt obstructions greatly increases the complexity of exact solutions.

Analogies between momentum, heat and mass boundary layer formation and transfer mechanisms are often used to relate one coefficient to another. One such analogy has been developed by Chilton and Colburn (1934). The complete heat and mass transfer Chilton-Colburn analogy as given by Welty et al. (1969) is

$$jH = jD = C_f/2 \tag{2.3}$$

where:

$$jH = h_c(Pr)^{2/3}/\rho a V_o c_p$$

and

$$jD = h_d(Sc)^{2/3}/\rho_a V_o$$

By this analogy, the mass transfer coefficient is related to the friction factor by

$$h_d = C_f \rho_a V_o / 2 \; Sc^{2/3} \qquad (2.4)$$

This analogy is exact for flat plates and satisfactory for other geometric forms provided form drag is not present. For systems with form drag, $j_H = j_D$, but does not equal $C_f/2$. The evaluation of the mass transfer coefficient from the heat transfer coefficient is possible, and visa versa. This is valid for gases and liquids within the ranges of $0.6 < Sc < 2500$ and $0.6 < Pr < 100$, respectively, (Welty et al. 1969).

Film transfer coefficients are most often expressed in terms of dimensionless relations. The ratio of the fluid's inertia forces to the viscous forces is called the Reynolds number, ($Re = V_o x/\nu$). It greatly influences the structure of the boundary layer development and thus, the value of the skin friction coefficient. The skin friction for laminar flow over a flat plate ($Re < 2 \times 10^5$) is exactly (Schlichting, 1968)

$$C_f = 1.328/Re^{1/2} \qquad (2.5)$$

The same coefficient for turbulent flow ($Re > 3 \times 10^6$) is approximately (Eckert and Drake, 1959)

$$C_f = 0.376/Re^{1/5} \qquad (2.6)$$

Thus, the mass transfer coefficient can be calculated using the Chilton-Colburn correlation and equations 2.5 and 2.6 depending on whether laminar or turbulent conditions prevail.

Where the body presents an obstruction to the air stream such that form drag is present, the resulting flow patterns

around the object are much more complicated and highly a function of the body geometry. Even where laminar flow prevails there may be points of stagnation, separation and reattachment which makes it difficult to estimate an over-all mean transport coefficient for the body. However, the form of the skin friction equations suggest the following:

$$h_d = (\rho_a V_o / 2Sc^{2/3})(m/Re^n) \qquad (2.7)$$

where m and n are constants depending upon the flow system and must be determined by experiment.

2.3 Vapor Transfer from the Wet Body to the Surrounding Environment

The rate of evaporation, $\dot{m}$, for a body with evaporative surface, A, is

$$\dot{m} = h_d A(H_s - H_o) \qquad (2.8)$$

where H_s and H_o are the concentrations immediately adjacent to the surface and in the free stream, respecitvely.

For a fluid with nearly constant properties, the mass concentration can be converted to partial densities. In addition, according to Eckert and Drake (1959), if the density can be assumed approximately constant and the temperature difference in the field small as compared with absolute temperature, Dalton's equation is obtained. Thus,

$$\dot{m}'' = h_D(p_s - p_o)/RT \qquad (2.9)$$

The mass diffusion coefficient, h_D, is equal to the mass transfer coefficient, h_d, divided by the density, ρ_a.

The rate of evaporation from a saturated surface is completely determined by the rate at which water vapor can be transferred through the film layer of air adjacent to the wet surface and mixed with the main air stream. Thus, for a time the rate of evaporation is independent of the kind of material of the body.

The concentration of vapor pressure in the free stream is determined by the thermodynamic properties of the free stream air. The corresponding value at the saturated surface is somewhat more difficult to determine. If saturation is complete and no heat is conducted or radiated to the surface, the layers immediately adjacent will be saturated at the thermodynamic wet-bulb temperature of the free stream. The actual surface temperature is influenced by the heat transfer rates and is therefore not solely a function of the air state.

2.4 Surface Heat and Mass Balance

Evaporation of moisture from the surface of a wet body involves two processes: (1) a transfer of heat to evaporate the liquid, and (2) a transfer of mass as vapor away from the surface. Heat is required at the surface to change the state of the moisture. If the only source of heat energy is supplied as convected heat from the air stream, evaporation is adiabatic. The heat and mass balance for such a steady state is

$$h_{fg}\dot{m}'' = h_{fg}h_d(H_s - H_o) = h_c(t_o - t_s) \qquad (2.10)$$

where h_{fg} is the latent heat of vaporization. This may be greater or less than that for a free water surface depending

on surface effects and liquid properties to be discussed later.

To account for heat radiated to the wet surface from the surrounding walls of the enclosure, a second heat flux term must be added to the right hand side of equation 2.10 as follows:

$$h_{fg}h_d(H_s - H_o) = h_c(t_o - t_s) + h_r(t_r - t_s) \quad (2.11)$$

where h_r is the radiation heat transfer coefficient and t_r is the temperature of the radiating walls. Threkeld (1970) states that for the case of a small body completely enclosed by a larger body, the radiation coefficient may be estimated by

$$h_r = 4.876\,\epsilon\left[(T_r/100)^4 - (T_s/100)^4\right]/(t_r - t_s) \quad (2.12)$$

where ϵ is the emissivity of the wet surface and the temperatures are absolute.

Heat may also arrive at the evaporating surface by conduction of heat through the body. In this case, the heat and mass balance of equation 2.11 must include an additional term, such as: $k(t_s - t_d)/d$, to account for the conducted heat source or sink.

Ideally, for the evaporative surface temperature to equal the theromodynamic wet-bulb temperature the heat and mass transfer process must involve pure turbulent mixing only (Threkeld, 1970). At a finite air velocity, the two temperatures, are identical providing that

$$Le\left\{1 + \left[h_r(t_r - t_s)\right] / \left[h_c(t_o - t_s)\right]\right\} = 1, \quad (2.13)$$

or in the case where the radiating wall temperatures are equal to the dry-bulb temperature of the air,

$$Le(1 + h_r/h_c) = 1 \qquad (2.14)$$

where the Lewis number, $Le = h_c/h_d$. At finite air velocities, radiation heat transfer may compensate for the Lewis number being less than unity. At low velocities, the Lewis number is approximately equal to the thermal diffusivity, α, divided by the mass diffisivity, D_v, of the air.

Rewriting equation 2.11 with equations 2.13 and 2.14 in mind we have

$$H_o - H_s = K(t_o - t_s), \qquad (2.15)$$

where K is the psychrometric wet-bulb coefficient and equals the left hand side of equation 2.13 or 2.14 divided by h_{fg}. In estimating surface temperatures, equation 2.15 can be solved by trial and error or graphically from the psychrometric chart assuming the coefficient, K, can be reasonably estimated.

2.5 Surface Constant Rate Drying

Basically, there are two major periods of drying materials initially saturated. In simple terms, they are called the constant and falling rate periods. During the first, the moisture content of the body changes at a constant rate. The temperature of the body remains nearly constant and as a rule, it equals the wet-bulb temperature of the environment (Harmathy, 1969). Drying takes place from the surface of the body by evaporation of moisture similar to evaporation from a free water surface. The rate is affected largely by the surroundings and little by the material being dried (Hall, 1958).

Moisture diffuses or moves to the surface in some manner as fast as the air stream is capable of removing it. In the porous body, it is often assumed that there are continuous threads of moisture. Harmathy (1969) refers to this as the funicular state. It is characterized by high moisture mobility.

There has been much research done on the drying of porous solids and on the drying of hygroscopic porous bodies. It is generally accepted that if a constant rate drying period exists, it takes place at a rate depending only on external conditions. This has been shown to be true with a wide variety of materials and further, the rates differ little from that of a free body of water. See, for example, Gilliland (1938). Most research has dealt with the constant-rate dyring period only in passing (Pearse et al., 1949; Harmathy, 1969; Nisson et al., 1959).

Equations 2.8, 2.9 and 2.10 all are suitable for predicting the rate of drying during the constant rate period. The parameter least likely to be known is the convective transfer coefficient. Estimates are usually made based on aerodynamic flow characteristics as suggested in section 2.2. However, in most cases there are certain constants that must be determined experimentally for the particular system in question. In calculating mass transfer coefficients from drying experiments, the partial pressure at the surface is usually inferred from the measured or calculated temperatures of the evaporative surface.

The use of the heat transfer coefficient is preferred in estimating drying rates because they are usually more reliable (Bagnoli et al., 1963). Small errors in temperature have negligible effect on the heat-transfer coefficient, but do introduce relatively large errors in partial pressure estimates and hence in the mass transfer coefficient.

In the absence of applicable specific data, Bagnoli et. al. (1963) suggest the following equation for estimating the heat-transfer coefficient for flow parallel to plane plates:

$$h_c = 0.01\ G^{0.8}/D_c^{0.2} \qquad (2.16)$$

where G is the mass flow rate of air and D_c is the characteristice dimension of the system. The value of the exponent of G has been selected to conform with the Colburn j factor for turbulent flow.

Krischer, as reported by Luikov (1966, page 143) suggests the introduction of a universal characteristic dimension to be the length of flow round the body. He recommended the following single formula for heat transfer in the flow of air streams with low velocities over bodies of different shapes:

$$Nu_{Dc} = 0.8\ Re_{Dc}^{1/2} \qquad (2.17)$$

with D_c as the length of flow around the body and with Re_{Dc} within a range of values greater than 10 but less than 10^5. For mass transfer he recommends:

$$Nu_{d,Dc} = 0.662\ Pr^{1/3} Re_{Dc}^{1/2} \qquad (2.18)$$

Thus, using the idea of a characteristic dimension of flow around the body, equation 2.7 can be written as follows:

$$h_d = \eta V_o^{1-n} / D_c^n \qquad (2.19)$$

where:

$$\eta = \rho_a m(\nu)^n / 2Sc^{2/3}.$$

2.6 Heat of Vaporization and Capillary Potential as They Effect Surface Drying Rates

Sobel (1969) found that water evaporation rates from chicken excreta surfaces in still air are not equal to those from a similarly situated body of free water. If in fact the manure surface is saturated and the surface factors control the rate of evaporation, this would indicate that the liquid exhibits characteristics somewhat different from those of a pure water surface.

The constant drying rate may be somewhat different than the free water evaporation rate because the liquid surface tension of the urine with all of its soluble contents is different from that of water. It is known that the latent heat of vaporization of a liquid is related to its surface tension. However, it is not known how much the surface tension of urine differs from that of water.

The simplest theory relating heat of vaporization to surface tension is Stephan's equation as given by Paddy (1969):

$$\gamma(M\sigma)^{2/3} = h_{fg}/2 \qquad (2.20)$$

where:

σ = the surface tension

M = the molecular weight of the liquid

and γ = the specific volume of the liquid.

Other equations have been developed to include temperature effects.

There are several methods for determining surface tension. In many cases, measurement of the height of capillary rise of the liquid in a small tube has been found satisfactory (Paddy, 1969).

A second possible reason for a drying rate different from a pure water surface is that the vapor pressure at the surface may not be the same. Slayter (1967) states that the vapor pressure is increased by a positive pressure exerted on the liquid and decreased by suction. The effect is only appreciable for comparatively large absolute values of pressure, however. As shown by Slayter, capillaries with radius of curvature of 10^{-5} cm reduce the relative vapor pressure approximately one percent.

3. MATERIAL DRYING CHARACTERISTICS

3.1 Falling Rate Drying Periods

a. Description

The rate of moisture diffusion to the surface from within the material eventually falls below the surface evaporation potential. At this time constant rate drying ends and the falling rate drying period begins. The moisture content at the surface of the body is called the critical moisture content and is a characteristic of the material. The average moisture content of the entire body is called the mean crticial moisture content and as Luikov (1966) points out, is a function of size and shape, as well as material and drying air characteristics.

The moisture content changes at a continuously, decreasing rate during the falling-rate period and the temperature of the body increases (Luikov, 1966). The mechanisms limiting the rate of moisture removal for the two periods are distinct, although all mechanisms may be present to varying degrees throughout. In fact, the transition from the constant rate to a well defined falling rate period may not be sharp. Harmathy (1966) saw need for defining upper and lower critical values for porous systems. The upper was defined as the mean value at the time when the rate of drying first deviated from constant, i.e., the usual definition of critical moisture

content. The lower was more arbitrarily taken to be at the time when all wet spots disappeared from the surface, indicating that from then on the drying rate would be primarily a function of internal characteristics.

For a non-shrinking porous body, the moisture distribution is basically constant until the upper critical point is reached, then the surface areas rapidly dry to the lower critical point causing the formation of steep moisture gradients at the surface with nearly constant values in the center regions.

As the zone of evaporation retreats deeper into the body of a non-hygroscopic material, the rate continues to decrease as the distance over which the water vapor must diffuse, increases. The rate remains finite until the last moisture is evaporated from the bottom. For hygroscopic solids the phenomena are more complex. The rate of weight loss typically falls off as drying progresses, but often not in a single, continuously smooth curve. Distinct break points are often discernable. For example, Gorling (1958), found two break points in the drying of a potato slice. The first break was interpreted to signify the beginning of evaporation within the porous body and the second occuring when no part of the sample piece contained moisture above the hygroscopic limit.

Newitt and Coleman (1952) also discerned two break points in the drying rates of china clay, a material that shrinks with drying. They postulated that the first period of constant

rate drying ends when surface layers have reached a moisture content equal to that of the material with the shrinkage water removed. The moisture gradient was then approximately linear with depth. During the first falling rate period the moisture gradient began to flatten as interior shrinkage water moved to the surface. Newitt and Coleman postulated that most of the shrinkage water was removed before the pore water was affected. During this period, the drying rate decreased at a constant rate as the distance the moisture traversed to reach the surface increased. The surface moisture content was considerably above equilibirum during this period. Eventually, the path became so toturous and the capillary potential so great that the minisci were drawn from the surface and the second falling rate drying period began. The surface moisture rapidly approached equilibrium and the moisture gradient within the material became parabolic.

Eckenfelder and O'Connor (1961) comment on the air drying of sludge from waste treatment plants. These beds initially contain as much as 95 percent water. They state that the drying process occurs in three stages, namely: a constant rate period, a falling rate period and a subsurface drying period. During the constant rate period, the sludge is completely wetted and the rate of evaporation is independent on the nature of the sludge and approximately the same as evaporation from a free liquid surface.

b. Modes of Moisture Movement Within the Porous Body

The moisture is transferred through the membranes and porous structure of the material as liquid and/or vapor. Hall (1958), lists five possible mechanisms that may control internal movement of moisture in agricultural products:

(1) Diffusion as liquid and/or vapor

(2) Capillary action

(3) Shrinkage and vapor pressure gradients

(4) Gravity

(5) Vaporization of moisture.

Gorling (1958), also pictures five physical mechanisms as being involved during the drying of materials such as wood, potato or macaroni.

They are:

(1) Liquid movement under capillary forces

(2) Diffusion of liquid caused by a difference in concentration

(3) Surface diffusion in liquid layers adsorbed at surface interfaces

(4) Water vapor diffusion in air-filled pores, caused by a difference in partial pressures

and (5) Water vapor flow under differences in total pressure, as for example in vacuum drying under radiation.

These are a little more specific and not quite the same as those listed by Hall because of the nature of the materials and drying processes involved. Number 4 would exist if a temperature gradient existed in the moist body.

Fresh chicken excreta contains a very high percentage of moisture and exhibits high volumetric shrinkage. Therefore, liquid movement and retention by the forces of osmotic inhibition and capillary suction are of the most interest here. Gravitational forces are considered to be relatively unimportant.

The physical unbalance of forces at an interface between a liquid and a gas or vapor produces the effect of a suction on the liquid. A wetting liquid will rise in a small tube due to this suction. Liquid will move from a region of lower potential to one of a higher potential. In a porous body, a narrow pore will draw water from a larger pore. Water will distribute itself in this manner until all potentials are equalized. Thus the porous structure of the system is very important in analysis of water movement by this method.

Pore water is dependent upon the inter-molecular attraction between solid and liquid and is common to all solids when wet. A certain class of porous solids exhibit an additional potential of electrochemical suction. These solids can imbibe osmotically an amount of water depending upon a quantity known as the base exchange capacity. Coloidal particles and organic humus material exhibit very high base exchange capacities (Slayter, 1967). These materials exhibit shrinking and swelling phenomena with desorption and sorption of water.

Newitt and Coleman (1952) do not consider capillary action responsible for the swelling and shrinking because of the required presence of a gas phase. They found that no such phase was necessary for clay to develop imbibitional suction. Newitt and Coleman consider pore-water to be substantially immobile because of its adsorbed nature and postulate that it vaporizes in situ. On the other hand, electrochemically adsorbed water is much more loosely bound and more likely to move to the surface under the influence of osmotic potential before evaporating. Therefore, Newitt and Coleman feel that it is this water that is associated with shrinkage and is referred to as shrinkage water.

In any case, it is a potential difference that causes water to move from one point in the system to another. When water is removed from the surface of a shrinking body, the discrete particles move closer together. The pore space between the particles thus exhibit a greater suction potential and are capable of drawing water from the larger pores within the material. Water is drawn from the interior through the narrowing channels at rates dependent upon the strength of force and viscous resistance of moisture to flow. This process can continue as long as there are continuous threads of liquid.

c. Approximate Drying Equations for Falling Rate Periods

The falling rate can frequently be expressed with fair accuracy by the following equation (Lapple et al., 1955; Hall, 1957);

$$dm/d\theta = -K_f(m - m_e) \qquad (3.1)$$

The value of the drying constant, K_f, depends on factors affecting rates of internal and external moisture movement. If the initial moisture content is above critical so that a period of constant rate drying proceeds the falling rate period, by continuity, the falling rate drying constant is a function of the constant rate as follows (Lapple et al., 1955; Bagnoli et al., 1963):

$$-K_f(m_{cr} - m_e) = dm/d\theta)_f = dm/d\theta)_c \qquad (3.2)$$

where $\theta = \theta_{cr}$.

Thus:

$$K_f = (dm/d\theta)_c/(m_{cr} - m_e) \qquad (3.3)$$

This approximation is especially suited for the period of unsaturated surface drying where the entire evaporative surface can no longer be maintained saturated by moisture movement within the material. The drying rate decreases for the unsaturated portion and hence the rate for the total surface decreases. Internal moisture movement is controlled by capillary flow and drying time varies inversely as thickness (Bagnoli et al., 1963).

For drying periods governed entirely by internal moisture diffusion, Fick's Law is applicable. It states that the flux is a product of the gradient of the concentration and the effective diffusion coefficient, D_e. It can be shown (Jason, 1958; Carslaw and Jaeger, 1959) that the solution for a three dimensional slab is

$$\frac{m - m_e}{m_o - m_e} \simeq \frac{8}{\pi^2} \exp \left[- \frac{\pi^2}{4} \left(\frac{D_x}{a^2} + \frac{D_y}{b^2} + \frac{D_z}{d^2} \right) \right] \theta \qquad (3.4)$$

Differentiation of equation 3.4 gives the drying rate of

$$\frac{dm}{d\theta} = - \frac{\pi^2}{4} \left(\frac{D_x}{a^2} + \frac{D_y}{b^2} + \frac{D_z}{d^2} \right) (m - m_e) \qquad (3.5)$$

If the medium is isotropic, $D_x = D_y = D_z = D_e$. Equation 3.5 is identical to equation 3.1 with $K_f = \frac{\pi^2}{4} D_e F$, where F is the shape factor and equal to $(1/a^2) + (1/b^2) + (1/d^2)$.

The diffusion coefficient has been regarded as a constant. Thus, K_f should be proportional to the shape factor, or inversely as the square of the thickness in situations where a and b are much greater than the thickness, d.

Thus far, it has been tacitly assumed that shrinkage does not occur. Calculations are based on initial dimensions. Danckwerts as reported by Fish (1957) handled shrinking systems by allowing the coordinates to shrink with the solid portion of the system. He has shown that where it can be considered constant, the diffusion coefficient is invarient with body size and shape and the shrinkage factor can then be ignored.

3.2 Characteristics of Biological Materials Related to Drying

a. Physical Structure, Moisture and the Hygroscopic Phenomena

Biological substances are characterized by complex and heterogeneous physical structure, of which water is an ubiquitous and fundamental part. Moisture contents of the different constituents may differ widely at equilibrium even though temperature and vapor pressure may be equalized throughout. In the course of drying shrinking materials the distance through which water must travel to reach the surface is decreasing, but if the material contains cellular tissues, the number of cell walls through which the water must pass does not change. In view of these complex relationships the term "moisture content" must be defined in terms of the exact procedure used to physically determine the quantity.

The hygroscopic point has been defined by Lewis (1921) as the product moisture content corresponding to a relative humidity of 100 percent. In general, a body with greater moisture content is saturated. The term "free moisture" is used to mean that moisture not bound to organic particles as chemical or adsorbed water, or in other words, water contained above the hygroscopic limit. "Removable moisture" refers to all moisture that will be removed from the material upon drying to its equilibrium moisture content (Van Arsdel, 1963). It is represented by the expression, $m - m_e$, where m is the amount of moisture present in grams and m_e is the amount of moisture contained in its equilibrium state.

Physically, if the material is saturated, it is a two-component system of water and solids, and if not, a three-component system of water, solids and gas (air).

A hygroscopic material exhibits a surface phenomena called sorption. Water bound to the body in this manner is called adsorbed moisture. The bonding may be physical, chemical, or both. The amount of water held in this manner is described empirically as a function of pressure and temperature. The relationship between the amount of vapor adsorbed by a solid and the vapor pressure is represented by the moisture equilibrium isotherm.

Moisture sorption isotherms of biological materials are noted for their striking S-shape and the phenomena of hysteresis. Hysteresis is the difference between equilibrium moisture content at a given vapor pressure according to whether the equilibrium point was reached from higher or lower moisture contents (Van Arsdel, 1963).

A limited number of equilibrium moisture isotherms have been determined for chicken excreta by Sobel (1969) and are included here in Figure 3.1. Values obtained from this figure were used extensively in analyzing the data of this research.

b. Shrinkage, Case-hardening and Distortion

By analogy with the definition of the coefficient of thermal expansion, the linear shrinkage with uniform moisture distribution has been characterized by the coefficient of linear shrinkage (Gorling, 1958) as follows:

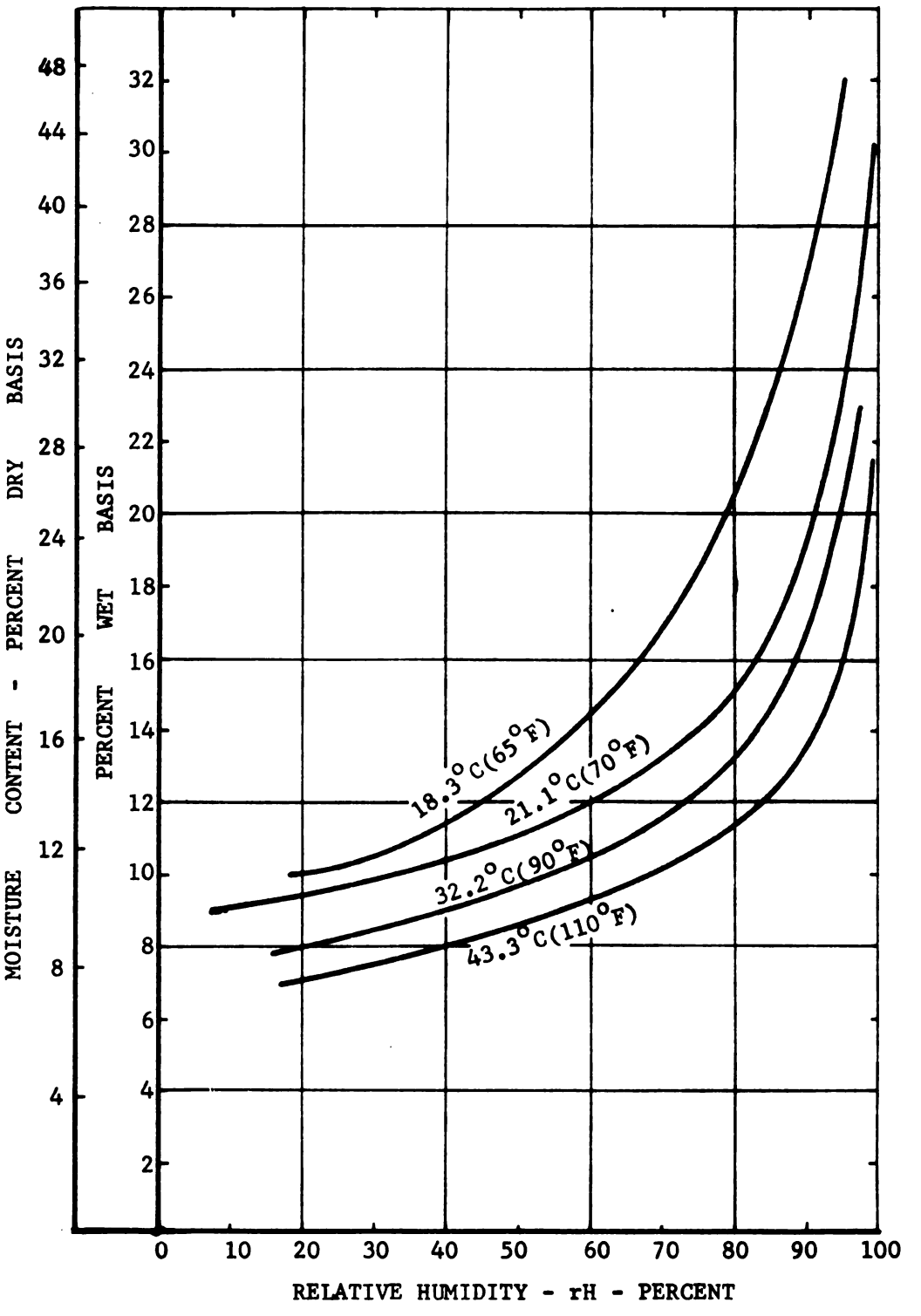

Figure 3.1 Equilibrium moisture content of chicken excreta (Sobel, 1969)

$$\alpha = (1/a_o)(\Delta a/\Delta m). \qquad (3.6)$$

As long as this relation holds, the shrinkage is called "unrestrained" or "free". Where additional forces caused by adherence or friction are present, the shrinkage is restrained.

During drying processes, the material layers next to the surface dry more quickly, so that the tendency to shrink is higher there but is restrained by the adjacent layers due to inner friction. Thus, shearing stresses appear along layers parallel to the surface, and at right angles there are either compressive or tensile stresses (Gorling, 1958). These stresses may cause deformations or, if the tensile strength is exceeded, surface cracks. The tensile strength of materials composed of discrete particles is relatively low. Increased drying rates cause greater moisture gradients and more cracking.

Chen and Rha (1971) investigated the shrinkage in dehydration of grapes and found that volume change was an exponential function of drying time in much the same manner as was moisture content. It was not stated how this would effect the diffusion model for high moisture foods.

Volume change of shrinking materials can follow different patterns for different moisture ranges. Philip and Smiles (1969) use the terms "normal", "residual" and "zero" to

describe patterns of volume change in collodiul soils. In the normal range, the material behaves as a two-component system and shrinks in direct proportion to the amount of water removed. The zero range is the other extreme where no volumetric change occurs upon drying, and residual refers to that range in between.

Formation of a crust like shell may occur while the interior of the body is still wet. This is sometimes called "case hardening" (Van Arsdel, 1963) and is a result of structural change and/or bonding by solute constituents. Soluble constituents such as sugars may migrate within pieces as drying occurs and be separated from the water by membranes. In addition to increasing the resistance of water flow through the membrane they may act as bonding agents as the shrinking system forces the particles together. The result is that resistance to moisture movement through these layers become much greater. A drastic decrease in drying rate will occur even though the mean moisture content of the body is relatively high.

Van Arsdel (1963) states that if migration of solutes or a chemical reaction does not change the character of the surface there is no advantage to preventing surface structure formation by slowing the initial drying rate. The moisture in the body always distributes itself through the solid in such a way that a low diffusivity in a zone of low-moisture content is compensated by a steeper moisture gradient in that zone.

Van Arsdel also states that the existance of a "wet center" is a condition which favors the most rapid further drying.

3.3 Characteristics of Chicken Excreta Related to Drying

The main points of the following discussion are taken from the article "Removal of Water from Animal Manures," by Sobel (1969).

Drying relationships established for agricultural products such as hay and grains, and for sewage sludge cannot be applied directly to animal manures because of their empirical nature. However, it has been established by Sobel and others that chicken manure has drying characteristics similar to other agricultural hygroscopic materials, such as, for example, equilibrium moisture contents and drying rates.

The following conclusions were made by Sobel:

a) Removal of water from chicken excreta results in a reduction in weight and volume.

b) The offensiveness of the odor of chicken excreta decreases with a decrease in moisture content.

c) Equilibrium moisture content of chicken excreta is comparable with other agricultural hygroscopic materials. Typical values for equilibrium moisture content at 70°F (21°C) are 19% w.b. at 90% rH and 9% w.b. at 10% rH.**

d) Drying times for chicken excreta under minimum velocity or "static" conditions are in terms of days. Typical drying times to equilibrium for the standard sample used at 80°F (26.7°C) were 45 hours at 35% rH and 70 hours at 56% rH.***

**For shelled corn equivalent values are: at 77°F(25°C), 19.6% at 90% rH and 5.1% at 10% rH (Hall, 1958).

***Standard sample thickness was 1/4 inch (0.635 cm).

e) Variation within samples has more effect on drying than humidity variation within a ± 15% range of relative humidity.

f) Reducing the thickness of the droppings has significant effect on the drying characteristics. The droppings must be thin, e.g. 1/4 inch, to enhance drying.

g) The loss of water from excreta surfaces are less than that from a free water surface.

Constants required for determining drying rates depend on environmental conditions, excreta characteristics and interaction between the material and its media. Parameters such as diffusivity and heat conductivity are difficult to establish for any biological material and especially so for materials of extreme heterogenity and biological variability as in the case of chicken excreta. In all likelihood, material parameters will vary with moisture content. No numerical values have been reported for chicken excreta.

Sobel also found that chicken excreta exhibited considerable shrinkage upon drying, as much as 50% when air dried from 75% w.b. to equilibrium moisture content. In addition, he found considerable cracking occuring as drying proceeded, cracking similar to that of cohesive soils.

4. SELECTING THE EMPIRICAL MODEL FOR DRYING CHICKEN EXCRETA

4.1 General Comments and Assumptions

Most drying models are empirical, or at most, semi-empirical in nature, based on experimental data and verified by how well they predict actual results. They are phenomenological in that they predict what will happen but not how.

The reason for any mathematical drying model is to predict moisture contents at a given time (or the amount of moisture removed over a period of time) or the time required to reach a given moisture content.

Drying data are most frequently presented in the form of drying rates, $dm/d\theta$. The rate of drying can usually be quite accurately described as a function of the moisture content of the drying body. Rate equations are straight forward in computational procedure but strictly empirical in nature. Drying constants must be determined by experiment for each new system. Direct integration of drying rates is theoretically allowable only if the rate of drying is strictly determined by the value of its mean moisture content and not at all by its previous drying history (Van Arsdel, 1963). This is never exactly true and further empirically restricts the methods.

Break points in drying rate curves indicate different dominating mechanisms involved in moisture movement. Better drying estimates are possible if distinct drying constants

are determined for each apparent period of drying. However, transition from one period to another is often gradual and the break point itself must be estimated.

As stated in the objectives, this research will be primarily concerned with the initial phases of drying of fresh chicken excreta including constant and initial falling rate periods. Rate equations will be used for prediction. Because of the distinct difference in mechanisms of drying and the factors involved, two distinct prediction equations are anticipated. However, drying is a continuous process. The equations must be compatable at the critical time when the rate changes from constant to falling. This compatability may be obtained through establishing initial conditions for each period based on the final conditions of the previous period.

The basic drying system to be analyzed is sketched in Figure 4.1. The drying body was dimensions of: a, the length parallel to the flow of air; b, the width perpendicular to the air flow; and d, the thickness. The surfaces are assumed hydraulically smooth and laminar flow conditions are assumed to prevail in the free stream. The top and four sides of the body are unrestricted and exposed to the air stream. The bulk free stream properties are maintained constant throughout the drying process and are unaffected by the process.

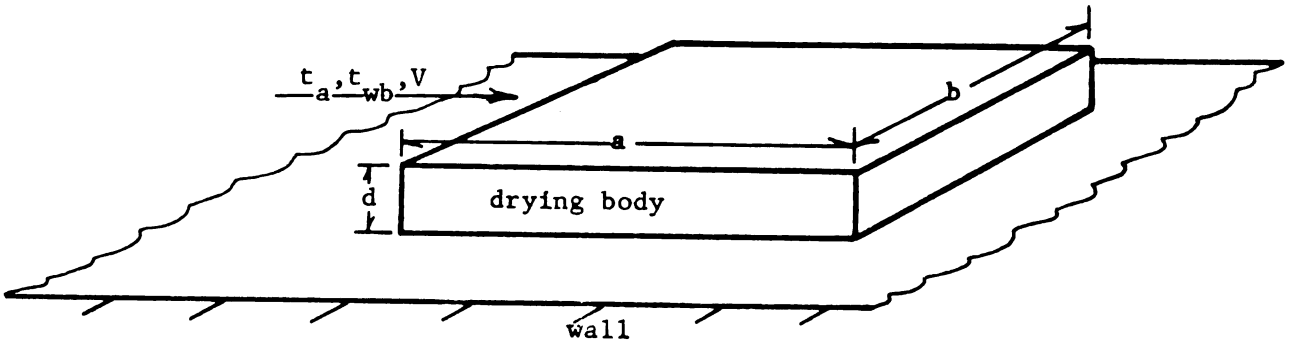

Figure 4.1 The basic drying system

4.2 Assumptions and Development: Constant Rate Period

The term, constant rate drying suggests that, during this period the rate will be constant and that it is simply a matter of evaluating this constant in terms of those factors that control the mechanisms of heat and mass transfer to and from the body.

The basic assumptions are that the body surface remains saturated and the adiabatic evaporative process prevails throughout the period. It is further assumed that no period of conditioning is required before the beginning of the constant rate period.

Under these conditions, equation 2.9 can be used to predict the rate of moisture removal. Equation 2.9 is reproduced below for convenience.

$$\dot{m}'' = h_D(P_a - P_s)/RT \qquad (4.1)$$

The transfer coefficient, h_D, takes the form of equation 2.19 with the characteristic length equal to a + 2d. Integration of 4.1 gives

$$m - m_o = \left[h_D(p_a - p_s)/RT\right] \theta \qquad (4.2)$$

In terms of moisture ratio this is equivalent to

$$M = 1 - K_c\theta \qquad (4.3)$$

The drying constant, K_c, is equal to the absolute value of $\left[h_D(p_a - p_s)A_s/RT(m_o - m_e)\right]$, and is dependent on the ambient air temperature, the wet-bulb depression, the free stream velocity and the body characteristic length.

In the development of equation 2.19 it was tacitly implied that the drying bodies were located far enough from the walls of the experimental chamber to be unaffected by the development of the momentum boundary layers along these walls. This is not the case for the situation depicted in Figure 4.1. However, it will be assumed that the basic factors affecting the development of the drying equations still hold and that the experimentally determined constants will allow for the differences in the systems geometry. The momentum boundary layer thickness at the wall of the experimental test section is estimated in Appendix A.1.

Equations 4.1 and 4.2 apply for all drying times between zero and the critical time when the mean critical moisture content is reached and the falling rate drying period begins. Thus, as long as the surface is saturated, the rate of moisture removed per unit area is constant.

4.3 Continuity Between Periods

The transition from constant to falling rates will be gradual. Theoretically the constant rate period will end

when the first water miniscus recedes into the body. Because of the shrinking nature of the material there is a time difference between the first deviation from constant rate drying and the complete disappearance of the surface pore water [lower critical point of Harmathy (1969)]. Therefore, the critical break point between constant and falling rate periods will not be well defined.

To satisfy the condition of continuity

$$\dot{m}''_f = \dot{m}''_c \text{ at } \theta = \theta_{cr} \tag{4.4}$$

where the critical time, θ_{cr}, is the time of the first deviation from constant rate. The critical time is directly related to the critical moisture ratio by equation 4.3 as follows:

$$\theta_{cr} = (1.0 - M_{cr})/K_c \tag{4.5}$$

4.4 Assumptions and Development: Falling Rate Drying

Definition of conditions during the falling rate period are much more difficult. Physical shape and internal characteristics make the problem extremely complex. The aim will be to develop a phenomenological rate equation of the type of equation 3.1, where the rate is a function of the mean moisture content of the material. Equation 3.1 is

$$dm/d\theta_f = -K_f(m - m_e) \tag{4.6}$$

As shown in Section 3.1c, the drying constant, K_f, is a function of the constant rate and the critical moisture content as follows:

$$K_f = K_c/M_{cr} \tag{4.7}$$

Thus, by this relation, the break point between the two periods of constant and falling rate is not as physically defined in the previous section but exactly determined by the ratio of drying constants. This more accurately defines the break point in analytical terms in the case where the transition is not well marked.

Shrinkage occurs throughout the drying process. However, original dimensions will be used as a basis. Shrinkage causes internal changes, but it will be assumed that these changes are a function of moisture content and not shape.

From previous discussion, it would be logical to expect more than one distinguishable falling rate phenomena. However, only the first falling rate constant will be determined.

5. EXPERIMENTAL DESIGN AND PROCEDURES

5.1 Controlled Environmental Variables

The controlled environmental factors were: ambient air temperature, thermodynamic wet-bulb temperature (absolute humidity) and free stream velocity. The barometric pressure was assumed constant at one atmosphere. Air flow was assumed laminar.

The range of air temperatures and velocities used for the experiments were somewhat higher than those anticipated in summer housing conditions in order to obtain better control and measure of these variables. It was difficult to maintain high humidities at lower temperatures with existing laboratory room temperatures. Higher temperatures were advantageous in that faster drying rates were obtained, thus decreasing the time required for each test. Velocities of less than 25 cm/sec (50 ft/min) were difficult to maintain constant and the air conditioning unit was designed to best handle somewhat greater mass flow rates.

Ambient air temperatures were controlled at values of 70 (21.1), 80 (26.7), 82 (27.8), 85 (29.4) and 90 (32.2) degrees fahrenheit (centigrade). Velocities were maintained at 50 (25), 150 (76), 240 (122) and 290 (147) feet per minute (centimeters per second). Absolute humidities ranged from

74 to 136 grains per pound of dry air (0.0106 to 0.0194 gm/gm or lb/lb). Corresponding relative humidities ranged from 40 to 76 percent and the wet-bulb depressions from 7 to 19°F (4 to 11°C). Selected values were held constant throughout each run.

5.2 Material and Process Variables

The only two material variables measured were initial moisture content and density, and these were not specifically controlled. They were found to vary randomly between 75 and 80 percent moisture content wet basis and 1.05 to 1.25 grams per cc, respectively. Age was also a material variable, but harder to define in quantitative terms. Most sample material was not older than three days, but in some cases was more than one week old; old enough that biochemical changes were apparent through color and smell.

Process variables include body shape and thickness, surface area and additional conducted heat input. Three primary thicknesses were used. They were: 1/8 (0.317), 1/4 (0.635) and 3/8 (0.952) inches (centimeters). Almost each run included at least one sample of each thickness. The sample shape was basically unchanged for all tests at 4 inches (10 cm) wide by 4 inches (10 cm) long. A few were 8 inches (20 cm) long. Two levels of surface area per thickness were obtained by placing the samples either on the floor of the test chamber or suspending them in the air stream on wire screens. The suspended samples effectively had almost twice the evaporative surface area.

Because of the extreme shrinking characteristics of the material, it was difficult to cover the sides such that no drying occured there and at the same time avoid effecting the normal shrinking patterns. In addition, there was the problem of keeping the top layer flush with the protective sides. It was decided to leave the sides exposed to the air stream and increase the top surface area to reduce the relative edge effects. The top to side area ratios were: 7.9, 4.0, and 2.6 for the respective thicknesses.

The thinnest thickness possible was about 0.3 cm due to the fiberous content of the material. Larger body dimensions of length and width insured a more representative material sample but, on the other hand, increased the difficulty of forming a continuous sample. Also, the experimental apparatus limited the sample size.

The experimental apparatus included two test sections. One section was provided with an electrical heater to supply additional heat input. The range of additional heat supplied was from 30.6 Btu/hr-ft^2 (8.4 cal/hr-cm^2) to 100 Btu/hr-ft^2 (27.1 cal/hr-cm^2).

5.3 Collection of Sample Material and Preparation of Test Samples

Chicken excreta was collected from one of the caged laying houses at the Michigan State University Poultry Research Farm. All material was collected from the same group of hens over a period of one month. The environment was typical to that

encountered in mild summer weather. Most of the sample material was collected within three days after deposit in plastic bags to prevent drying by natural ventilation. The rest was collected directly from the open pit area. The amount of spilled water and feed in the sample material was minimized by the collection techniques.

The material was stored as collected in sealed bags at refrigeration temperatures of approximately 7°C for one day to allow for moisture equalization throughout the material. The material was removed from the refrigerator 2-3 hours before the test samples were made.

Samples were formed by spreading 1/8 inch (.31 cm) layers within a 4 by 4 by 1/8 (10 x 10 x .317 cm) form. The 3/8 inch samples were composed of three such layers. The resulting density ranged from 1.10 to 1.25 gm/cc. It will be noted that this was considerably greater than the fresh excreta values reported by Sobel (1966). There was no correlation between thickness and material density or initial moisture content.

Some samples were formed using minimum disturbance techniques. The material was collected on plates with the excess material trimmed away to form the test samples. The fiberous nature of the material made it difficult to obtain smooth surfaces of constant dimensions. The density of these samples were approximately 1.05 gm/cc. One additional sample was tested completely undisturbed. In this case the surface area could only be roughly estimated.

The object of molding the samples was to obtain hydraulically smooth surfaces of known area.

All samples, except the two surface drying samples, rested on 1/8 x 5 x 5 inch (.31 x 12.7 x 12.7 cm) plexiglas plates. These plates were required so that the samples could be removed from the experimental chamber for weighing.

The two surface drying samples rested on screens of approximately 40 gage wire were 0.3 cm openings. The two surface samples were somewhat thicker than nominal dimensions because some of the material was squeezed into the grid openings upon forming.

5.4 Brief Description of Experimental Test Chamber

The following discussion will be clarified by referring to Figure 5.1.

The experimental chamber consisted of a settling chamber, two test sections and an exit section. Conditioned air entered the settling chamber through a 10 cm diameter pipe. The air was spread by diverging walls and screens into a 12 x 26 inch (30.48 x 66 cm) plenum chamber. Then it passed through a converging throat, two screens and a honeycomb flow straightener into the main test chamber measuring 4 inches (10.1 cm) deep and 26 inches (66 cm) wide. The flow straightener was 1.4 cm thick with 0.25 cm openings and was located approximately 30 cm from the leading edge of the samples in the first test section.

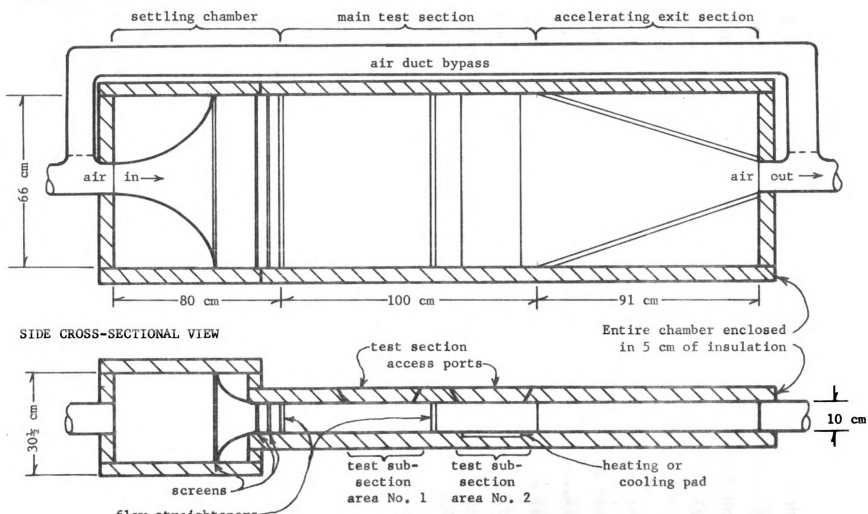

Figure 5.1 Sketch of the experimental test chamber

Following the first test section was another flow straightener identical to the first. This flow straightener was about 15 cm from the leading edge of the samples in the second test section. Following the second test section was a converging exit about 90 cm in length reducing the flow cross-section to 10 x 10 cm.

Each test section contained a removable lid for access to the samples. The samples had to be removed from the chamber to be weighed. When closed the chamber presented a continuous 10 x 66 cm flow cross-section. The entire test chamber was enclosed in 2 inches (5 cm) of insulation board and 1 inch (2.5 cm) of plywood. The combined conductance coefficient was estimated to be 0.15×10^{-4} cal/sec-cm^2-^{o}C.

The velocity variation was less than $\pm$ 5 percent of the mean free stream velocity throughout the cross-section to within 2-1/2 cm of each side wall and to within 1/2 cm of the ceiling and the floor. The measured velocity of the second section was approximately 2-1/2 percent less the velocity of the first.

Wet-bulb and dry-bulb temperature values of incoming and outgoing air varied less than $\pm$ 1^{o}C without the heater in the second section. The heater increased the outgoing temperature approximately 1^{o}C, but since it was on the downstream side did not effect the first (unheated) section.

The electrical heater was made up to #34 copper wire with resistance of 5 ohms per meter. The wire was strung back and

forth across an asbestos sheet with spacings of approximately 1/4 cm. The heater was enclosed in plexiglas. The temperature variations 1/4 cm above the heater was less than $\pm$ 2°C throughout the length. The samples were placed on top of the heater enclosure. Thus, the heat passed through 0.635 cm of plexiglas before reaching the sample (.317 cm sample plate plus .317 cm heater plate).

In addition to the heater plate, a cooling plate was designed to fit the same space upon removing the heater plate. By circulating tap water through this plate, plate temperatures of 58 to 60°F (14.4 to 15.5°C) were maintained. This plate was used to simulate winter floor conditions in the poultry house. One test was run simulating winter environment conditions.

5.5 Experimental Apparatus

An Amico-Aire* air conditioning unit was used to pre-condition the recirculated air. Dry bulb temperatures could be maintained at $\pm$ 1°C. Dew point of the air was maintained by the water bath temperature. Line voltage variations, especially between night and day, required that close watch be maintained and fine adjustments made during the test run. Thus, the maximum variations per run were a degree or two greater than experiment variations.

---

*American Instrument Co., Inc., Silver Spring, Md.

Air speed was controlled by a universal variable rpm motor and voltage regulator. The motor seemed to be extremely sensitive to changes in line voltage. Air speed fluctuations were approximately $\pm$ 10 percent of the mean value. Minor control changes were necessary to maintain a uniform mean value throughout the 24 hour period.

A 25 cm diameter radial type fan was used to move the air. There was approximately a 5°C temperature rise across this fan at the higher air speeds, which increased the difficulty of maintaining lower chamber temperatures.

A 24 point potentiometer was used to record temperatures at a frequency determined by a time clock. The time required to record 24 points was 90 seconds.

Twenty-four gage copper-constantine thermocouples were used as sensors. Finer gage wire would have been desirable for in-sample readings, but were difficult to position and too easily broken. In some cases, shrinkage strains were enough to break them. In any case, position was not accurately determined. Temperature recordings were estimated to be accurate to $\pm$ 1°C of recorded value.

Samples used for material temperature measurement could not be used for weight measurements. Therefore, at most, there were only two samples reserved for temperature measurements for each test run. Themocouples were placed at the bottom, in the center and on the surface as the sample was formed.

Free stream velocity was measured in the center of the cross-section midway between the first and second test sections by a single hot wire anemometer of the constant current type with accuracy of ± 2 fpm (1 cm/sec) or ± 3 percent of the indicated value.

Normal sample loading reduced the free stream cross-section by about 8 percent. Comparisons of free stream velocity measurement over the samples with the above mentioned recording position indicated the free stream velocity was no more than 10 percent greater than the recorded value. Cross flow was minimal in the free stream. Of course, the flow patterns around the samples were more random. No attempt was made to measure velocities near the sample except at the top surface. Velocities at a position 1/4 cm above the sample were roughly 1/2 the mean free stream velocity.

A Mettler** balance positioned near the experimental chamber was used to measure the sample weights. The capacity was 800 grams with accuracy to the nearest 0.1 gram. Weight was estimated to the nearest 0.05 gram.

Accurate humidity measurement proved to be the most difficult measurement to make. The simplest and most accurate measurement was obtained with calibrated mercury-in-glass thermometer with wet wick. This was inserted at the 10 x 10 cm exit section when a wet-bulb reading was desired. The wick

---

**Mettler Instrument Co., Hightstown, N.J.

was wet with distilled water at temperatures near the estimated wet-bulb temperature. Minimum velocities in this section were 320 feet per minute (160 cm/sec) which were more than enough to avoid an error of more than 1/2°C due to insufficient velocity (Threlkeld, 1970).

The heater input was controlled by a voltage regulator. The voltage input varied from 30 to 55 volts. The actual heat flow was estimated to be ± 20% of the value recorded. It took this variable considerably more time to reach steady state than the other variables. In addition, because of the complex interaction between the heater, air velocity and sample thickness, temperature differences within the samples could not be duplicated from test to test or from sample to sample.

5.6 Test Procedures

It took approximately one hour to form 10 samples and place thermocouples in two. To minimize moisture loss to natural air circulation during this period, the samples were placed in a closed box until the start of the experiment. During this period, the desired environmental conditions of the experimental chamber were established.

The samples were weighed for intial values immediately before being placed in the chamber. While the chamber was open the conditioned air was diverted past the main chamber.

Ten samples were placed in position, five to each section, side by side across the chamber on the floor, unless they were two-surface samples. Two-surface samples were suspended in the airstream midway between the top and bottom. The samples were placed randomly as to thickness. Some preliminary tests were made with all samples of the same thickness. Drying rates did not vary significantly with horizontal position.

Vertical position of the top surface relative to the floor introduced a greater variation. The surface of the thinner samples were closer to the floor than the thicker unless lifted by equalizing blocks and, thus, submerged in the natural momentum boundary layer formed along the experimental chamber walls. The disadvantage of lifting the thinner samples to equalize surface position was the possibility of increasing heat flow underneath and through the bottom of the sample, and also further reducing the free stream cross sectional flow area. Most samples were placed directly on the floor with only the support plate underneath. Estimated momentum boundary layer thicknesses are given in Appendix A.1.

Samples reached quilibirum chamber temperatures in less than one hour. Drying data indicated that the initial drying rate had been established by that time. Total drying times were always more than 24 hours except for the heated samples in the second section.

Samples were removed from the chamber for weighing once every hour, two hours or four hours, depending on the test and

time since beginning the test. Total time required to open the chamber, weigh eight samples and close the chamber was approximately 5 minutes. Sample recovery time, based on temperature samples, was estimated to be no more and probably much less than 5 minutes. Chamber recovery time was almost instantaneous because of the by-passing air arrangement. One reason for the quick sample recovery was that none of the test temperatures were more than 10°C above the room temperatures.

The frequency of weighing was determined by balancing the need for a large number of data points on the one hand, with the desirability of minimal sample disturbance on the other. Initial readings were more frequent to make certain the initial drying rates were established.

One difficulty encountered in optimizing recording frequency was the extreme variation of drying rates due to thickness and conducted heat inputs. Thin samples with conducted heat input should have been weighed three to four times more frequently than the thicker samples without heat input.

Each sample was rotated 90 degrees in place after each weighing to present a different leading edge to the air stream, thus, equalizing the uniformity of drying over the surfaces. Samples, divided into nine equal parts and dried, indicated that drying after a period of 8-10 hours was essentially uniform, with the center section containing the most water.

Sample moisture determinations were made at the end of each test run by oven drying the samples 24 hours at 84°C and

atmospheric pressure. Higher oven temperatures were not used to avoid warping the sample support plates.

No volumetric measurements were made. Time when sample cracking started was noted.

6. REGRESSION ANALYSIS AND DEVELOPMENT OF DRYING MODEL

6.1 Data Summation and Limitations

Initial conditions for each sample tested are listed in Table 2 of Appendix B. The samples are listed by run number (the first two figures of the sample number) and thickness, starting with the thinnest of each run.

The following information is given in Table B.2: nominal thickness, d, based on the depth of the form used to make the sample; effective thickness, d_e, which is the volume divided by the evaporative surface area; the characteristic dimension, D_c, of the sample or length of air flow path over the sample; the area of evaporative or exposed surface, A_s; the initial weight of the sample, m_i; the initial and assumed unchanging weight of dry solids, m_s; the amount of removable moisture, $m_o - m_e$; the initial moisture content in percent wet basis, IMC; the desnity, ρ; and, in the most general sense, the age of the material used to make the samples. The age identification symbol of 0 represents material that was collected from the pit area after periods of exposure exceeding 72 hours. The figure 1 represents sample material collected in plastic bags for periods of 24 to 48 hours before being sealed and stored in the refrigeration unit.

The mean density of 88 samples is 1.20 gm/cc with standard deviation of 0.05. There is no significant difference between the "old" and "new" samples or with the thickness of the sample. Due to the method of sample formation, the mean value is approximately 15 percent greater than the values of 1.04 to 1.07 gm/cc reported by Sobel (1966).

The initial moisture contents of 29 "old" samples averaged 74.5 percent wet basis with standard deviation of 1.9. Sixty-five "new" samples averaged 70.6 percent with a standard deviation of 1.4. Again, there is no significant difference with sample thickness. In addition, initial moisture content and density could not be shown to be statistically correlated. No sample material contained moisture equivalent to fresh manure because of unavoidable moisture evaporation during the collection period. Estimates using Stephan's Law for diffusion of water into still air predicted a moisture reduction from 88 to 82 percent under conditions similar to the collection system with plastic bags.

The environmental test-run conditions and number of samples in each test section are given in Table B.1 as well as the average body temperatures of the samples.

All weight data are transposed into a dependent variable of dimensionless moisture content ratio, M, referred to as moisture ratio. The moisture ratio is used instead of sample weight or weight of water in the sample because of its normalizing aspect. It is a term that is independent of

sample size and initial mass of moisture in the sample. Physically, it is the ratio of the amount of removable moisture remaining at a given time to the total amount of removable moisture that was present at the beginning of the drying process. Symbolically it is

$$M = (m - m_e)/(m_o - m_e) \qquad (6.1)$$

Figures 6.1 through 6.6 are some typical drying curves plotted on cartesian and semi-logarithmic coordinate paper after the moisture ratio transformation. These figures show effects of sample thickness and various drying situations. Their shape is similar to those found for most hygroscopic materials. However, distinct straight line segments are not apparent in most of the semi-logarithmic plots. This makes analysis of the falling rate data difficult, especially for samples in which the number of data points is limited.

Drying rates must be obtained from the original data by some process of differentiation. Graphical differentiation is impossible with the small amount of data available. The only alternative is mathematical curve fitting and then differentiation of this mathematical expression.

Complete falling rate data were not attained in all cases, particularly for thin samples in fast drying situations. The frequency of weight measurements for all samples provided for only two or three falling rate data points for the thin samples. The samples that could not be used in the falling rate analysis are noted in the tables.

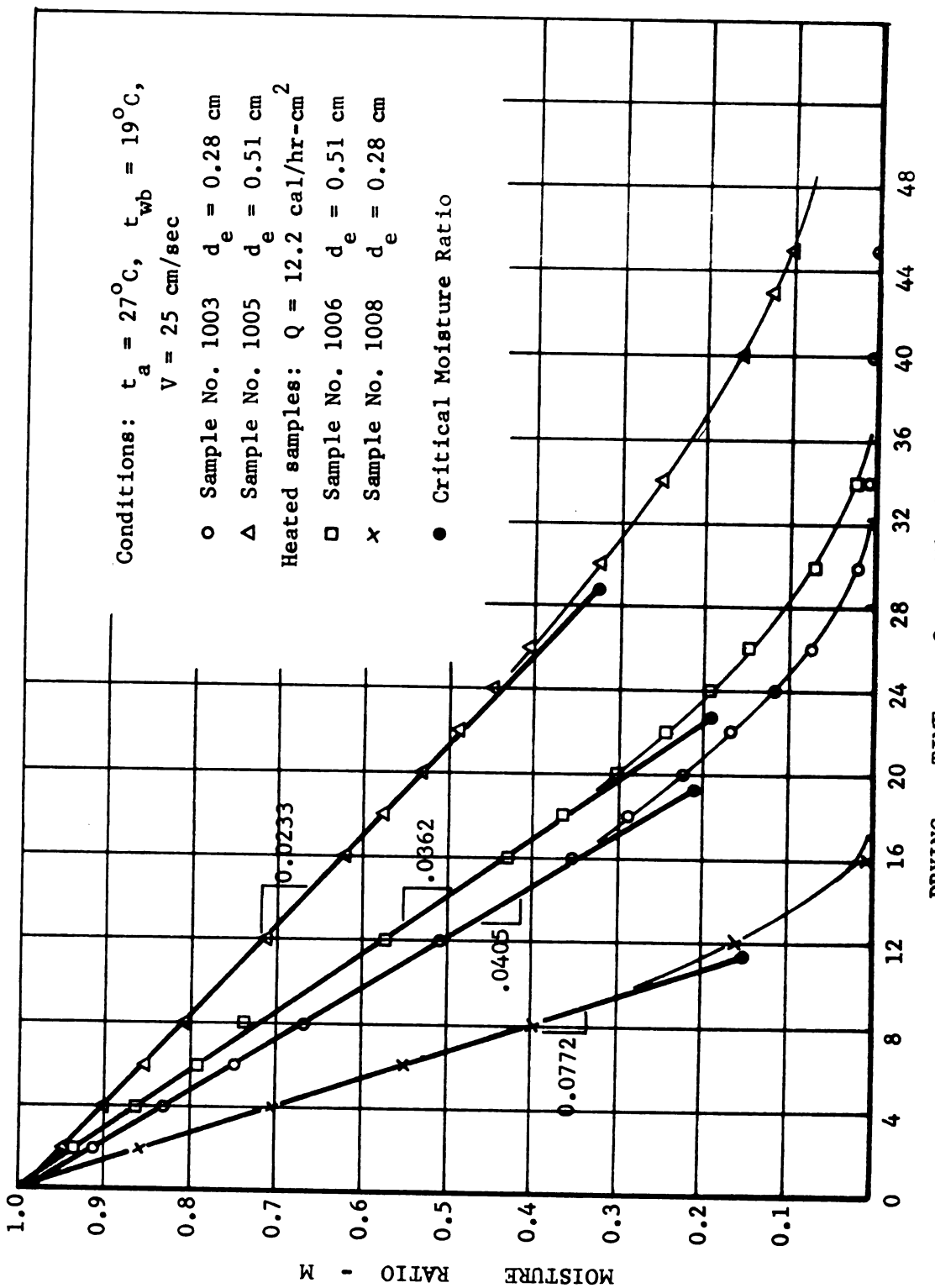

Figure 6.1 Drying curves for test-run 1000

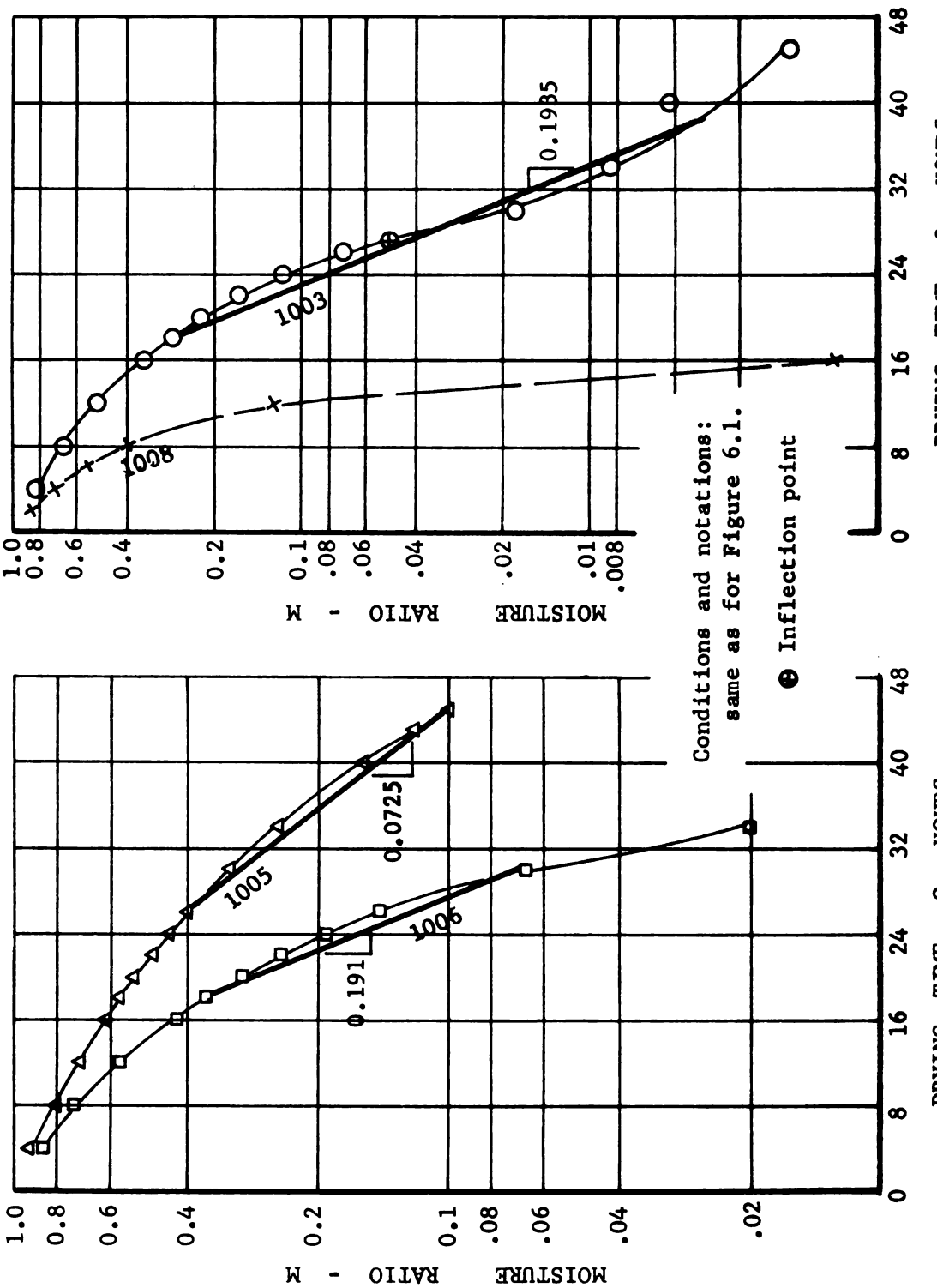

Figure 6.2 Semi-logarithmic drying curves for test-run 1000

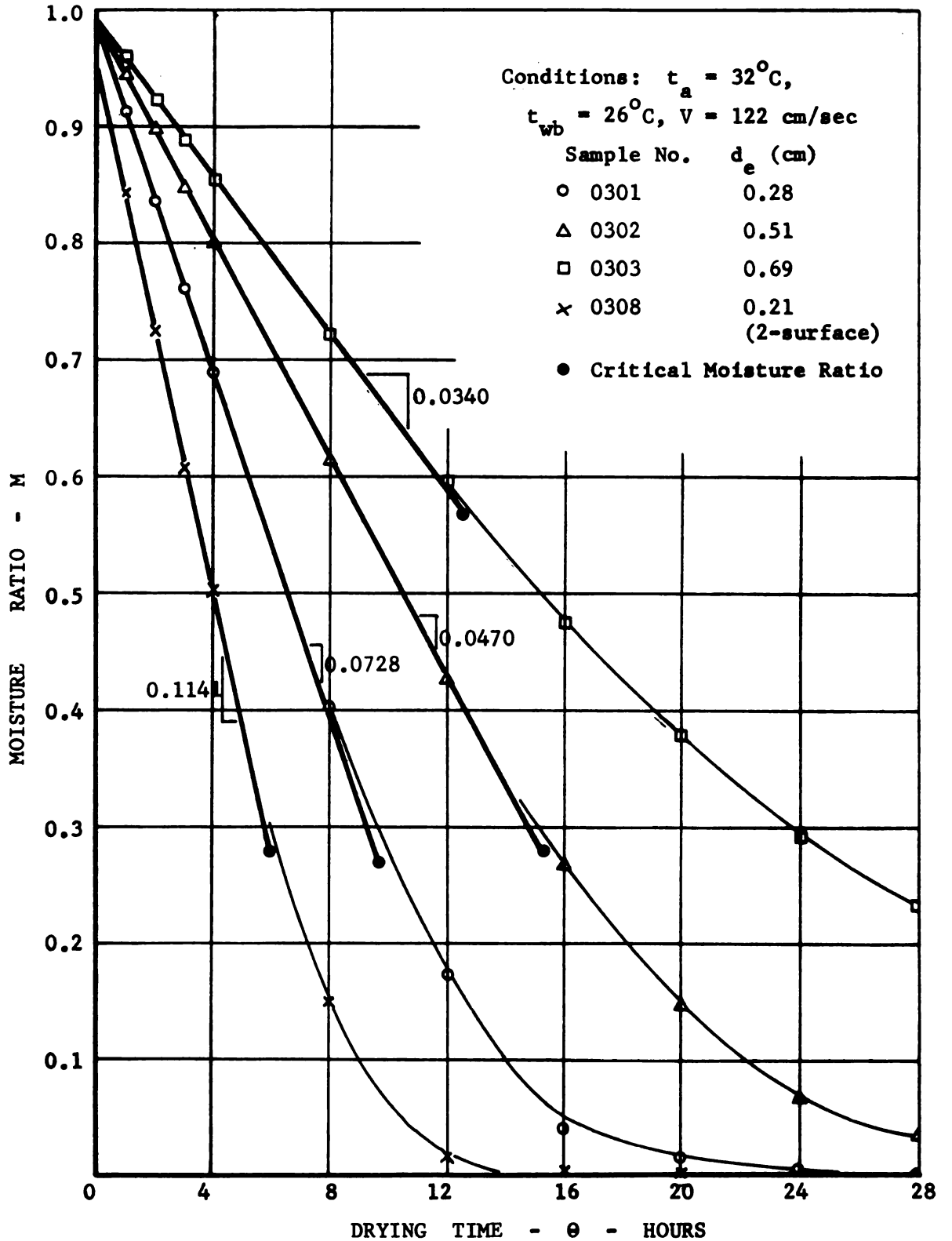

Figure 6.3 Drying curves for test-run 0300

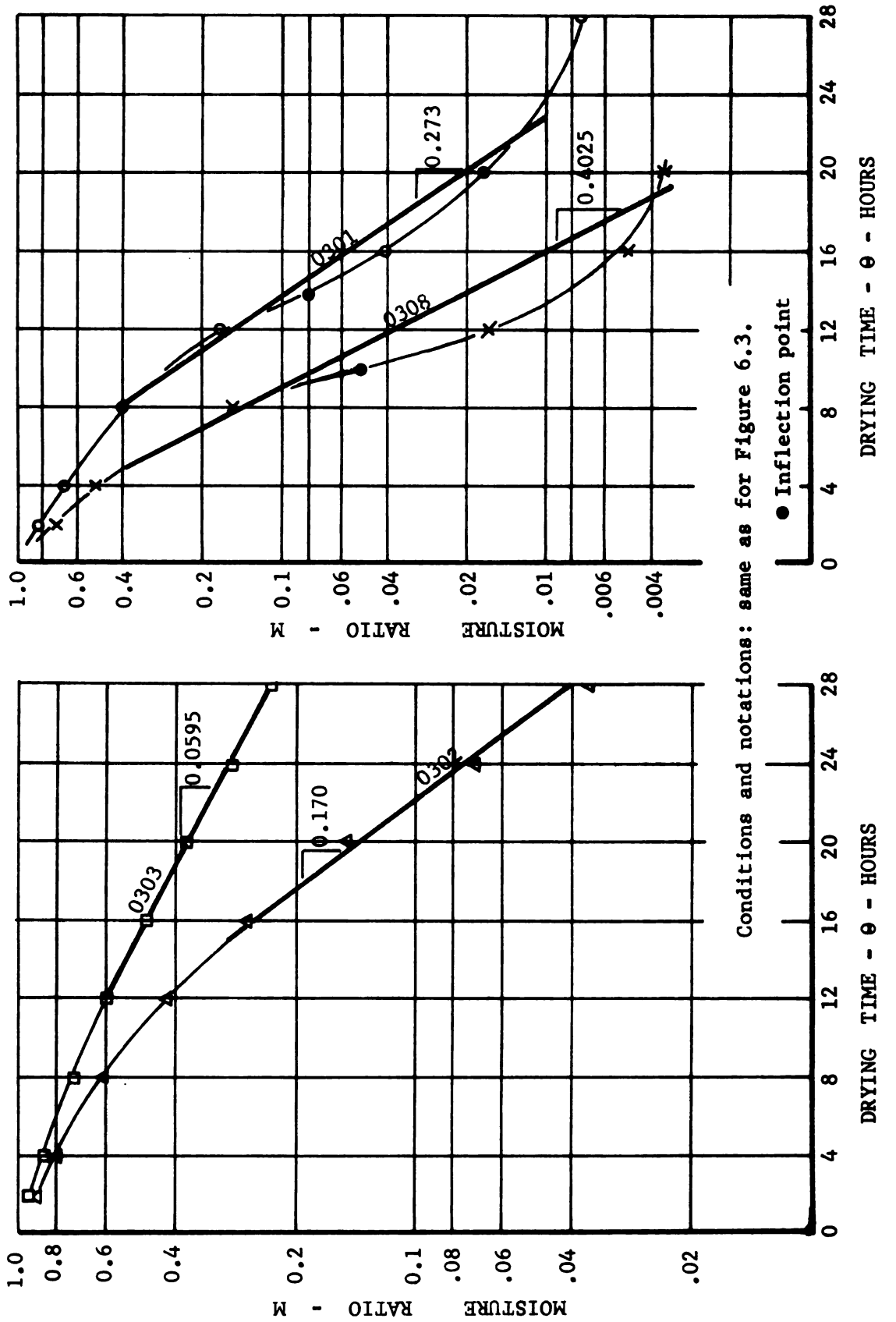

Figure 6.4 Semi-logarithmic drying curves for test-run 0300

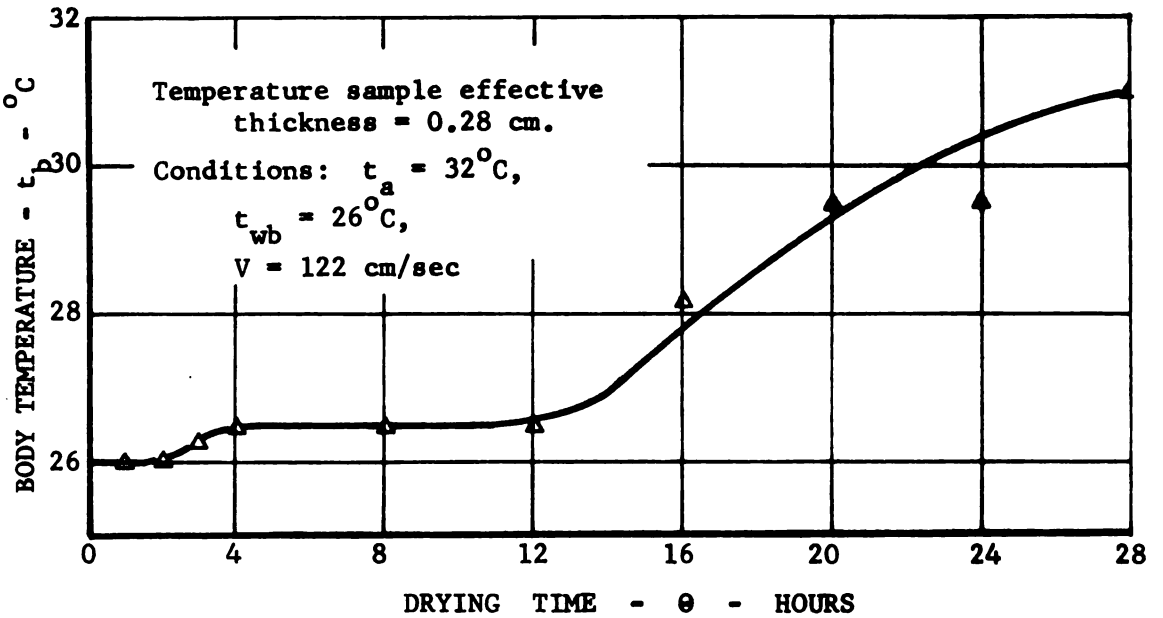

Figure 6.5 Sample temperatures for test-run 0300

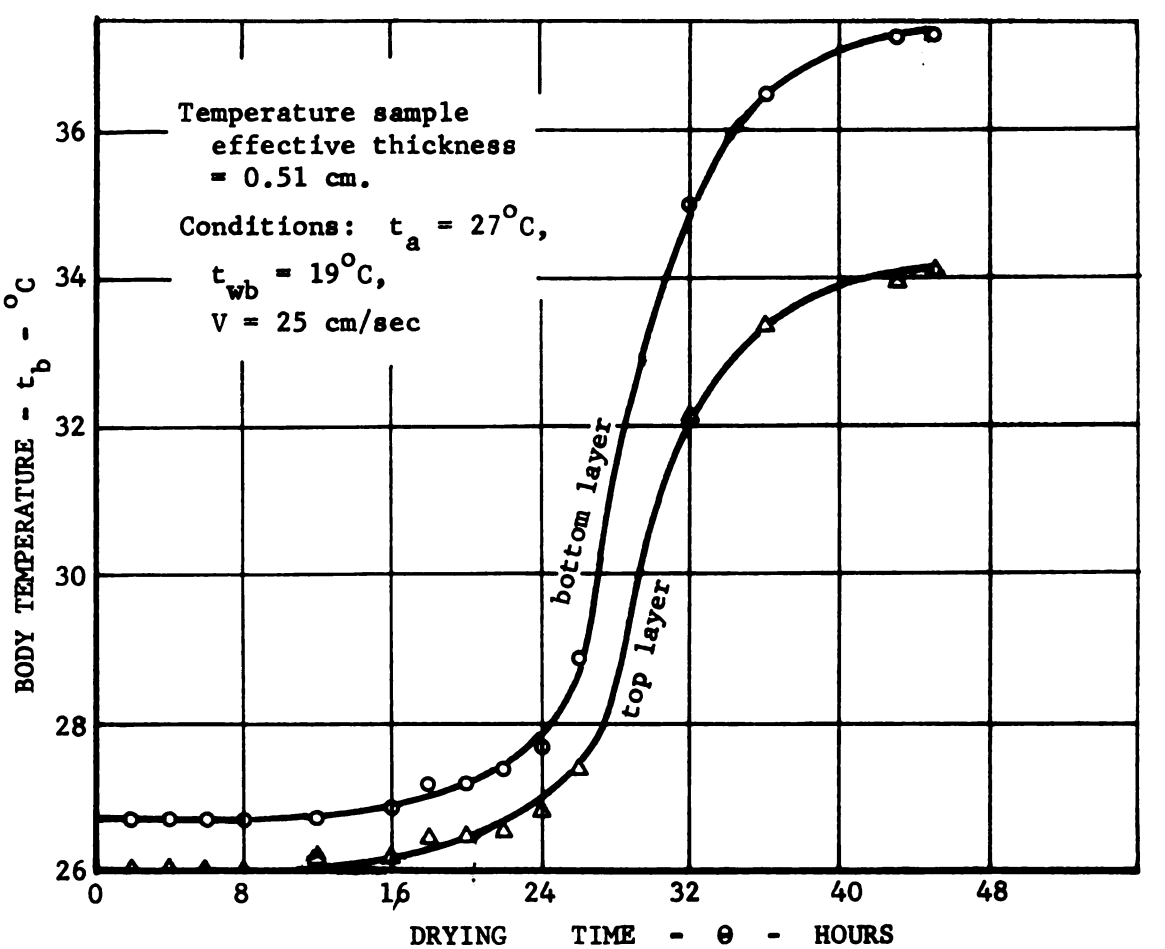

Figure 6.6 Heated sample temperatures for test-run 1000

Bias may result through the data recording time sequence relative to the beginning of the falling rate period or through undetected nonrandum measurement error. In some cases it is possible to combine data from more than one sample to improve on the reliability of the estimates. These are also noted.

Another minor limitation arose from the fact that, in order to shorten the time required for experimentation, most samples were not dried to equilibrium. Equilibrium moisture contents are assumed using the results reported by Sobel (1969). (See Figure 3.1) Low values of the moisture ratio, M, are extremely sensitive to small errors in equilibrium moisture content, but relatively insensitive to such errors at high values.

Immediately evident from Figures 6.1 and 6.3 is the presence of an initial period of constant rate drying, or at least a period that can be approximated by a constant rate model. Therefore, as suggested in previous chapters, the analysis for the initial period will be separated from the following falling rate period or periods. Determining the break or critical point between the constant and falling rate periods is a major problem.

Preliminary tests indicated that uncontrolled sample variability could cause as much as plus or minus five percent variation from the mean in drying rates. This variability becomes of primary concern in the analysis of the falling rate period because of its dependence on material characteristics.

6.2 Analytical Techniques

Drying rates for each sample were approximated by straight lines fitted to the drying data by the least-squares method. For the constant rate period this line was linear with respect to time and for the falling rate period the rate was assumed exponential with time (See Figures 6.2 and 6.4).

To relate the drying constants and rates to the independent environmental, process and material variables, multiple regression and least squares elimination procedures were used where other methods and theories could not be applied.

For all of the statistics calculated, it was assumed that the dependent variables are normally distributed random variables with (1) mean based on the value of the independent variables for each observation, (2) constant variance over all observations, and (3) independence between observations.

Michigan State University computer facilities as well as those of the Agricultural Engineering Department were used for these calculations. The Michigan State University Agricultural Experiment Station routines for the CDC 3600 computer were used extensively. The computer programs used are relatively straight forward.

6.3 Initial Drying Constants

The initial portion of the drying curves can be approximated very well by straight lines fitted by the least-squares method. There slopes are the bulk drying constants,

K_C, of the sample for the constant rate period. The initial portion of the drying curves are straight lines without correction for change in surface area, even though some volumetric change was observed during this period.

The regression equation is

$$M = A - K_C\theta \qquad (6.2)$$

The number of points used were determined by trial, using the standard error of estimate and confidence limits to indicate at what time the drying rate deviated significantly from constant. In most cases, the plotted data quite clearly indicated where the experimental measurements began to deviate from the initial straight line. It was a simple matter to calculate the linear regression using those points that fell on the line and check the correlation between the two variables. Then one additional data point was added to the number of observations used in the analysis and again the correlation checked. Often two calculations were sufficient to find significant deviation. The standard error of estimate did not exceed 0.005 and the confidence limits at the 95 percent level were well below plus or minus five percent of the estimated value in most cases.

At the beginning of the drying period, the moisture ratio is ideally equal to one. This point was not used in the analysis because of possible non-linear conditioning periods. In all cases, the first data point used occured between one and two hours after the beginning of drying. Even so, the

estimated straight line passed very close to one at zero time. Often, the value of one fell within the 95 percent confidence intervals of the estimated intercept.

These results are shown in Table B.3 for unheated samples and Table B.4 for heated samples. Ninety-five percent confidence limits are listed in column (5) in terms of percent of the calculated value recorded in column (4). In column (6) are the intercept values, A, of the regression analysis.

It should be noted here that although the correlation between the moisture ratio and time (better than .999) is very good, close examination of the regression equations, its intercept and slope, their conficence limits and change as data points are added one by one, indicate a very slight concave tendency. There is some evidence of a change in surface area by body shrinkage. However, the straight line estimate fits the data so well that the initial drying period will be considered constant without correction for surface area changes.

6.4 Initial Constant Drying Rates

To obtain the constant drying rates, equation 6.2 is differentiated with respect to time. The resulting rate equation for the constant rate period is

$$\dot{m} = -K_c(m_o - m_e) \qquad (6.3)$$

Dividing by the evaporative surface area gives the rate per unit area or dividing by the weight of solids in the sample,

m_s, gives the rate per unit solid. These two rates are listed in Table B.3 in columns (7) and (8) and in Table B.4 in columns (10) and (11) for the heated samples.

The rates per unit area are nearly the same for all sample thicknesses within any given run. Thinner samples tend to show rates less than the thicker because they are more affected by the hydrodynamic boundary layer of the test chamber walls. The theoretical thickness and the local velocities within this layer are calculated in Appendix A.1.

It was shown in Chapter 2 that surface evaporation rates from free water bodies are a function of convective transfer coefficients and a concentration potential difference. Combination of equations 2.9 and 2.19 gives the following relation between drying rate and the independent variables that effect drying during the constant rate period:

$$\dot{m}'' = \eta(V^{1-n}/D_c^{\,n})(P_a - P_s) \qquad (6.4)$$

Laminar flow over a flat plate with length equal to sample length will be considered first. The coefficients η and n are 25.0 and 0.5, respectively. The vapor pressure at the surface is assumed to be the saturated vapor pressure at 1/2^{o}C above the thermodynamic wet bulb temperature of the air.

This value of vapor pressure is selected for two reasons. First, experimental temperature measures indicated body temperatures approximately 1/2 degree higher than the measured wet-bulb temperature of the air during the initial drying period.

This, in itself does not demand that the surface temperature also be higher. However, surface heat and mass balance equations using the Colburn analogy to estimate the convective heat transfer as a function of the mass transfer coefficient, show a heat deficit. (See Appendix A.2 for details). It is assumed that there is either heat production within the body or that heat is conducted through the body, thus raising the average body and surface temperatures.

In Table 6.1 are shown the average evaporation rates per unit area for each run, the estimated value by laminar flow conditions as described above, and their difference. Even with the assumed surface temperature increase, the laminar flow estimation is almost always less than the experimental value. This is also true for the 2-surface samples suspended in the air stream and unaffected by the experimental chamber wall boundary layers.

For high mass transfer rates, the transfer coefficients depend on the mass transfer rate. Using methods outlined by Bird et al., (1965) it was found that the mass transfer rate was small enough not to affect the transfer coefficients as developed by the laminar boundary layer theory.

Because of the thickness of the sample and its blunt leading edge, there will be local regions of flow disturbances. The experimental values of the drying rates of the unheated samples are now used to evaluate statistically the coefficients

Table 6.1 Experimental and estimated laminar flow drying rates

Run Number	Average Value Experimental Rate ($gm/hr\text{-}cm^2$)	Estimated Laminar Flow Rate ($gm/hr\text{-}cm^2$)	Estimated Minus Experimental ($gm/hr\text{-}cm^2$)	Percent Difference Based on Experimental Value
0200	.0156	.0169	+.0013	8
0300	.0188	.0182	-.0006	3
0400	.0205	.0185	-.0020	10
0500	.0065	.0053	-.0012	23
0600	.0156	.0132	-.0024	16
0700	.0110	.0072	-.0038	35
0800	.0332	.0318	-.0014	4
0900	.0127	.0127	0	0
1000	.0108	.0090	-.0018	17
1100	.0092	.0092	0	0
1200	.0058	.0048	-.0010	23
2-surface samples				
0300	.0202	.0192	-.0010	5
0900	.0146	.0129	-.0015	10
1200	.0108	.0092	-.0016	15
samples with 8 inch length				
0304	.0192	.0182	-.0010	5
0501	.0054	.0053	-.0001	2
1104	.0087	.0092	+.0005	6

*cooled samples of test section 2

η and n. Only the first sample of each group listed in Table B.2 is used to avoid weighting in favor of those runs with repeated samples. The characteristic dimension, D_c, used is the path length of flow over the sample, that is the top length plus two times the thickness (two times one-half the thickness of the 2-surface samples). The vapor pressure at the surface is assumed as before. Velocity adjustments based on the calculations of Appendix A.1 are made for the 0.31 cm thick samples in runs 0200, 0300, 0400, 0800 and 0900. Rate differences of these runs with higher air velocities seemed to be more marked than those of lower velocities.

With these assumptions and adjustments, the parameters of equation 6.4 are calculated to be: $n = 0.6$ and $\eta = 55.6$. The multiple correlation coefficient of this estimate is 0.9637. The estimated results are tabulated in column (12) of Table B.3. In column (13) of this table are listed the percentage differences between the estimated and experimental values. The standard deviation of the differences is 9.27 and the 95 percent confidence limits are $\pm$ 20 percent of the experimental values.

The main conclusion of this section is that the initial drying of wet chicken excreta is controlled by environmental conditions and the rate can be predicted if the hydrodynamic boundary layer conditions and surface temperatures can be estimated.

6.5 Conducted Heat Sources and Utilization Efficiencies

Additional heat sources greatly increased the drying rates as is seen by comparison of the results of heated samples with non-heated samples. Under steady-state conditions, the summation of convective and conductive heat sources at the surface equals the latent heat required to evaporate the moisture being removed. In mathematical terms

$$h_c(t_a - t_s) + k(t_d - t_s)/d = h_{fg}h_D(p_s - p_v)RT \quad (6.5)$$

where p_s is a function of the surface temperature, t_s, and t_d is the temperature at distance d from the surface. The second term on the left hand side of this equation is the heat flow through the material and to estimate its value requires knowledge of several unknown factors.

Although the conductivity of wet excreta can reasonably be assumed approximately equal to that of water, heat flow estimation by temperature measurement is impossible because of the necessity for accurate sensor placement and response beyond that obtained in this experiment. The most reasonable estimate of heat input is obtained by calculating the electrical energy input and assuming conversion to heat evenly distributed over the hot plate with no heat loss through the floor of the test chamber.

Disregarding slight differences in density and moisture content, the only variable difference between the heated and

unheated samples is the heat input. Heat and mass balance for the unheated samples is

$$h_{fg}\dot{m}'' = h_c(t_a - t_s), \tag{6.6}$$

and with conductive heat input

$$h_{fg}\dot{m}''h = h_c(t_a - t_b) + Q \tag{6.7}$$

where t_b is the measured body temperature and also assumed to be the surface temperature of the heated sample. Q is the heat input as tabulated in Table B.1.

The ratio of heated to non-heated drying rates is then

$$\dot{m}''_h/\dot{m}'' = \left[(t_a - t_b)/(t_a - t_{wb})\right] + (Q/h_{fg}\dot{m}'') \tag{6.8}$$

Estimated drying rates of heated samples based on this equation are presented in Table 6.2. The estimates range up to 25 percent greater than the experimental values indicating that the original assumptions of no heat loss and uni-directional heat flow are not quite true.

A measure of the utilization efficiency of the additional heat input is the heat energy required to cause the observed increase in evaporation rate compared to the amount of heat ideally required to evaporate the same amount of water under the same environmental conditions. The utilization factor, U, in heat energy per unit weight may be stated as follows:

$$U = Q/\left[(h_c \ t/h_{fg}) + (Q/h_{fg}) - (h_D \ p/RT)\right] \tag{6.9}$$

In many cases, with moderate heating, the temperature difference

Table 6.2 Experimental and Estimated drying rates for heated samples

Run Number	Average Drying Rate No Heat (gm/hr-cm^2)	Average Drying Rate With Heat (gm/hr-cm^2)	Rate Ratio Heat to No heat	Estimated Drying Rate by Eq. 6.8 (gm/hr-cm^2)	Percent Difference
0200	.0156	--	--		
0300	.0188	--	--		
0400	.0205	.0305	1.5	.0370	+14
0500	.0065	.0222	3.4	.0236	+ 2
0600	.0156	.0312	2.0	.0428	+24
0700	.0110	.0161	1.45	.0180	+ 7
0800	.0332	.0472	1.4	.0607	+19
0900	.0127	.0339	2.7	.0389	+ 9
1000	.0108	.0184	1.7	.0222	+14
1100	.0092	.0226	2.5	.0251	+ 6

is nearly zero and the term, h_c t, is small relative to the other terms in the denominator. Thus

$$U \simeq Q/\left[(Q/h_{fg}) - (h_D \Delta p/RT)\right] \qquad (6.10)$$

The utilization efficiency, U_{eff}, in percent is

$$U_{eff} = (h_{fg}/U)100 \qquad (6.11)$$

In Table 6.3, the following results are shown: utilization factor of equation 6.10; the convective heat transfer coefficient, h_c, estimated by the Colburn analogy based on the experimental value of h_D for the non-heated samples of each run; the

Table 6.3 Utilization factors and efficiency

Run Number	Utilization Factor by Eq. 6.10 (cal/kgm)	Convective Heat Transfer Coefficient ($cal/hr\text{-}cm^2\text{-}^oC$)	Utilization Factor by Eq. 6.9 (cal/kgm)	Utilization Efficiency by Eq. 6.11
0400	1485	1.38	1350	43
0500	712	0.66	925	63
0600	950	0.58	907	64
0700	2480	0.58	1575	37
0800	1880	1.24	1270	46
0900	780	1.32	949	61
1000	1215	0.59	1150	50
1100	796	0.85	1004	56

utilization factor of equation 6.9; and the utilization efficiency. Discussion of utilization efficiencies will be continued in Section 7.6.

6.6 Analysis of the Falling Rate Data

As has been stated, the data did not show any distinct period during the falling rate drying process. On rare occasions, portions of the data did form a locus for a straight line on semi-logarithmic coordinates but, in general, the curves were

S-shaped as clearly shown in Figures 6.2 and 6.4 Indications are that for complete drying analysis, more than one falling rate drying constant is needed. Only one will be considered here to estimate the falling rate drying period between the critical moisture ratio and a moisture ratio of approximately 0.1.

As pointed out in Section 4.4, falling drying rates for thin layers frequently can be expressed in terms of the mean moisture content of the layer as follows

$$\dot{m}_f = (dm/d\theta')_f = -K_f(m - m_e) \qquad (6.12)$$

The falling rate time, θ', is the total drying time minus the time at which the falling rate period began.

Integration of equation 6.12 leads to an equation describing the drying curve in terms of moisture ratio:

$$M = M_{cr} \exp(-K_f\theta') \qquad (6.13)$$

Regression equations of this type approximated the falling rate data with fairly high correlation.

All experimental falling rate data was used to estimate the falling rate drying constant, K_f. Deleted were those points beyond the inflection point (see Figures 6.2 and 6.4) that greatly reduced the correlation between the moisture ratio and time.

The 95 percent confidence interval of the drying constant, K_f, is given in terms of its estimate in column (5) of Table B.5. Even though some of these intervals seem relatively

large, examination of the curves (see, for example, figure 6.4) suggest that this is not due to random measurement errors and that, at least qualitatively, the estimate can be considered meaningful. The fact is that a linear estimate is being made of what is in reality non-linear.

A more serious limitation insofar as general model development is concerned is the fact that the relative segment of the falling rate drying curve being estimated by linear regression varies from sample to sample. This can be seen by comparing the drying curves of samples 0303 and 0301 in Figure 6.4. The observations of sample 0303 cover only the beginning of the falling rate period while those of 0301, although limited in number, cover the entire period. The true falling rate drying constant of 0303 may be somewhat different from the estimated value even though the correlation of those observations available are good. Those samples that did not reach a moisture ratio of 0.1 by the end of the test-run are marked with an asterisk to the right of Table B.5.

Upper and lower values of confidence at the 95 percent level are given for the estimates of the moisture ratio at critical time (see next section for method of calculation) and at the time of the last ovservation used in the analysis, which in some cases is also the last observation of the test-run. These are tabulated in Table B. 5 in columns (8) and (9), and (13) and (14), respectively. If the lower limit is negative, zero is tabulated because, physically, the moisture

ratio will not be less than zero if the equilibrium moisture content has been assumed or calculated correctly. The confidence band over the midrange of the analysis will be less than at the two end points so that what is tabulated is the worst situation for each sample.

As much as 84 percent of the variation in the falling rate constant can be accounted for by the variation in the constant rate drying constant. For 24 estimates under adiabatic conditions

$$K_f = 0.12 + 3.2\ K_c - 0.25\ d_e \qquad (6.14)$$

with a multiple correlation coefficient of 0.938. For the 18 estimates with added heat input

$$K_f = 0.25 + 3.8\ K_c - 0.37\ d_e \qquad (6.15)$$

with a multiple correlation coefficient of 0.966. Including the variable of heat input did not improve on this correlation. These relations and their significance will be discussed in Section 7.4.

6.7 Critical Moisture Ratios and Time

Continuity is assumed between the constant and falling rate periods. Thus, at critical time, $\theta = \theta_{cr}$, the falling drying rate, $\dot{m}''_f$, must be equal the constant drying rate, $\dot{m}''_c$. Setting equation 6.12 equal to equation 6.3 and substituting m_{cr} for m, gives

$$-K_c(m_o - m_e) = -K_f(m_{cr} - m_e) \qquad (6.16)$$

From this it can be seen that the ratio of the constants are equal to the critical moisture ratio:

$$M_{cr} = (m_{cr} - m_e)/(m_o - m_e) = K_c/K_f \qquad (6.17)$$

The critical time, θ_{cr}, is calculated by rearranging equation 6.3 and setting $M = M_{cr}$:

$$\theta_{cr} = (1 - M_{cr})/K_c \qquad (6.18)$$

The critical values calculated by this method can be found in Table B.5. They do not affect the falling rate constant if the same data are used for the estimation of K_f, but they do affect the upper and lower limits of moisture ratio confidence intervals and thus, are necessary for the compilation of Table B.5.

The assumption is that the constant rate period ends when the moisture content at the surface reaches a specific value. Since the critical moisture ratio is the average through the material, its value depends on the rate of drying, the thickness of the material, and the factors influencing moisture movement and resulting gradients within the solid. As a result it is to be expected that the critical moisture ratio increases with increased drying rate and with increased thickness of the mass of material being dried.

The drying rates of the adiabatic drying situation do not cover a sufficiently broad range to significantly change the critical moisture ratio within the sensitivity of this experiment. The critical moisture ratio could only be related to the thickness as follows:

$$M_{cr} = 0.68\ d_e \qquad (6.19)$$

where the multiple correlation coefficient is 0.826.

In the case of the heated samples, surface temperatures are higher resulting in increased drying rates. But heating also increases the material temperatures and temperature gradients within the body, thus increasing the rate of internal moisture movement. The overall result is an increased amount of moisture removed at the constant rate, lowering the critical moisture ratio. However, no correlation could be made with any of these variables. The presence of conducted heat input did lesson the effects of depth, however, as indicated by comparing the following relation for the heated samples with equation 6.19.

$$M_{cr} = 0.1 + 0.19\ d_e \qquad (6.20)$$

The multiple correlation coefficient for equation 6.20 is 0.925.

To determine the critical time from the relation of continuity rather than the critical moisture ratio, such as:

$$A \exp(-K_f \theta_{cr}) = 1 - K_c \theta_{cr} \qquad (6.21)$$

(where A is the exponential moisture ratio intercept at drying time of zero), in many cases resulted in an initial falling rate higher than the constant rate because of the inexact determination of the falling rate constant. The critical time solution determined by trial, (the left hand side of the above equation is not linear), resulted in two, one or no solutions depending on the pre-calculated values of the drying constants.

Table B.6 summarizes the estimated drying constants and critical ratio by sample thickness and rank of the constant

rate drying constant from low to high values. Environmental variables are also included for convenience.

Because of the method of development, this model will slightly underestimate moisture ratios during the transitional period from the constant to falling rate periods by over extending the constant rate time period. This is illustrated graphically for a typical sample in Figure 6.7. The experimental data are plotted, and the falling rate estimate and confidence limits of the estimate are shown. The error of the estimate during the transitional period reaches a maximum at the critical time and decreases as falling rate drying progresses. The estimated experimental value (estimated because experimental data are seldom recorded at the exact critical time) is shown in the last column of Table B.6 beside the estimated critical moisture ratio in column (13). Greater error usually occurs with the more rapid drying situations. A difference of 0.01 in the moisture ratio represents approximately one percent difference in percent moisture content for the experimental sample sizes and less than five percent estimated error in total moisture removed.

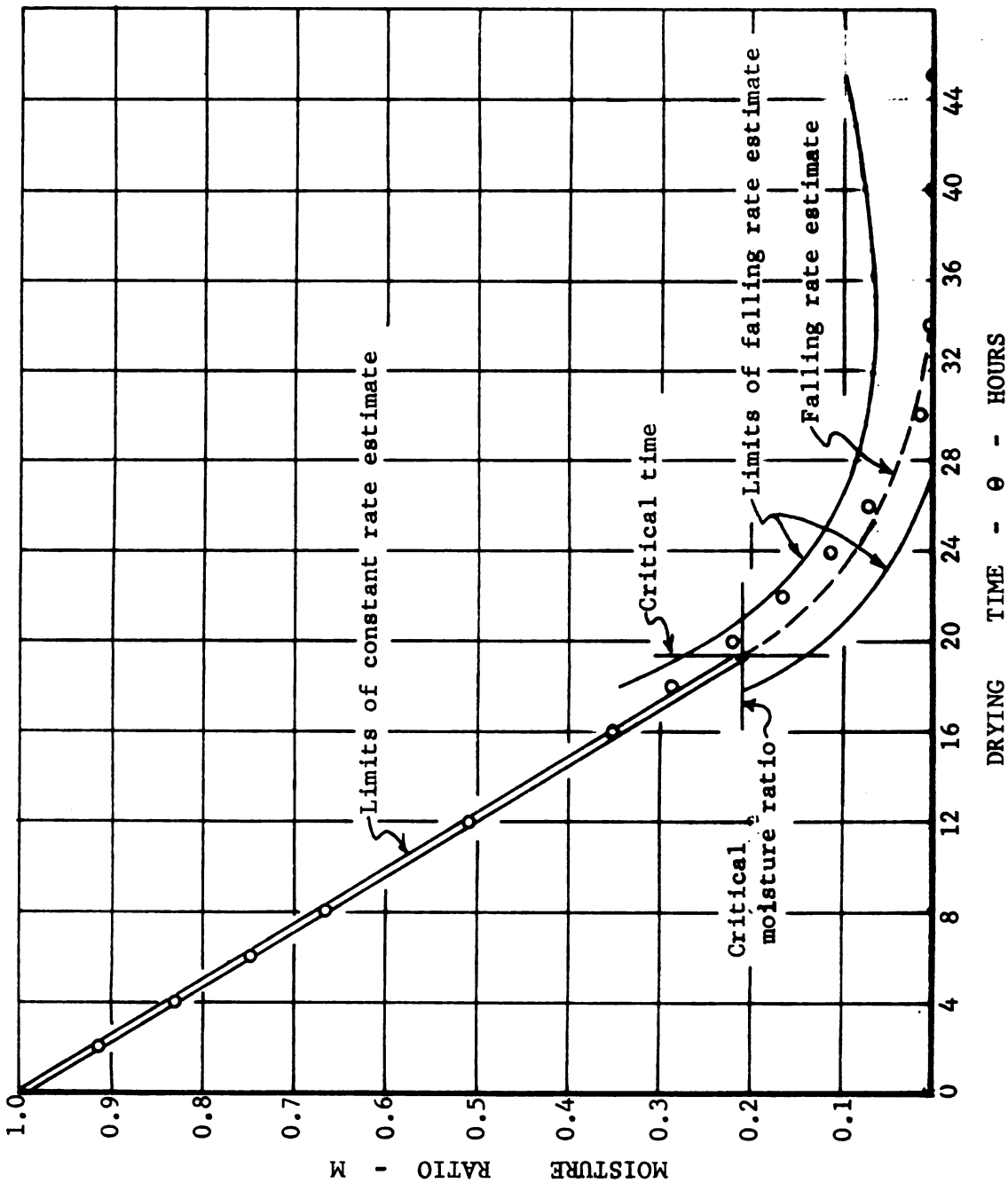

Figure 6.7 95 percent confidence limits of estimate for sample No. 1003

7. DISCUSSION OF METHODS AND RESULTS

7.1 Drying Rates as a function of Time and Moisture Content

The process of complete drying of fresh chicken excreta was expected to be complex. However, large portions of moisture are removed by the relatively simple process of constant rate drying because of the extremely high initial moisture contents and because a large portion is free (non-hygroscopic) moisture.

It was shown in the previous chapter that the falling rate can be estimated as a linear function of the moisture content of the material. Figure 7.1 graphically shows the drying rates as a function of time and moisture ratio as derived from the analysis of Chapter 6. Average constant rate values are used for the run. The experimental data points are estimated by

$$\dot{m}''_f = K_f(m_o - m_e)\, M/A_s \qquad (7.1)$$

where the moisture ratio M is the experimental value and K_f is the falling rate constant of Table B. 6. There is some descrepency between the solid curves and experimental data points because the curves are based on average values for the run and the points are calculated using individual sample data.

The slopes of the falling rate portion of the right hand drying curves are: $K_f(m_o - m_e)/A_s$, so that the falling rate equation 7.1 applies. This is equivalent to equation 6.12,

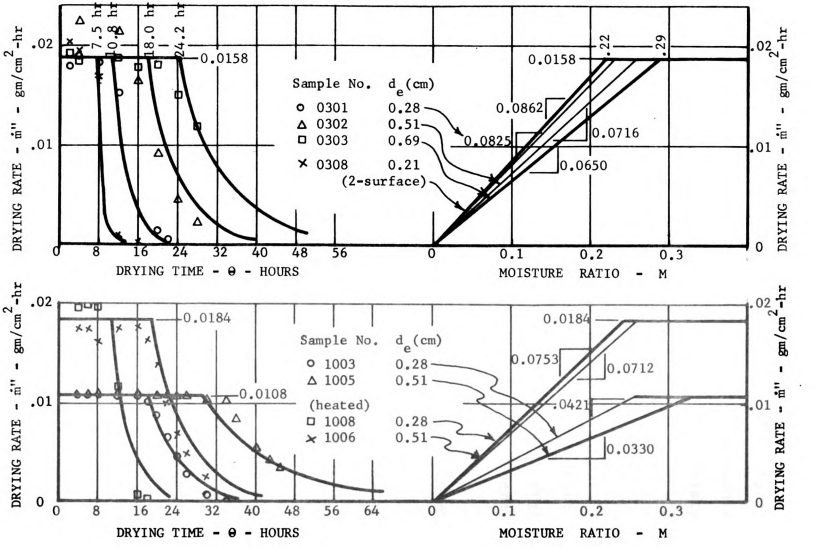

Figure 7.1 Estimated drying rates for runs 0300 and 1000

namely, $\dot{m}_f = -K_f(m - m_e)$. Note that this is a linear relation with zero intercept because the equilibrium moisture content, m_e, is chosen to be the final dried moisture content. This relation then assumes zero drying rate at zero moisture ratio and precludes any secondary falling rate period.

A more general expression would be

$$dm/d\theta = K_f(m - m_1), \tag{7.2}$$

where m_1 is the moisture content at zero drying rate if the material continued drying at the same rate (with drying constant K_f) and would be different from m_e if there were secondary falling rate drying periods.

Writting equation 7.2 in terms of equilibrium moisture content and moisture ratio gives

$$dm/d\theta = K_f(m_o - m_e)(M - M_1) = K_f(m_o - m_e)M - \dot{m}_1 \tag{7.3}$$

where $M_1 = (m_1 - m_e)/(m_o - m_e)$ and $\dot{m}_1 = K_f(m_o - m_e)M_1$. Graphically, the situation is sketched in Figure 7.2 The critical moisture ratio would then be adjusted by the amount M_1. This would allow for a second falling rate period, but since the experiment was not aimed at distinguishing falling rate drying periods, no values are available to estimate the necessary adjusting parameters.

The selection of equilibrium moisture content as the lower limit of the falling rate drying period could effectively be used within the range of analysis because most of the moisture ratios are little affected by small changes in the selected value of the final dried moisture content.

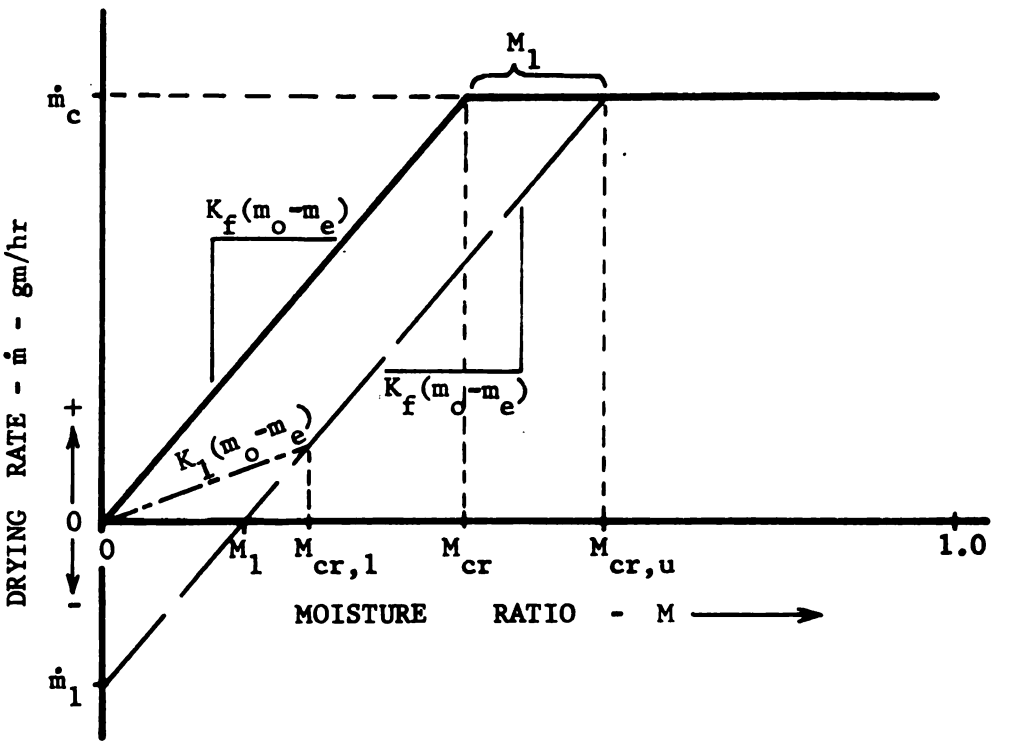

Figure 7.2 Critical moisture ratios with more than one falling rate period

7.2 Factors Influencing Rate of Drying

a. Temperature, Humidity, and Air Velocity

The most important single factor correlated with constant rate drying is the absolute humidity or wet-bulb depression of air flowing past the wet surface (Van Arsdel, 1963). The drying rate is a function of the vapor pressure differential and if the air is saturated, no drying can take place by convection. The saturated vapor pressure is a function of the absolute temperature while the partial vapor pressure of the air is, by definition, its saturated vapor pressure times the relative humidity (Brooker, 1966).

In Figure 7.3, the constant drying rates for the ten experimental conditions are plotted against the wet-bulb depression. Only two points at any one condition of constant velocity and ambient air temperature are available. Although the psychrometric relation between vapor pressure difference and wet-bulb depression at different ambient air temperatures are not exactly linear, it is nearly so within the narrow range of these tests and straight lines are drawn through those points of similar experimental velocity to clarify their possible association.

The wet-bulb depression is a very simple measure of the drying potential of the stream of air, but has little effect on the falling rate period where internal diffusion rates are controlling. It is, in the main, a surface phenomena. The material temperature has the most affect on the localized vapor potential within the body during the falling rate period. It has been shown that for similar hygroscopic materials the critical break points between surface and internal evaporation at different temperatures of the substance can be predicted according to the change in ratio of surface tension to the viscosity of the liquid of the product (Gorling, 1963). In this research there is insufficient evidence to indicate what the temperature effects are except to note that the heated samples did exhibit lower critical moisture ratios. However, this may have been caused by the temperature gradient rather than the sample temperature, per se.

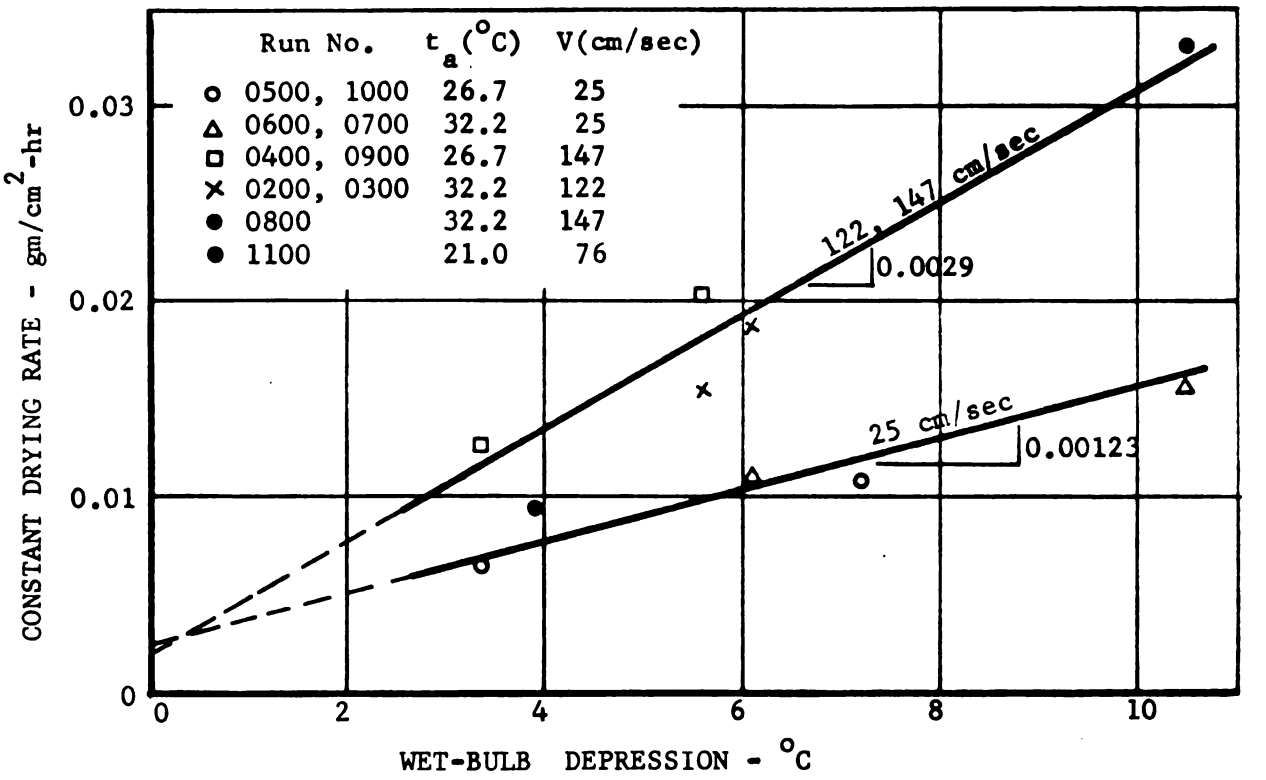

Figure 7.3 Influence of wet-bulb depression on constant rate drying

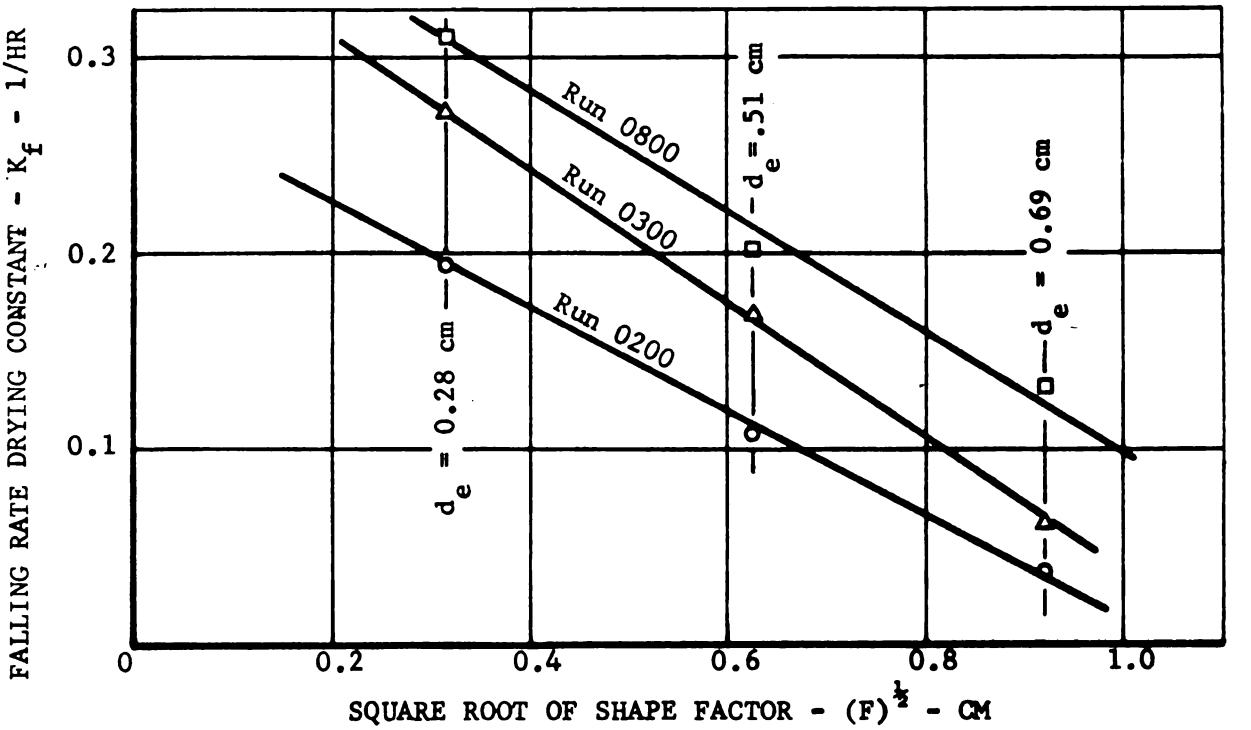

Figure 7.4 Influence of thickness on falling rate drying

In the low moisture range, drying is so slow that the cooling effect of evaporation is inappreciable and the material assumes very nearly the dry-bulb temperature of the air as shown in Figure 6.5. The internal redistribution of moisture, which is the rate determining factor at this stage, is accelerated by a rise of the material temperature.

Free stream air velocity affects the constant drying rate through its hydrohynamic effects on heat and mass transfer. These effects have been demonstrated to be a fractional exponential function of velocity. For laminar flow, it is a function of the square root of the velocity. In such a case, an increase of velocity by 4 times should double the drying rate. This is roughly the case as shown in Figure 7.3 even though pure laminar boundary flow was not attained in the experiment. The velocity associated with the upper line is approximately 5-6 times that of the lower and the slope is approximately the square root of 5 times that of the lower.

That the velocity, as well as the wet-bulb depression has some combined affect on the falling rate period because of larger heat transfer coefficients is demonstrated by the close correlation of the constant and falling rate drying constants. However, the real controlling factors of falling drying rates are those that control the rate of moisture movement to the surface. It is prophesized that further

analysis would indicate that of the three environmental factors only ambient air temperature, as it affects body temperature, will affect falling rate drying.

b. Material and Process Factors

Of the many possible factors associated with the biological and physical material characteristics, and sample size and shape, only the thickness and the ratio of volume to evaporative surface area were studied in any detail.

The rate of drying per unit area is a function of the environmental factors and thus the rate of drying per unit dry solid is a function of how much surface area can be exposed to the drying air. For a given mass of material, an increase in surface area also decreases the internal path length the moisture must traverse to reach the surface. Thus, not only is the rate per unit mass increased, the moisture content at the critical level is decreased, or in other words, the amount of moisture removed at the faster constant drying rate is increased. Exposing both surfaces of a mat of material to the drying air as was done in three experimental runs by suspending samples on wire screens, effectively doubled the rate of moisture removal and also decreased the critical moisture ratio.

By referring to Figures 6.1 and 6.3, it will further be noted that drying time varies approximately inversely as the thickness. This is true for most of the falling rate period

as well as the constant rate period. In situations where internal vapor diffusion is the controlling drying mechanism, the rate varies inversely as the square of the thickness and it would take nine times as long to dry a sample three times as thick to the same moisture content (Van Arsdel, 1963). The linear relation of falling rate constants to the thickness is illustrated in Figure 7.4.

Supplemental conductive heat sources will be discussed in more detail in a later section, but it will be noted here that drying rates are increased by increasing the material and surface temperatures. During the constant rate drying period the increase in surface temperature increases the vapor pressure potential difference, as the partial pressure of the air remains the same. Internal moisture movement is increased not only through increased material temperature, but also due to an increase in the temperature gradient across the body. It has been shown by several researchers (Cary and Taylor, 1962; Luikov, 1966; among others) that liquid phase moisture diffusion is affected by thermal gradients as well as by concentration and pressure gradiets. Luikov also states that liquid transfer by means of selective diffusion such as an osmotic pressure gradient is a function of moisture content and temperature.

7.3 Volumetric Shrinkage, Shrinkage Water and Stresses

Chicken excreta contains a high percent of shrinkage moisture, moisture that results in body shrinkage when removed. However, the rate of shrinkage apparently is not directly related to the rate of moisture removal during the constant rate drying period. This is shown by the simple fact that a bulk constant drying rate does exist without adjustment for volumetric and surface area changes. Considerable amounts of moisture are evaporated before any apparent change in drying rates are noted. For example, one calculation predicted a 35 percent surface area change (see Appendix A.3) if the sample should shrink in proportion to the amount of moisture removed during the constant rate period. Volumetric changes of this magnitude were not observed during the constant rate drying period.

There are two possible explanations for this phenomena. The first is that as water is evaporated, the mean pore diameter decreases through surface shrinkage and structural changes resulting in an increase in the osmotic and capillary moisture potential in the surface layers. Water is drawn from interior regions of lower moisture potential leaving air pockets. If the liquid threads remain continuous throughout the drying period, most of the non-hygroscopic water will be removed by surface evaporation.

The second possible reason that little shrinkage occurs during this period is that water is "manufactured" through biological and enzimatic breakdown of the fats and starches

present in the material. There is no data to support this statement because there is no measurable difference in the calculated moisture content of samples dried quickly and those dried slowly.

Part of the change of drying rate during the early part of the falling rate period is because no correction is made for reduction in evaporative surface area through shrinkage. The real beginning of the falling rate drying period cannot be determined until accurate measurements of shrinkage rates are made. Surface area change does not account for the entire falling rate phenomena, however.

In addition to the associated surface area changes, shrinkage creates stresses causing surface cracks to form. Shrinkage stresses are discussed more fully in Section 3.2b and by Gorling (1958). It is to be noted here that the first signs of surface fissures and cracks did not appear until near the end of the constant rate drying period. This would indicate that steep moisture gradients did not develop until near the beginning of the falling rate process. In addition, thinner samples developed many hair line cracks while the thicker samples formed fewer but wider cracks as drying progressed. This would indicate steeper moisture gradients in the thinner samples.

It might be asked, does cracking expose new evaporative surfaces to compensate for the volumetric shrinkage such that apparent constant bulk drying rates are maintained? Probably

not, because these cracks are at first so small in width that moving air does not penetrate and moisture would have to diffuse in the vaporous form through still air, or affectively through a thicker boundary layer. This was demonstrated with one sample (#1001) in which were scored V-cuts the thickness of the sample and approximately 1/4 cm wide at the surface at the beginning of the test. The increase in exposed surface area was nearly 10 percent, yet the bulk drying constant was not significantly different from the unscored counterparts.

Further research involving drying, associated shrinkage rates and linear shrinkage coefficients are needed to further the understanding of drying of chicken excreta.

7.4 The Falling Rate Drying Constant and Internal Diffusion

During the falling rate period, evaporation may be at or near the surface or it may occur below the surface. The relative resistance to the movement of water and heat through the surface gas film and through the solid determines the position of evaporation. Thus, if liquid water moves easily through the solid and the rate of evaporation is low, the water will be able to equalize throughout with only a small concentration gradient within the drying material, and evaporation will take place mainly near the surface.

The falling rate constant is highly correlated to the initial drying constant indicating that the surface film

resistance still plays a part in limiting drying rates. That this is so is not surprising considering that the raw data are weighted in favor of the early phases of drying and that the material still contains large amounts of non-hygroscopic water at the beginning of the falling rate period.

That falling rate drying has not reached the stage where internal diffusion rates are the sole controlling factor is shown by the relation of the drying constant, K_f, to the shape factor, F. As shown in Section 3.1c K_f will equal $\pi^2 D_e F/4$ if the medium is considered isotropic and the diffusion coefficient, D_e, constant. The drying constant is not a linear function of F but rather of the square root of F, or if the dimensions of a and b are much larger than d, a linear function of the inverse of thickness, 1/d. This linearity is shown graphically in Figure 7.4.

The temperature difference between the top and bottom of the sample will help indicate whether or not the plane of evaporation is retreating within the material (Gilliland, 1938). If the evaporation continues to take place at the surface, the resistance to heat transfer will be largely in the film layers around the body and the temperature difference across the body will remain essentially constant. Sample temperatures are shown in Figures 6.5 and 6.6 for a heated and unheated case. The adiabatic unheated sample showed no significant temperature difference across the body thickness. The heated sample showed nearly constant differences until near the end

of the drying process. Because of the limited sensitivity and relative size of the sensors, this does not conclusively support the hypothesis of surface evaporation during the initial stages of the falling rate period, but does suggest the probability.

Although there is insufficient data with which to examine the mechanisms of internal moisture movement, it appears that the so-called falling rate period dealt with in this study is largely transitional in nature, the true limits being the upper and lower critical moisture ratios of the transition period as defined in Section 3.1a. At the upper critical point, surface shrinkage begins to have an effect. Dry patches begin to show on the surface in the form of surface cracks. In these regions, the funicular state (Harmathy, 1969) begins to break down, greatly reducing moisture mobility. Over the remaining surface regions, constant surface evaporation rates continue.

The scope of this research does not warrent a discussion of the falling rate period in great detail. Owing to the lack of raw data, the rate data obtained for this period cannot be considered equally reliable as those obtained for the constant rate period and further data are desirable before an accurate analysis is attempted. However, indications are that large proportions of the non-hygroscopic water are removed from the material by the time the lower critical point is reached where the internal moisture movement takes place predominately

in the gaseous phase. This is particularly true for thinner drying layers of the material.

7.5 Some Comparisons with Drying Rates in Existing Housing Units

Esmay and Sheppard (1971) recently reported results of their research involving in-house drying of poultry droppings. Some of the data from that report are used to evaluate the possibility of extending the methods of drying analysis of Chapter 6 to cover the more general case of existing drying situations. Several assumptions must be made regarding the environmental conditions in the pit area.

It immediately becomes apparent that not enough is known about the boundary layers along the surface of the droppings. Surface roughness, mean path length of surface flow and fluctuations in flow patterns caused by obstructions in the house favor turbulent boundary layer development. On the other hand, extremely low velocities support thick laminar boundary layers. In any case, undulated surfaces and wet and dry regions would preclude uniform boundary layer development and transfer rates. A measure of the mean mass transfer film thickness is needed, based on some simple measure of free stream air movement and possibly, some measure of surface roughness.

Esmay and Sheppard reported summer removal rates of 95 grams of water per hen-day (4 gms/hen-hr) which converts to 0.0128 gm/hr-cm^2 where the population density is 3 hens per

929 cm^2 (1 square foot). Assuming a vapor pressure differential of 0.068 atm (0.1 psi) and a room temperature of 26-1/2°C (80°F), the convective mass transfer coefficient for the above drying rate is 43 cm/min (85 ft/hr).

Summer ventilation rates are 132 m^3/min (4650 cfm) through a room with cross-sectional area of 21.4 m^2 (320 ft^2). Velocities beneath the cages are assumed to be three times the room average. The result of 30.8 cm/sec (60 ft/min) is of the same order of magnitude as those reported by Lilleng (1969). Under these conditions, the transfer coefficient of 43 cm/min is approximated by laminar flow conditions over a 10 cm (4 in) smooth surface. On the other hand, if the pit surface area is assumed saturated over its entirety and the mean path length is assumed to be the width of the pit (122 cm or 4 ft), there would be turbulent transfer conditions with a mean coefficient of 71 cm/min. Assumption of laminar transfer would decrease the transfer coefficient to 13 cm/min. This would indicate that neither pure laminar or turbulent flow conditions can be assumed. This analysis completely neglects the random dropping patterns and the possibility of initially faster drying rates followed by slower falling rate periods.

Total production of excreta was reported to be 220 grams per hen-day. At a density of approximately one cc per gram, this would cover 310 cm^2 (1/3 ft^2) approximately 0.95 cm

(3/8 in) deep. At 88 percent initial moisture content, 26.5 grams are dried solids and 3-5 grams of moisture are not removable under these drying conditions. With these conditions the constant rate drying constant, K_c, is 0.0208/hr. It would take 48 hours to dry to equilibrium at a constant rate. The estimated critical moisture ratio is 0.5. The constant rate drying period would last 24 hours and the moisture content at the end of this period would be 78-1/2 percent wet basis, approximating the reported values of moisture content in dropping pits during the summer.

The initial drying rate of 0.0128 gm/hr-cm^2 is matched by test-runs 0700 (V = 25 cm/sec, t_a = 32°C), 0900 (V = 147 cm/sec, t_a = 26-1/2°C) and 1000 (V = 25 cm/sec, t_a = 26-1/2°C), of which only run #1000 closely matches the above in-house environmental conditions. In run 1000, the wet-bulb depression is 7.3°C (13°F), the relative humidity 52 percent, and the vapor pressure differential at the saturated surface 0.0544 atm (0.08 psi). Although direct comparisons cannot be made, indications are that a prediction model of this type does have potential in predicting in-house drying providing a mean boundary layer thickness or convective transfer coefficient can be determined for each particular housing situation.

Because of the lack of fresh, wet-weight fecal production figures, similar calculations could not be made for winter conditions. Increases in moisture removal rates with heating panels are discussed in the next section.

7.6 Utilization Rates of Energy Inputs

The rate equations indicate the following five alternatives available for increasing drying rates and decreasing drying times: (1) increase air temperatures, (2) increase wet bulb depression (decrease humidity), (3) increase the air flow rate, (4) increase material evaporative surface area (decrease effective depth), and (5) increase evaporative surface temperature through material heating. There is little opportunity to use the first two alternatives to advantage as there limits are narrowly determined by environmental conditions required for optimum production.

Opportunity for increasing the air velocity is also somewhat limited unless the pit area is deep and the air flow can be partially confined to this region. However, local increase of the circulation rate without increasing ventilation rates would be quite beneficial.

Increasing the evaporative surface area would be very effective for decreasing drying times. The initial rate per unit area remains constant but the amount of moisture removed from a given mass of material is directly proportional to the surface area. Not only is the bulk drying rate greater, as seen in Figure 6.3, but generally lower moisture contents are reached before the falling rate period begins as indicated by the discussion of critical moisture ratio in Section 6.7.

This simple alternative does require rather complex handling systems to maintain thin layers. Energy inputs are required for whatever scraping, mixing and handling called for. Stirring the bed to expose new surfaces without breaking up the structure of the conglomerate masses would not be of much help as long as all surfaces are saturated. However, chickens confined to cages will tend to concentrate their droppings near the center of the floor area beneath. Stirring will spread the wet surfaces more uniformly over the pit area. Esmay and Sheppard (1971) reported that approximately 10 percent more moisture was removed from areas with once a day stirring over those without any.

The final alternative to increasing drying rates is the addition of heat sources. Conductive heat panels beneath the manure are considered here.

King and Newitt (1955) studied drying of granular materials with heat transfer by conduction. An initial constant drying rate was observed, the rate of evaporation largely determined by the flow of heat through the material. Since the heat conductivity of the material is a function of its moisture content, decreasing as the bed dries, the flow of heat will gradually diminish, resulting in a progressive reduction in drying rates.

The increase in drying rate due to conducted heat is a complex function of existing environment conditions and rate of heat input. Figure 7.5 shows the heat utilization

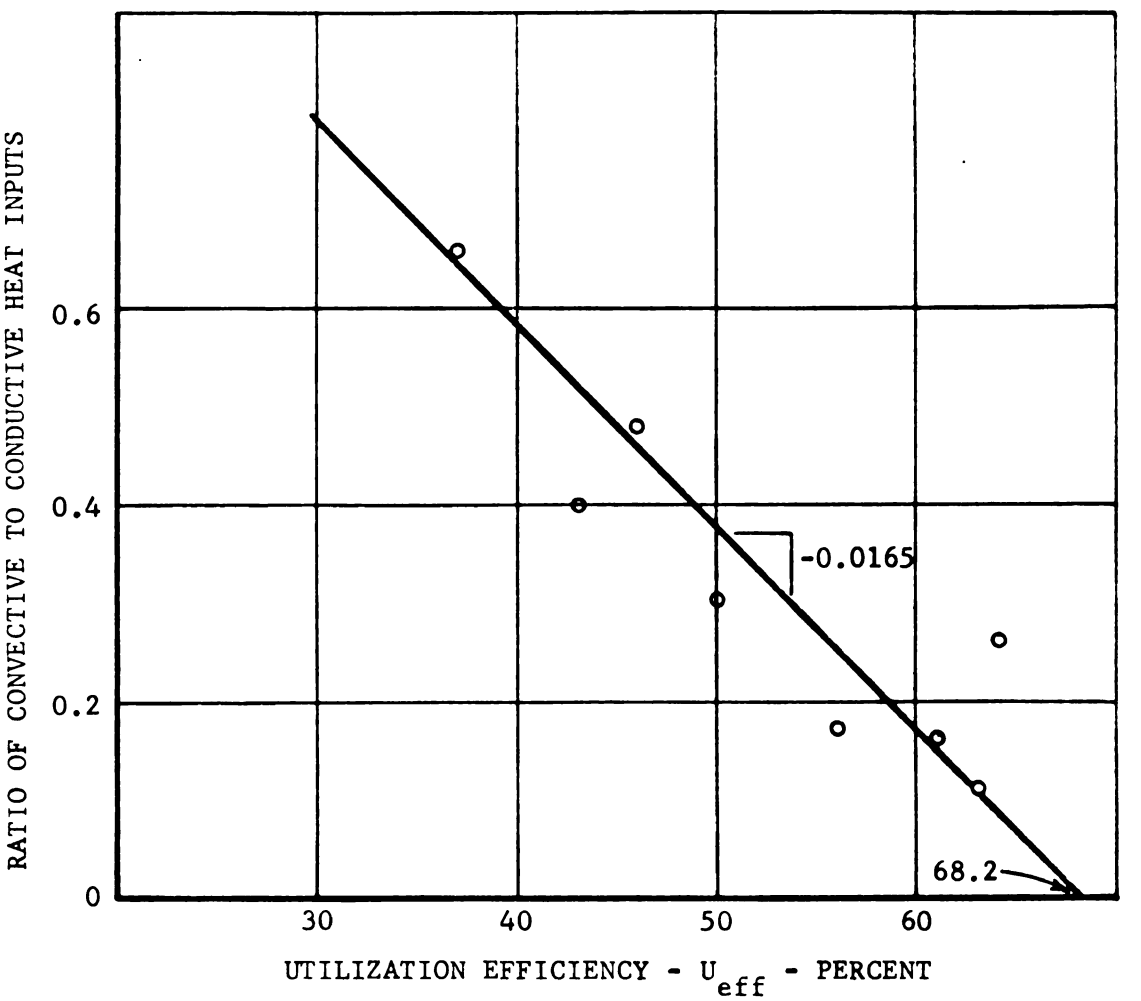

Figure 7.5 Utilization efficiencies

efficiency as a function of convective to conductive heat source ratio for the 8 runs with heated sub-sections. The equation of best fit is linear with slope and intercept as shown, although over a broader range of values the relation may not be linear. As the ratio of convective to conductive heat sources increases, the efficiency decreases. Utilization efficiencies at a given level of conductive heat input decreases as the convective source, or in other words, convective drying potential increases. This is because by increasing the surface temperature, the convective heat potential is decreased, eliminated or even turned into a sink depending on how much the surface temperature is raised. Thus, some of the conducted heat input is potentially lost for moisture evaporation in replacing the convective heat source. The greater this source, the less efficient will be the conducted heat source.

The average heat utilization of 8 runs was 50 percent. Esmay and Sheppard (1971) reported similar efficiency figures for in-house, winter drying conditions with somewhat lower efficiencies under summer conditions. In-house summer conditions generally consist of higher air temperatures, greater wet-bulb depressions and higher ventilation rates, all creating more favorable convective drying conditions. Assuming heating sources well insulated from the ground beneath, summer utilization efficiencies would be lower because of the greater drying potential of the air itself.

In conclusion, for moderate drying requirements, greater efficiency will be obtained with more efficient use of the heat energy already available in the air, with conducted heat used as a supplementary source to increase drying rates where convective drying is insufficient, such as wintertime conditions. This would require improved circulation patterns of air over the droppings. Although, with laminar flow, air velocities must be increased four times to double the convective transfer rate, the total increase in power would not be great because only that air near the surface is involved in the transfer of heat and moisture. Bulk vertical mixing is required to bring more air into contact with the surface.

8. SUMMARY AND CONCLUSIONS

8.1 Summary

Ninety-five samples of chicken excreta were dried in eleven laboratory controlled environments, simulated to typify those found in poultry houses. Samples of three basic thicknesses were used. Drying rates of some samples were increased by supplemental heat inputs and by increasing the exposed surface area per unit mass by suspending the sample on a fine mesh wire screen. The results are summarized in Table B.6.

Basically, it was found that the drying rates were a function of free stream velocity, wet-bulb depression and ambient air temperature as it affects the saturated vapor pressure. Process variables of increased surface area and conducted heat source also increased the drying rate.

More than half of the removable moisture was evaporated from the body surface at constant rates which can be predicted by film resistance and concentration gradients. Because the rate of shrinkage was not measured, the end of the constant rate period could not be accurately defined, but critical moisture ratios were calculated for each sample tested.

The free stream conditions were found to be of major importance throughout the drying periods analyzed. Falling rate drying was predicted as a function of moisture content.

The falling rate drying constant was estimated as a function of the initial drying constant and the sample thickness. Indications are that most of the non-hygroscopic water moves to the surface in liquid form and is evaporated there.

Although only two drying periods are clearly defined by this research, it is hypothesized that, because chicken excreta is hygroscopic at lower moisture contents, drying to equilibrium consists of one or more falling rate periods. Vapor diffusion is expected to control drying rates when the surface moisture content falls below the hygroscopic limit.

Drying rates were compared to some in-house drying data. It was shown that constant rate drying will predict the in-house drying rate if a measure of the mean boundary layer thickness and area of wet surface can be approximated.

8.2 Conclusions

The following four conclusions have been supported by this research dealing with drying of chicken excreta in thin layers of less than 1 cm (1/2 inch):

(1) The initial drying rate of fresh chicken excreta is constant. Falling rate drying periods follow the constant rate period.

(2) The constant rate is a function of the boundary layer thickness and boundary layer concentration gradients with the surface at saturated conditions.

(3) Falling rate drying periods can be identified and the rate predicted as a function of removable moisture content as in thin layer drying.

(4) In-house drying of fresh chicken excreta can be predicted on the basis of constant drying rates.

In addition, there is some support for the following:

Non-hygroscopic moisture moves to the surface in liquid form at a rate nearly equal the surface evaporation potential until the surface falls below the hygroscopic limit.

8.3 Suggestions for Future Research

Based on this study, there are two major areas of research of concern to in-house drying that need to be pursued. Basic research is needed to determine material properties and their relation to such parameters as heat and moisture conductivity, specific heat and etc. Also, the degree of micro-biological activity and its affects need to be studied in more detail. The hygroscopic limit needs to be determined as well as shrinkage rates and coefficients.

Applied research is needed in the area of micro-environmental conditions in the pit area and along the manure surfaces. Parameters physically describing manure surfaces and its interaction with the enviornmental ventilation air are needed. A systems approach to develop an economically optimum system for in-house drying would be of great practical value.

Specifically, it is felt that the following three suggestions would reap the most immediate benefits:

(1) Determination of the volumetric shrinkage rates with drying.

(2) Develop some one basic measure of air movement in the region immediately above the manure surface that would satisfactorily predict the effective mass transfer film thickness and/or coefficient.

(3) Determine heat conduction and moisture diffusion coefficients as a function of moisture content.

LIST OF REFERENCES

REFERENCES

Bagnoli, E., F. H. Fuller and R. W. Norris (1963). Humdification and drying. Section 15, in J. H. Perry, et. al., Ed. Chemical Engineers Handbook. 4th Ed. McGraw-Hill Book Company, New York.

Bird, R. B., W. E. Stewart and E. N. Lightfoot (1960) Transport Phenomena. John Wiley and Sons, Inc., New York, New York.

Bressler, G. O. (1968). Preliminary report on drying poultry manure inside a poultry house. ASAE Paper No. NA 68-502.

Brooker, D. B. (1966). Mathematical model of the psychrometric chart. ASAE Paper No. 66-815.

Carslaw, H. S. and J. C. Jaeger (1959). Conduction of Heat in Solids. Oxford, Clarendon Press, London.

Cary, J. W. and S. A. Taylor (1962). The interaction of the simultaneous diffusion of heat and water vapor. Soil Sci. Soc. Proc. 26:413.

Chen, C. S. and C. K. Rha (1971). Investigation of shrinkage in dehydration of grapes. ASAE Paper No. 71-387.

Chilton, T. A. and A. P. Colburn (1934). Mass transfer (absorption) coefficients: Prediction from data on heat transfer and fluid friction. Ind. Eng. Chem. 26:1183.

Cross, O. C. (1966). Removal of moisture from poultry waste by electr-osmosis (Part 1). pp. 91-93, in Proc. Nat. Symp. Animal Waste Management. ASAE Pub. No. SP-0366.

Dixon, J. M. (1958). Investigation of urinary water reabsorption in the cloaca and rectum of the hen. Poultry Sci. 37:410.

Eckenfelder, W. W. and D. J. O'Connor (1961) Biological Waste Treatment. Pergamon Press, New York.

Eckert, E. R. G. and R. M. Drake, Jr. (1959). Heat and Mass Transfer. McGraw-Hill Book Company, Inc., New York, New York.

Esmay, M. L. (1966). Poultry Housing for Layers. Extension Bulletin 524. Cooperative Extension Service, Michigan State University, East Lansing, Michigan, 16. pp.

Esmay, M. L. (1969). Principles of Animal Environment. AVI Publishing Company, Westport, Connecticut.

Esmay, M. L., M. Saeed, and G. D. Wells (1966). Psychrometrics of summer-ventilization air exchange in windowless poultry houses. ASAE Paper No. 66-912.

Esmay, M. L. and C. C. Sheppard (1971). In-house drying of poultry droppings. ASAE Paper No. 71-917.

Fish, B. P. (1957). Diffusion and equilibrium properties of water in starch gel. Food Investigation Technical Paper No. 5.

Gilliland, E. R. (1938). Fundamentals of drying and air conditioning. Ind. Eng. Chem. 30:506.

Gorling, P. (1958). Physical phenomena during the drying of foodstuffs. Fundamental Aspects of the Dehydration of Foodstuffs. Society of Chemical Industry, London.

Hall, C. W. (1957). Drying Farm Crops. Agricultural Consulting Associates, Inc., Reynoldsburg, Ohio.

Harmathy, T. Z. (1969). Simultaneous moisture and heat drying. I&EC Fundamentals. 8:92.

Jason, A. C. (1958). A study of evaporation and diffusion processes in the drying of fish muscle. pp. 103, in Fundamental Aspects of Dehydration of Foodstuffs. Society of Chemical Industry, London.

Kays, W. M. (1966). Convective Heat and Mass Transfer. McGraw-Hill Book Company, New York, New York.

King, A. R. andD. M. Newitt (1955). The mechanism of drying of solids. Part 7. Drying with heat transfer by conduction. Trans. Inst. Chem. Engr. 33:64.

Lapple, W. C., W. E. Clark and E. C. Dybdal (1955). Drying design and costs. Chem. Engr. 62:11:177.

Lewis, W. K. (1921). The rate of drying of solid materials. Ind. Eng. Chem. 13:427.

Lilleng, H. (1969). An investigation of How the Inlet Air Velocity, Direction and Temperature Affect Air Flow Patterns and Temperature Distribution in Cage-Laying Houses. AE class 899 Research Report, Michigan State University, East Lansing, Michigan.

Loehr, R. C. (1969). Animal wastes - a national problem. J. San. Engr. Div., ASCE. 95:189.

Ludington, D. C., A. T. Sobel and B. Gormel (1971). Control of odors through manure management. Trans. ASAE. 14:177.

Luikov, A. V. (1966). Heat and Mass Transfer in Capillary-Porous Bodies. English translation. Pergamon Press Ltd., London.

Newitt, D. M. and M. Coleman (1952). The mechanism of drying of solids. Part 3. The drying characteristics of china clay. Trans. Inst. Chem. Engr. 30:28.

Nissan, A. H., W. G. Kaye and J. R. Bell (1959). Mechanism of drying thick porous bodies during the falling rate period: I. The pseudo-wet-bulb temperature. A.I.Ch. E. Journal. 5:1:103.

Padday, J. F. (1969). Surface Tension. Part 1. The theory of Surface Tension in E. Matijevic, Ed. Surface and Colloid Science. Vol. 1. Wiley-Interscience Div. of John Wiley and Sons, Inc., New York.

Pearse, J. F., T. R. Oliver and D. M. Newitt (1949). The mechanism of the drying of solids. Part 1. The forces giving rise to movement of water in granular beds during drying. Trans. Inst. Chem. Engr. 27:1.

Philip, J. R. and D. E. Smiles (1969). Kinetics of sorption and volume change in three component systems. Aust. J. Soil Sci., 7:1.

Phillips, R. E. (1969). A Systems Analysis of Summer Environment for Laying Hens. Unpublished Thesis, Michigan State University, East Lansing, Michigan.

Schlichting, H. (1968). Boundary Layer Theory. 6th Ed. English Translation. McGraw-Hill Book Company, Inc., New York, New York.

Slayter, R. O. (1967). Plant-Water Relationships. Academic Press, New York, New York.

Sobel, A. T. (1966). Some physical properties of animal manures associated with handling. pp. 27-32, in Proc. Nat. Symp. Animal Waste Management. ASAE Pub. No. SP-0366.

Sobel, A. T. (1969). Removal of water from animal manures. pp. 347-362, in Animal Waste Management. Proceedings of the Cornell University Conference on Agricultural Waste Management.

Sturkie, P. D. (1965). Avion Physiology. 2nd Ed. Cornell University Press, Ithaca, New York.

Threlkeld, J. L. (1970). Thermal Environmental Engineering. 2nd Ed. Prentice-Hall, Inc., Englewood Cliffs, New Jersey.

Van Arsdel, W. B. (1963). Food Dehydration. Vol. 1. Principles. AVI Publishing Company, Inc., Westport, Connecticut.

Welty, J. R., C. E. Wicks and R. E. Wilson (1969). Fundamentals of Momentum, Heat and Mass Transfer. John Wiley and Sons, Inc., New York, New York.

APPENDICES

APPENDIX

A.1 Hydrodynamics of Experimental Chamber

Figure A.1 is a sketch of the physical situation and the assumed hydrodynamic boundary layer development between the point of air entry at the flow straightener and the test section, as well as the assumed velocity profile near the leading edge of the test samples. The distance between the straightener and samples is approximate because no attempt was made to position the samples exactly each time.

Air is assumed to leave the straightener at uniform velocity. Non-uniformities caused by momentum boundary layer development through individual passages of the straightener and minor turbulence caused by rough edges will quickly dissappear with the low flow rates used in this experiment.

The momentum boundary layer along the test chamber wall is assumed to begin immediately following the flow straightener. The samples are located well within the hydrodynamic entry length far removed from the theoretical region of fully developed duct flow. Therefore, boundary layer development along the chamber floor is considered to be that of laminar flow over a flat plate. The length Reynolds number at the leading edge of the sample location is, at the maximum test velocity of 147 cm/sec, approximately 27800, well below the turbulent transition Reynolds number of 2×10^5.

The momentum thickness, δ, at this point is calculated by equation A.1 (Eckert and Drake, 1959) and the results are tabulated below along with the ratios of sample top surface position to the momentum thicknes, δ. (Refer to figure A.1.)

$$\delta = 4.64(x)/(Re_x)^{1/2} \text{ where } x = 30.5 \text{ cm.} \qquad (A.1)$$

V (cm/sec)	Re_x	δ(cm)	d_1/δ	d_2/δ	d_3/δ	d_4/δ
25.4	4628	2.080	.1526	.3053	.4580	.6106
76.3	13888	1.200	.2644	.5290	.7935	1.057
122.0	22222	0.948	.3347	.6695	1.004	
147.5	26850	0.829	.3677	.7355		

A velocity profile of

$$u/u_s = (3/2)(d/\delta) - 0.5(d/\delta)^3 \qquad (A.2)$$

is assumed (Eckert and Drake, 1959). The resulting velocities at support plate and sample heights are tabulated below:

V(cm/sec)	u_1	u_2	u_3	u_4
25.4	5.8	11.2	16.3	20.8
76.3	29.5	55.4	73.2	76.3
122.0	59.0	88.0	122.0	122.0
147.5	77.8	136.0	147.5	147.5

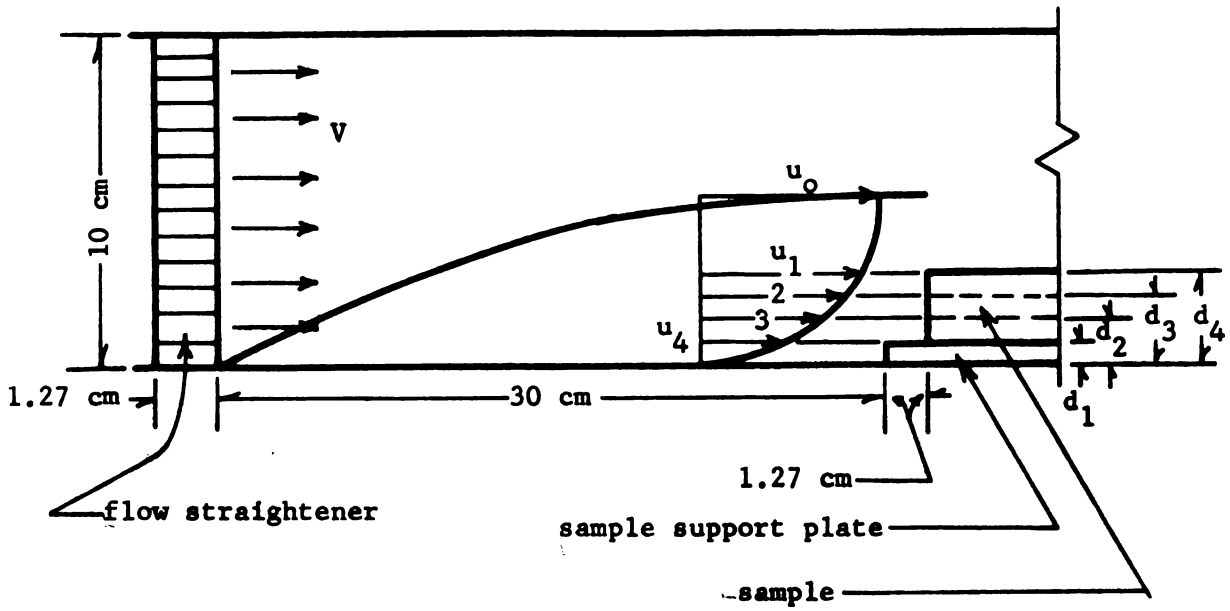

(Sketch not drawn to scale)

u = velocity in boundary layer

u_1 = velocity at d_1 (d_1 = 0.32 cm plate thickness)

u_2 = velocity at d_2 (d_2 = .32 cm plate + .32 cm thick sample)

u_3 = velocity at d_3 (d_3 = .32 cm plate + .64 cm thick sample)

u_4 = velocity at d_4 (d_4 = .32 cm plate + .96 cm thick sample)

u_o = velocity at δ = V cm/sec

Figure A.1 Boundary layer and velocity profile development along chamber floor

APPENDIX

A.2 Evaporative Surface Heat Balance

The adiabatic heat balance at the evaporative surface of the sample is, according to equation 2.11,

$$h_{fg}\dot{m}''_c = h_c(t_a - t_s) + h_r(t_r - t_s).$$

The radiation coefficient, h_r, is estimated by equation 2.12 with the surface emmisivity assumed to be 0.95. The temperatures of the radiating walls of the chamber are equal the air temperature. So calculated, the radiation heat transfer coefficient value is approximately 3 to 4 percent that of the convective heat transfer coefficient. The convective transfer coefficient is calculated in the same manner as in Section 6.5. Evaporative surface temperatures are assumed equal the wet bulb temperature plus 1/2°C as before.

The following table includes the heat required to vaporize the moisture at the experimental rate assuming latent heat of vaporization equal that of free water, the calculated value of available heat through convection and radiation, and the heat deficit. The deficit is approximately 1/3 to 1/2 the value of the combined heat source and averages 3.1 cal/hr-cm^2.

There are at least four possible reasons for the calculated heat deficit of this magnitude. First, it is

Table A.1 Heat deficits

Run Number	Evaporation Rate ($\frac{gm}{hr\text{-}cm^2}$)	Evaporation Heat Required ($\frac{cal}{hr\text{-}cm^2}$)	Combined Heat Transfer Coeff. ($\frac{cal}{hr\text{-}cm^2\text{-}^oC}$)	Combined Convective Heat Source ($\frac{cal}{hr\text{-}cm^2}$)	Heat Deficit ($\frac{cal}{hr\text{-}cm^2}$)
0200	.0156	9.2	1.15	6.25	3.0
0300	.0188	10.9	1.30	7.2	3.5
0400	.0205	11.9	1.54	7.1	4.8
0500	.0065	3.8	0.72	2.0	1.8
0600	.0156	9.15	0.64	6.4	2.8
0700	.0110	6.4	0.72	4.0	2.4
0800	.0332	19.4	1.32	13.1	6.3
0900	.0127	7.4	1.37	3.8	2.6
1000	.0108	6.3	0.70	4.7	1.6
1100	.0092	5.35	0.90	3.0	2.3

possible that the latent heat of vaporization of the contained water is less than that for free water. There seem to be no solvents contained in the urine that would be expected to reduce the surface tension of the solution to any extent, and in fact, Sobel (1969) observed lower evaporation rates from a manure surface compared to a free water body in the same environment. Until it is shown that the surface tension is less than that of water this possibility will be discounted.

Secondly, there is the possibility of heat production within the sample. Based on work by Minor (1969), it is estimated that active digestion rates may produce as much as one cal/cc-hr. The temperature increase caused by this internal heat source will be maximum at the wall and equal to (Eckert and Drake, 1959)

$$t = Q'd^2/2k + Q'd/h_c$$

where Q' is the internal heat source and the thermal conductance is assumed to be roughly that of water, i.e., 0.0014 cal/sec-cm-^oC. For a 0.64 cm thick sample, the increase in temperature is approximately 0.04^oC at the wall and progressively less toward the surface. This is quite insufficient to account for the calculated heat deficit.

The third and most reasonable possibility is that ideal adiabatic conditions are not achieved. The heat source from outside the experimental chamber is minimal due to the thick insulated walls and the fact that in most cases the laboratory air temperatures were nearly the same as the thermodynamic wet-bulb temperatures of the experimental chamber. A more real source is heat conducted through the edges of the sample support plate and through the walls of the experimental chamber directly from the air as shown in the sketch below.

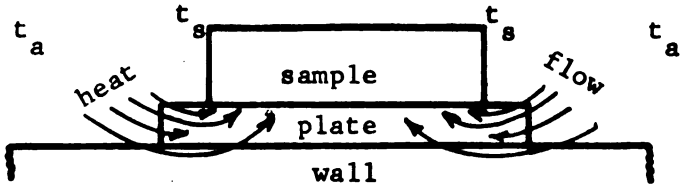

In any case, a temperature differential of less than $1/2^{o}C$ across a 1/4 inch sample thickness is sufficient to make up the heat deficit assuming conductivities of the order of water. It has previously been assumed that the body temperature was uniform. However, a slight difference in temperature was measured, but it was felt that the precision of the measurement was not good enough to justify reporting exact values.

Finally, the fourth reason for the deficit is in the calculations. First, the convective mass transfer coefficient calculations are based on the vapor pressure differential. This differential, in turn, is not measured directly but is calculated from measured and assumed temperature values and is extremely sensitive to variations in these values. Thus, the estimated mass transfer coefficient may be in error. Secondly, the Colburn analogy does not hold exactly for gases with a Schmidt number less than 0.6. The calculated Schmidt number in this case is 0.51.

APPENDIX

A.3 Example of Normal Shrinkage

The example referred to on page 94 is sample number 0301. Its drying curve is shown in Figure 6.3 where it will be noted that after 8 hours of drying, has reached a moisture ratio of 0.4 at constant rate drying. This means that 18 (0.4x30) gms of water have been removed at this time. With initial sample volume of approximately 33 cc, this would mean approximately 50 percent volumetric change under normal shrinkage conditions. If unstrained shrinkage is assumed, dimensional change will be proportional to length and physically independent of the 3-dimensional shape.

By the coefficient of linear shrinkage (see Section 3.1c)

$$\alpha = (1/a_o)(\Delta a/\Delta m)$$

or $$a/a_o = (1 - \Delta m\, \alpha) = c = b/b_o = d/d_o$$

and $$A/A_o = c^2;\ Vol/Vol_o = c^3$$

Thus: $$A/A_o = (Vol/Vol_o)^{2/3}$$

With these assumptions, the evaporative surface area after 8 hours should be 65 percent of the initial surface area. Individual dimensions would be approximately 0.8 of their original value. As noted, such dimensional changes were not observed.

APPENDIX

B.1 Tables

Table B.1 Experimental test-run conditions

								Test sub-section one			Test sub-section two			
	t_a		t_{wb}	H	V		EMC		t_b		t_b	Q	
Run No.	^oF	^oC	^oC	grains	ft/min	cm/sec	%wb	No. of samples	^oC	No. of samples	^oC	cal/hr-cm^2	Btu/hr-ft^2
(1)	(2)	(3)	(4)	(5)	(6)	(7)	(8)	(9)	(10)	(11)	(12)	(13)	(14)
0200	82	27.8	22.2	102	240	122	11.0	5	22.8	4	22.8	--	--
0300	90	32.2	26.1	134	240	122	9.5	5	26.7	8	26.7	--	--
0400	80	26.7	21.1	94	290	147	11.0	5	21.7	3	26.1	19.5	72
0500	80	26.7	23.3	117	50	25	13.0	5	23.9	4	32.2	19.5	72
0600	90	32.2	21.7	84	50	25	9.0	4	22.2	4	31.1	23.0	85
0700	90	32.2	26.1	136	50	25	10.0	5	26.7	3	30.6	8.4	31
0800	90	32.2	21.7	84	290	147	8.0	4	22.2	6	28.9	27.1	100
0900	80	26.7	23.3	117	290	147	12.5	5	23.9	7	29.4	27.1	100
1000	80	26.7	19.4	80	50	25	10.0	5	20.0	5	26.1	12.2	45
1100	70	21.1	17.2	75	150	76	11.0	4	17.8	4	25.0	19.5	72
1200	70	21.1	17.2	75	150	76	11.0	3	17.8	2	16.1	cooled samples	

Table B.2 Experimental sample data: Initial conditions

Sample Number	d	d_e	D_c	A_s	m_i	m_s	m_o-m_e	IMC	ρ	Age	
	#in	cm	cm	cm^2	gm	gm	gm	%wb	gm/cc	##	Comments
(1)	(2)	(3)	(4)	(5)	(6)	(7)	(8)	(9)	(10)	(11)	
0202	1/8	.282	10.8	116	39.0	10.0	27.6	74.2	1.19	0	
0205					38.8	10.0	27.5	74.2	1.18	0	
0208					39.1	10.0	27.8	74.5	1.19	0	
0203	1/4	.508	11.4	129	77.4	20.1	54.8	74.0	1.18	0	
0206					77.1	20.5	54.1	73.5	1.18	0	
0209					78.1	20.0	55.6	74.5	1.19	0	
0204	3/8	.692	12.1	142	117.1	32.7	80.2	72.0	1.19	0	
0201					116.7	32.2	80.6	72.5	1.19	0	
0207					119.8	31.5	84.4	73.7	1.21	0	
0301	1/8	.282	10.8	116	41.6	10.2	30.3	75.4	1.27	0	
0305					43.5	11.0	31.5	74.9	1.33	0	
0313					36.1	10.0	25.0	72.1	1.10	0	
0302	1/4	.508	11.4	129	80.0	18.8	59.2	76.5	1.22	0	
0312					76.1	17.7	56.5	76.7	1.16	0	
0304		.535	21.6	245	152.7	34.8	114.2	77.2	1.16	0	8" length
0303	3/8	.692	12.1	142	120.4	30.3	86.9	74.8	1.22	0	
0310					125.2	30.3	91.8	75.8	1.27	0	
0311					109.9	25.6	81.6	76.7	1.12	0	
0308	1/8	.213	10.5	225	56.1	15.8	38.6	71.8	1.17	0	2-surface
0307	1/4	.336	10.8	238	94.8	24.2	68.1	74.5	1.18	0	"
0309					94.1	27.8	63.3	70.5	1.18	0	"
0306	3/8	.440	11.1	250	135.1	33.1	98.5	75.5	1.23	0	"
0402	1/8	.282	10.8	116	36.1	8.2	26.9	77.4	1.10	1	
0406					35.2	7.7	26.5	78.1	1.07	1	heated
0401	1/4	.508	11.4	129	76.5	16.6	57.9	78.3	1.17	1	
0407					73.2	14.9	56.4	79.6	1.12	1	heated
0403	3/8	.692	12.1	142	115.8	24.4	88.4	78.9	1.18	1	
0408					111.6	23.5	85.2	79.0	1.14	1	heated
0405	1/2	.845	12.7	155	148.2	30.1	114.5	79.7	1.13	1	
0404	--	.852	12.2	135	117.8	23.1	91.8	80.4	1.05*	1	undisturbed
0503	1/8	.282	10.8	116	37.1	6.1	30.0	83.5	1.13	1	
0507					35.9	6.3	28.7	82.5	1.10	1	heated
0502					40.9	10.0	29.4	75.6	1.25	0	
0501		.290	20.9	226	75.0	12.7	60.4	83.1	1.14	1	8" length
0504	1/4	.508	11.4	129	78.1	12.9	63.2	83.5	1.19	1	
0508					82.5	15.2	65.2	81.6	1.26	1	heated
0505	3/8	.692	12.1	142	116.8	21.0	92.7	82.0	1.19	1	

Table B.2 cont. page 2 of 3

(1)	(2)	(3)	(4)	(5)	(6)	(7)	(8)	(9)	(10)	(11)	
0603	1/8	.282	10.8	116	36.4	7.3	28.3	79.9	1.11	1	
0606					35.7	8.0	27.0	77.7	1.09	1	heated
0602	1/4	.508	11.4	129	78.2	15.8	60.8	79.8	1.19	1	
0604					78.1	15.5	61.1	80.1	1.19	1	
0605					78.2	16.0	60.6	79.6	1.19	1	heated
0608					78.7	15.5	61.6	80.2	1.20	1	"
0601	3/8	.692	12.1	142	119.5	23.8	93.3	80.1	1.22	1	
0607					115.5	22.9	90.3	80.2	1.18	1	heated
0704	1/8	.282	10.8	116	40.1	7.8	31.5	80.7	1.22	1	
0708					42.1	8.3	32.8	80.3	1.28	1	heated
0705	1/4	.508	11.4	129	76.2	15.2	59.1	80.0	1.16	1	
0707					75.8	14.7	59.6	80.6	1.16	1	heated
0701					82.5	23.6	56.2	71.4	1.26	0	
0703					65.0	12.2	51.3	81.2	1.05*	1	undisturbed
0702	3/8	.692	12.1	142	114.0	23.1	88.2	79.7	1.16	1	
0706					117.2	23.5	90.9	79.9	1.19	1	heated
0801	1/8	.282	10.8	116	43.5	9.1	33.6	79.1	1.33	1	
0805					40.1	8.1	31.3	79.8	1.22	1	heated
0806					44.0	11.9	31.1	73.0	1.34	0	"
0807					41.1	11.0	29.2	73.3	1.25	0	"
0808					37.1	7.7	28.7	79.2	1.13	1	"
0803	1/4	.508	11.4	129	79.8	16.6	61.8	79.2	1.22	1	
0809					79.4	15.9	62.1	80.0	1.21	1	heated
0804	3/8	.692	12.1	142	118.2	23.7	92.5	79.9	1.20	1	
0810					118.1	25.1	90.9	78.7	1.20	1	heated
0802	--				74.2	17.2	55.4	76.7	1.05*	1	individual droppings
0903	1/8	.282	10.8	116	39.7	7.8	30.8	80.4	1.21	1	
0905					40.8	8.4	31.2	79.4	1.25	1	
0901					40.9	8.1	31.7	80.2	1.25	1	
0902					37.7	7.8	28.8	79.3	1.15	1	raised 1/8"
0904	1/4	.508	11.4	129	74.6	16.2	56.1	78.3	1.14	1	
0907					79.4	16.2	60.8	79.5	1.21	1	heated
0906					79.2	17.6	59.1	77.8	1.21	1	"
0909					84.1	18.2	63.4	78.4	1.28	1	"
0908					61.3	13.4	46.1	78.2	1.05*	1	heated and undisturbed
0910	1/8	.213	10.5	225	57.8	13.0	43.0	77.5	1.28	0	2-surface
0911					56.1	12.3	42.1	78.1	1.25	0	"
0912					51.1	10.8	38.8	78.9	1.14	0	"

Table B.2 cont. Page 3 of 3

(1)	(2)	(3)	(4)	(5)	(6)	(7)	(8)	(9)	(10)	(11)	
1003	1/8	.282	10.8	116	41.1	9.0	31.1	78.1	1.25	1	
1008					40.0	9.2	29.7	77.0	1.22	1	heated
1010					42.1	10.5	30.4	75.1	1.28	0	"
1005	1/4	.508	11.4	129	80.5	18.0	60.5	77.7	1.23	1	
1001					81.5	17.6	61.9	78.4	1.24	1	scored
1002					73.3	12.6	59.3	82.8	1.05*	1	undisturbed
1004					79.3	18.9	58.2	76.2	1.21	0	
1006					83.0	18.2	62.8	78.1	1.27	1	heated
1007					77.5	15.4	60.4	80.1	1.05*	1	heated and undisturbed
1009	3/8	.692	12.1	142	121.6	25.8	92.9	78.8	1.24	1	heated
1102	1/8	.282	10.8	116	39.5	8.2	30.1	79.2	1.21	1	
1106					39.5	8.5	29.8	78.6	1.21	1	heated
1109					38.1	7.1	29.9	81.4	1.16	1	"
1101	1/4	.508	11.4	129	81.4	16.2	62.8	80.1	1.24	1	
1105					78.7	16.3	60.0	79.3	1.20	1	heated
1104		.535	21.6	245	157.8	31.8	121.3	79.9	1.20	1	8" length
1103	3/8	.692	12.1	142	119.4	25.1	90.6	79.0	1.22	1	
1107					118.9	25.6	89.4	78.4	1.21	1	heated
1201	1/8	.231	10.5	225	57.5	12.3	43.4	78.7	1.19	1	2-surface
1202	1/4	.349	10.8	238	99.5	21.1	75.3	78.8	1.20	1	"
1203	3/8	.444	11.1	250	134.3	27.5	102.7	79.6	1.21	1	"
1204	1/8	.282	10.8	116	39.5	8.6	29.6	78.2	1.21	1	cooled
1205	1/4	.508	11.4	129	79.8	16.6	60.8	79.2	1.22	1	"

* Estimated density

/ Nominal thickness (1/8 in. = 0.317 cm., 1/4 in. = 0.635 cm. and 3/8 in. = 0.952 cm.)

// Age: 0 - sample material collected after remaining in the pit area 72 hours or longer.
1 - sample material collected within 24 hours of being deposited in the pit area.

Table B.3 Constant rate analysis: Unheated samples

Sample Number	d_e cm	Observations	K_c 1/hr	Limits ± %	Intercept	Rate $\frac{gm}{hr/cm^2}$	Rate $\frac{gm}{gm/hr}$	h_D cm min	$\hat{h}_D$ cm min	$h_{D,L}$ cm min	$\hat{Rate}$ $\frac{gm}{hr/cm^2}$	% Difference
(1)	(2)	(3)	(4)	(5)	(6)	(7)	(8)	(9)	(10)	(11)	(12)	(13)
0202	.28	6	.0581	3	1.007	.0138	.160					
0205		7	.0580	1	1.010	.0138	.160					
0208		6	.0612	2	1.011	.0147	.171					
202,5,8		18	.0590	3	1.009	.0141		69	80	85	.0156	+6
0203	.51	7	.0378	1	1.007	.0161	.103					
0206		7	.0398	1	1.005	.0168	.105					
0209		7	.0383	1	1.006	.0165	.106					
203,6,9		21	.0386	3	1.006	.0165		80	87	85	.0174	+5
0204	.69	6	.0292	2	1.003	.0165	.0715					
0201		7	.0285	2	1.001	.0162	.0714					
0207		7	.0267	1	1.004	.0160	.0715					
204,1.7		20	.0278	3	1.001	.0162		82	85	85	.0168	+4
0301	.28	5	.0728	2	.984	.0190	.215					
0305		5	.0677	4	.999	.0184	.194					
0313		5	.0736	2	.996	.0158	.182					
301,5,13		15	.0714	4	.991	.0177		87	80	87	.0175	-1
0302	.51	6	.0470	1	.992	.0216	.148					
0312		6	.0387	1	1.003	.0170	.124					
						.0193		97	87	87	.0193	0
0303	.69	5	.0340	2	.993	.0208	.0975					
0310		7	.0304	1	.997	.0196	.0920					
0311		7	.0312	1	.998	.0179	.0992					
3,10,11		19	.0278	16	.947	.0194		94	85	87	.0186	-4
0402	.28	4	.0707	4	.992	.0164	.235	85	91	94	.0180	-10
0401	.51	6	.0493	2	.996	.0221	.172	116	94	94	.0186	-16
0403	.69	6	.0370	2	.997	.0230	.134	116	91	94	.0180	-22
0405	.85	6	.0335	2	.997	.0247	.128					
0404		5	.0403	3	.993	.0274	.160					

Table B.3 cont. page 2 of 3

(1)	(2)	(3)	(4)	(5)	(6)	(7)	(8)	(9)	(10)	(11)	(12)	(13)
0503	.28	9	.0243	3	.979	.0063	.112	50	48	39	.0066	+5
0502		6	.0250	5	.982	.0063	.0736					
0504	.51	14	.0138	4	.990	.0068	.0676	50	47	39	.0064	-6
0505	.69	14	.0103	1	.989	.0067	.0454	52	45	39	.0062	-7
0603	.28	4	.0628	2	1.014	.0153	.244	45	48	40	.0165	+8
0602	.51	7	.0340	1	1.014	.0160	.131	47	47	40	.0159	-1
0604		6	.0337	1	1.012	.0159	.132					
0601	.69	9	.0231	1	1.009	.0152	.090	44	45	40	.0154	+2
0704	.28	6	.0408	3	1.002	.0110	.165	50	48	40	.0106	-3
0705	.51	7	.0254	1	1.007	.0117	.099					
0701		5	.0215	1	1.005	.0094	.051					
0705		6	.0262	1	1.005	.0103	.062					
705,1.3		18	.0247	7	.991	.0110		53	47	40	.0102	-7
0702	.69	7	.0179	2	1.008	.0112	.0688	51	45	40	.0099	-11
0801	.28	4	.0964	4	.977	.0297	.356	84	88	96	.0300	+1
0803	.51	4	.0660	3	.986	.0316	.245	92	94	96	.0322	+2
0804	.69	5	.0589	2	.985	.0383	.230	112	91	96	.0311	-19
0802	--	3	.0821	5	.971	.0337	.264					
0903	.28	3	.0440	4	.976	.0117	.174					
0905		5	.0448	6	.970	.0121	.167					
0901		5	.0470	12	.983	.0128	.184					
0902		3	.0487	10	.922	.0121	.180					
3,5,1,2		16	.0481	10	.984	.0122		77	88	93	.0122	0
0904	.51	5	.0347	4	.981	.0151	.120	109	94	93	.0130	-14
1003	.28	5	.0405	1	.993	.0108	.140	44	48	39	.0118	+9
1005	.51	7	.0233	1	.996	.0109	.0783					
1001		7	.0230	1	.999	.0110	.0809					
1002		7	.0240	1	.995	.0110	.113					
1004		6	,0227	2	.991	,0103	.070					
05,1,2,4		27	.0232	2	.990	.0108		45	47	39	.0114	+4
1102	.28	6	.0362	1	.986	.0094	.133	65	75	66	.0108	+15
1101	.51	11	.0181	1	.990	.0088	.070	61	72	66	.0105	+19
1103	.69	12	.0150	1	.994	.0096	.0544	66	70	66	.0101	+6

Table B.3 cont. page 3 of 3

(1)	(2)	(3)	(4)	(5)	(6)	(7)	(8)	(9)	(10)	(11)	(12)	(13)
samples with 8 inch (20.3 cm) top surface length												
0304	.53	6	.0412	1	.997	.0192	.135	87	71	87	.0157	-18
0501	.29	12	.0201	3	.994	.0054	.096	39	32	39	.0045	-16
1104	.53	11	.0176	1	.994	.0087	.067	60	58	66	.0085	-2
2-surface samples												
0308	.21	4	.1141	6	.962	.0196	.279	89	99	87	.0220	+12
0307	.34	4	.0731	7	.989	.0209	.206	95	97	87	.0217	+4
0309		4	.0697	3	.974	.0185	.159					
0306	.44	4	.0549	5	.988	.0216	.163	98	96	87	.0213	-2
0910	.21	2	.0775	-	1.004	.0148	.256					
0911		2	.0800	-	.992	.0150	.275					
0912		2	.0810	-	.990	.0140	.291					
910,11,12		6	.0797	9	.995	.0146		116	99	93	.0137	-6
1201	.23	5	.0544	3	.996	.0105	.193	73	76	66	.0111	+5
1202	.35	6	.0346	1	.998	.0109	.123	75	75	66	.0109	0
1203	.44	7	.0265	2	.993	.0109	.099	75	74	66	.0107	-2
cooled samples												
1204	.28	5	.0227	2	1.008	.0058	.0782	78	76	66	.0056	-4
1205	.51	8	.0125	1	.998	.0059	.0457	79	74	66	.0054	-7

Table B.4 Constant rate analysis: Heated samples

Sample Number	d_e cm	Observations	$K_{c,h}$ 1/hr	± Limits %	Intercept	$\frac{K_{c,h}}{K_c}$ --	q kcal/hr	$(t_b - t_{wb})$ °C	Rate gm/hr/cm²	Rate gm/gm/hr	$\hat{Rate}$ gm/hr/cm²	% Difference
(1)	(2)	(3)	(4)	(5)	(6)	(7)	(8)	(9)	(10)	(11)	(12)	(13)
0406	.28	3	.1413	6	.983	2.00	2.00	5	.0323	.487	.0365	+8
0407	.51	5	.0668	2	1.003	1.35			.0292	.253	.0371	+18
0408	.69	5	.0500	2	1.002	1.35			.0300	.182	.0372	+16
0507	.28	4	.0959	2	.985	3.94	2.00	8	.0237	.436	.0239	-3
0508	.51	7	.0411	1	1.000	2.97			.0208	.177	.0220	+6
0606	.28	3	.1367	23	1.127	2.18	2.37	9	.0318	.463	.0427	+23
0605	.51	5	.0658	1	1.030	1.94			.0309	.250	.0428	+25
0608		5	.0599	2	1.030				.0286	.237		
0607	.69	5	.0487	1	1.023	2.11			.0310	.192	.0427	+25
0708	.28	5	.0554	2	1.004	1.36	0.86	4	.0157	.219	.0180	+9
0707	.51	7	.0367	2	1.022	1.44			.0169	.148	.0183	+4
0706	.69	5	.0260	1	1.018	1.45			.0166	.101	.0182	+5
0805	.28	3	.1804	11	.936	1.87	2.79	7	.0487	.697	.0595	+15
0806		2	.1910	-	.973				.0512	.499		
0807		3	.1611	18	.943				.0405	.429		
0808		2	.1990	-	.990				.0493	.743		
5,6,7,8		10	.1777	6	.955				.0474			
0809	.51	4	.0948	3	.985	1.44			.0457	.371	.0600	+21
0810	.69	4	.0748	3	.998	1.27			.0479	.271	.0624	+20
0907	.51	4	.0728	4	.988	2.10	2.79	6	.0343	.273	.0368	+3
0906		4	.0728	5	.993				.0334	.245		
0909		4	.0692	1	.989				.0340	.242		
0908		4	.0822	5	.978				.0294	.283		
907,6,9		12	.0716	4	.987							
1008	.28	4	.0772	1	1.015	1.91	1.26	7	.0198	.249	.0221	+7
1010		4	.0695	2	.995				.0182	.202		
1006	.51	5	.0362	1	1.009	1.55			.0176	.125	.0222	+17
1007		6	.0416	1	1.015				.0195	.163		
1009	.69	8	.0259	1	1.011	--			.0170	.094	.0222	+20
1106	.28	4	.0898	5	.994	2.48	2.37	8	.0231	.316	.0249	+3
1109		3	.0885	8	.965				.0228	.373		
1105	.51	5	.0504	1	.999	2.78			.0234	.185	.0255	+5
1107	.69	7	.0335	1	1.002	2.24			.0211	.117	.0247	+11

Table B.5 Falling rate analysis

Sample Number	d_e	Observations	K_f	± Limits	Correlation	Moisture ratio estimates at: Critical time M_{cr}			θ_{cr}	MC_{cr}	Time of last observation used M			θ	MC	
							Upper **	Lower				Upper **	Lower			
	cm		1/hr	%		--			hr	% wb	--			hr	% wb	
(1)	(2)	(3)	(4)	(5)	(6)	(7)	(8)	(9)	(10)	(11)	(12)	(13)	(14)	(15)	(16)	
0202	.28	4	.196	27	.992	.30	.42	.18	12.0	49	.03	.15	0	24.0	18	
0205		4	.210	28	.991	.28	.39	.16	12.5	47	.03	.15	0	24.0	17	
0208		4	.222	2	.999	.28	.28	.27	12.0	47	.05	.05	.04	20.0	20	
202,5,8		11	.2025	11	.986	.29	.32	.24	12.2	48	.03	.07	0	24.0	16	
0203	.51	7	.0946	2	.999	.40	.41	.39	16.0	54	.05	.06	.02	40.0	20	
0206		8	.103	7	.998	.39	.43	.34	15.5	53	.03	.07	0	40.0	17	
0209		7	.107	5	.999	.36	.38	.34	16.7	53	.03	.05	0	40.0	18	
203,6,9		22	.102	5	.994	.38	.41	.35	16.0	53	.03	.06	0	40.0	18	
0204	.69	10	.0387	5	.998	.75	.79	.72	8.5	67	.16	.19	.13	48.0	33	*
0201		10	.0415	2	.999	.68	.69	.67	11.0	65	.15	.15	.14	48.0	33	*
0207		10	.0387	1	.999	.68	.69	.68	12.0	66	.17	.18	.16	48.0	37	*
204,1,7		30	.0397	3	.998	.70	.72	.68	10.8	66	.16	.18	.14	48.0	35	*
0301	.28	4	.273	23	.994	.27	.38	.16	9.7	48	.02	.15	0	20.0	14	
0305		4	.273	33	.988	.25	.37	.13	11.0	45	.02	.19	0	20.0	13	
0313		4	.228	38	.985	.32	.50	.14	9.0	47	.03	.23	0	20.0	15	
301,5,13		12	.258	12	.983	.28	.33	.22	10.0	48	.02	.08	0	20.0	14	
0302	.51	4	.170	10	.999	.28	.31	.24	15.3	49	.04	.07	0	28.0	17	
0312		4	.1575	22	.995	.25	.29	.20	19.5	48	.06	.13	0	28.0	22	
302,12		8	.1635	29	.949	.26	.36	.19	17.2	48	.05	.14	0	28.0	20	
0303	.69	5	.0595	4	.999	.57	.58	.56	12.5	64	.23	.24	.21	28.0	43	*
0310		4	.0639	9	.999	.48	.49	.46	17.0	61	.24	.26	.21	28.0	45	*
0311		4	.0633	9	.999	.49	.51	.47	16.0	63	.24	.25	.21	28.0	46	*
3,10,11		12	.0625	6	.996	.51	.53	.49	15.2	61	.23	.24	.21	28.0	43	*
0402	.28	4	.320	23	.994	.22	.30	.13	11.0	46	.03	.11	0	17.3	17	
0401	.51	5	.158	12	.996	.31	.36	.26	13.9	55	.04	.09	0	27.3	20	
0403	.69	6	.0720	2	.999	.52	.53	.51	13.0	67	.14	.15	.13	31.3	28	*
0405	.85	6	.0610	1	.999	.55	.56	.54	13.3	69	.18	.19	.17	31.3	45	*
0404		6	.0787	4	.999	.51	.53	.49	12.0	68	.11	.13	.09	31.3	37	*

Table B.5 cont. page 2 of 4

(1)	(2)	(3)	(4)	(5)	(6)	(7)	(8)	(9)	(10)	(11)	(12)	(13)	(14)	(15)	(16)	
0503	.28	4	.0967	16	.997	.25	.27	.22	30.0	58	.09	.11	.05	41.7	37	
0502		↓														
0504	.51	3	.0262	10	.999	.52	.53	.51	33.7	73	.43	.44	.42	41.7	69	*
0505		↓														
0603	.28	3	.3475	94	.992	.18	.34	.02	13.2	44	.04	.28	0	17.7	20	
0602	.51	3	.0933	32	.999	.36	.40	.33	19.0	60	.23	.27	.19	23.7	50	*
0604		3	.0936	33	.999	.36	.39	.33	19.3	60	.24	.28	.20	23.7	51	*
602,4		6	.0934	7	.998	.36	.37	.35	19.0	60						
0601	.69	↓														
0704	.28	5	.1635	7	.994	.25	.28	.22	18.5	53	.06	.08	.03	27.5	27	
0705	.51	5	.0502	6	.999	.50	,51	.49	20.0	67	.34	.35	.33	27.5	59	*
0701		5	.0327	4	.999	.65	.66	.64	16.0	63	.45	.45	.44	27.5	55	*
0703		5	.0514	7	.999	.50	.51	.49	19.2	69	.33	.34	.32	27.5	60	*
705,3		10	.0510	5	.999	.50	.51	.49	19.5	68	.33	.35	.32	27.5	60	*
0801	.28	3	.311	82	.994	.31	.47	.15	7.0	55	.11	.32	0	10.2	33	
0803	.51	5	.202	9	.999	.33	.37	.28	10.0	57	.03	.07	0	22.2	16	
0804	.69	5	.1335	3	.999	.44	.45	.43	9.2	64	.08	.09	.07	22.2	28	
0802	--	7	.144	2	.999	.57	.59	.55	4.9	66	.05	.06	.03	22.2	20	
0903	.28	5	.154	13	.996	.28	.32	.25	15.7	56	.06	.10	.01	26.2	27	
0905		5	.184	18	.992	.25	.29	.20	16.2	51	.04	.10	0	26.2	22	
0901		5	.165	14	.995	.28	.33	.24	14.8	56	.05	.09	0	26.2	25	
0902		5	,202	13	.996	.24	.28	.19	14.0	51	.03	.07	0	26.2	19	
03,5,1,2		20	.176	19	.925	.26	.31	.21	15.2	53	.04	.10	0	26.2	23	
0904	.51	5	.0855	8	.997	.40	.42	.39	16.5	61	.18	.20	.15	26.2	44	*
1003	.28	9	.1935	13	.987	.21	.27	.14	19.3	46	.01	.10	0	34.0	13	
1005	.51	6	.0725	9	.997	.32	.34	.30	29.0	54	.10	.12	.08	45.0	31	
1001		6	.0687	9	.997	.33	.35	.31	28.8	56	.11	.13	.09	45.0	34	
1002		6	.0865	13	.993	.28	.30	.25	30.0	58	.07	.10	.04	45.0	32	
1004		6	.0606	8	.997	.37	.39	.35	27.0	56	.14	.16	.11	45.0	35	
05,1,2,4		24	.0721	12	.963	.32	.35	.30	28.9	56						
1102	.28	7	.224	15	.987	.16	.21	.10	22.7	42	.04	.07	0	31.2	22	
1101	.51	4	.0580	13	.998	.31	.33	.29	37.5	57	.17	.18	.14	47.2	46	*
1103	.69	↓														

Table B.5 cont. page 3 of 4

(1)	(2)	(3)	(4)	(5)	(6)	(7)	(8)	(9)	(10)	(11)	(12)	(13)	(14)	(15)	(16)	
samples with 8 inch (20.3 cm) top surface length																
0304	.53	4	.195	26	.993	.21	.27	.16	10.0	44	.04	.12	0	28.0	18	
0501	.29	4	.0566	12	.998	.35	.37	.34	31.7	65	.20	.22	.18	41.7	52	*
1104	.53	4	.0515	10	.999	.34	.35	.33	37.0	59	.20	.21	.19	47.2	48	*
2-surface samples																
0308	.21	4	.4025	27	.992	.28	.46	.10	6.0	44	.01	.23	0	16.0	11	
0307	.34	5	.2455	11	.997	.30	.38	.22	9.5	49	.01	.10	0	28.0	11	
0309		5	.235	10	.997	.30	.37	.23	9.5	44	.01	.10	0	28.0	10	
307,9		10	.240	6	.997	.30	.34	.26	9.5	45						
0306	.44	5	.169	15	.995	.33	.40	.24	12.0	52	.03	.10	0	28.0	16	
0910,0911,0912																
	.21	6	.1775	28	.971	.45	.49	.41	6.9	61	.28	.33	.23	9.5	51	*
1201	.23	4	.409	30	.990	.13	.22	.04	16.0	38	.01	.12	0	25.2	14	
1202	.35	4	.159	40	.983	.22	.31	.13	22.5	48	.04	.14	0	33.2	23	
1203	.44	6	.1125	13	.993	.24	.27	.20	28.6	51	.03	.08	0	47.2	21	
heated samples																
0406	.28	↓														
0407	.51	4	.360	44	.979	.18	.32	.05	12.2	45	.04	.19	0	17.3	21	
0408	.69	4	.183	31	.990	.27	.35	.19	14.0	53	.05	.15	0	23.3	24	
0507	.28	3	.428	28	.999	.22	.27	.18	7.9	54	.09	.13	.05	10.0	36	
0508	.51	4	.200	40	.983	.21	.27	.14	19.3	51	.05	.15	0	25.5	26	
0606	.28	↓														
0605	.51	3	.472	--	.988	.14	.33	0	13.5	39	.05	.32	0	15.0	22	
0608		3	.278	78	.994	.21	.34	.09	13.6	49	.06	.30	0	17.7	26	
605,8		6	.375	59	.909	.17	.25	.08	13.7	45						
0607	.69	4	.213	30	.990	.23	.30	.16	16.2	50	.04	.13	0	23.7	21	
0708	.28	4	.452	25	.993	.12	.19	.05	16.0	37	.01	.06	0	23.5	12	
0707	.51	5	.145	16	.994	.25	.27	.23	21.0	53	.09	.12	.07	27.5	33	
0706	.69	4	.0630	9	.999	.41	.42	.40	23.2	63	.31	.32	.30	27.5	57	*
0805,0806,0807,0808																
	.28	8	.865	46	.881	.20	.40	0	4.2	41						
0809	.51	4	.381	28	.992	.25	.34	.16	7.7	52	.02	.16	0	14.2	14	
0810	.69	4	.250	27	.992	.30	.38	.22	9.3	54	.05	.15	0	16.2	22	

Table B.5 cont. page 4 of 4

(1)	(2)	(3)	(4)	(5)	(6)	(7)	(8)	(9)	(10)	(11)	(12)	(13)	(14)	(15)	(16)
0907	.28	4	.389	37	.985	.18	.28	.09	11.0	45	.02	.15	0	16.7	16
0906		4	.379	41	.982	.19	.30	.08	11.0	44	.02	.17	0	16.7	16
0909		4	.406	41	.982	.17	.30	.04	11.7	42	.01	.14	0	18.7	15
0908		3	.539	--	.986	.15	.43	0	10.0	40	.01	.42	0	14.7	15
906,7,9		12	.370	15	.973	.20	.24	.15	11.0	44					
1008,1010															
	.28	4	.476	67	.954	.15	.29	.02	11.5	36	.09	.17	0	14.0	27
1006	.51	6	.191	22	.981	.19	.24	.14	22.7	44	.07	.10	0	30.0	26
1007		5	.191	19	.991	.22	.25	.19	19.0	49	.06	.09	.02	26.0	26
1009	.69	6	.103	12	.993	.25	.28	.22	29.3	50	.05	.08	.02	45.0	23
1106,1109															
	.28	3	.438	71	.995	.20	.31	.09	8.7	50	.06	.22	0	11.2	26
1105	.51	4	.2085	35	.987	.24	.31	.17	15.0	51	.05	.17	0	21.2	26
1107	.69	5	.121	13	.996	.28	.30	.25	21.0	53	.09	.11	.06	31.2	32
cooled samples															
1204	.28	5	.0623	7	.998	.36	.38	.34	28.5	58	.12	.13	.09	47.2	37 *
1205	.51	5	.0204	5	.999	.61	.62	.60	31.0	70	.44	.45	.43	47.2	64 *

* Value at end of test-run, end of falling rate drying period not reached.

/ Insufficient data.

** Confidence limits at the 95 percent level.

Table B.6 Summary

		t_a		rH	V		Q	d_e	F	K_c	K_f	M_{cr}	M_{cr} exp**
	Run No.	°F	°C	%	cm/sec	ft/sec	cal/hr/cm^2	cm	cm^2	1/hr	1/hr	--	--
(1)	(2)	(3)	(4)	(5)	(6)	(7)	(8)	(9)	(10)	(11)	(12)	(13)	(14)
1	0500	80	27	67	25	1	--	.28	.10	.0245	.0967	.25	.28
2	1100	70	21	68	76	2½				.0362	.224	.16	.20
3	1000	80	27	52	25	1				.0405	.1935	.21	.24
4	0700	90	32	64	25	1				.0408	.1635	.25	.27
5	0900	80	27	76	147	5				.0460	.176	.26	.32
6	0200	82	28	62	122	4				.0590	.196	.29	.31
7	0600	90	32	40	25	1				.0628	.3475	.18	.21
8	0400	80	27	60	147	5				.0707	.320	.22	.25
9	0300	90	32	63	122	4				.0714	.273	.28	.28
10	0800	90	32	40	147	5				.0964	.311	.31	.32
11	0500	80	27	67	25	1	--	.51	.39	.0138	.0262	.52	.53
12	1100	70	21	68	76	2½				.0181	.0580	.31	.31
13	1000	80	27	52	25	1				.0232	.0725	.32	.34
14	0700	90	32	64	25	1				.0245	.0502	.50	.50
15	0600	90	32	40	25	1				.0340	.0933	.36	.36
16	0900	80	27	76	147	5				.0347	.0855	.40	.43
17	0200	82	28	62	122	4				.0386	.102	.38	.41
18	0300	90	32	63	122	4				.0415	.170	.26	.30
19	0400	80	27	60	147	5				.0493	.158	.31	.31
20	0800	90	32	40	147	5				.0660	.202	.33	.34
21	0500	80	27	67	25	1	--	.69	.85	.0103	--	--	--
22	1100	70	21	68	76	2½				.0150	--	--	--
23	1000	80	27	52	25	1				--	--	--	--
24	0700	90	32	64	25	1				.0179	--	--	--
25	0600	90	32	40	25	1				.0231	--	--	--
26	0900	80	27	76	147	5				--	--	--	--
27	0200	82	28	62	122	4				.0280	.0387	.70	.71
28	0300	90	32	63	122	4				.0315	.0625	.51	.50
29	0400	80	27	60	147	5				.0370	.0720	.52	.51
30	0800	90	32	40	147	5				.0589	.1335	.44	.45
31	1200	70	21	67	76	2½	*	.28	.10	.0227	.0623	.36	.37
32	0700	90	32	64	25	1	8.4			.0554	.428	.12	.15
33	1000	80	27	52	25	1	12.2			.0733	.476	.15	.16
34	1100	70	21	68	76	2½	19.5			.0890	.438	.20	.24
35	0500	80	27	67	25	1	19.5			.0959	.428	.22	.23

Table B.6 cont. page 2 of 2

(1)	(2)	(3)	(4)	(5)	(6)	(7)	(8)	(9)	(10)	(11)	(12)	(13)	(14)
36	0600	90	32	40	25	1	23.0	.28	.10	.1367	--	--	--
37	0400	80	27	60	147	5	19.5			.1413	--	--	--
38	0900	80	27	76	147	5	27.1			--	--	--	--
39	0800	90	32	42	147	5	27.1			.1800	.865	.20	.23
40	--												
41	1200	70	21	67	76	2½	*	.51	.39	.0125	.0204	.61	.61
42	0700	90	32	64	25	1	8.4			.0367	.145	.25	.28
43	1000	80	27	52	25	1	12.2			.0390	.191	.19	.23
44	0500	80	27	67	25	1	19.5			.0411	.200	.21	.22
45	1100	70	21	68	76	2½	19.5			.0504	.2085	.24	.26
46	0600	90	32	40	25	1	23.0			.0630	.375	.17	.17
47	0400	80	27	60	147	5	19.5			.0668	.360	.18	.22
48	0900	80	27	76	147	5	27.1			.0716	.389	.20	.22
49	0800	90	32	42	147	5	27.1			.0948	.381	.25	.30
50	--												
51	1200	70	21	67	76	2½	--	.69	.85	--	--	--	--
52	0700	90	32	64	25	1	8.4			.0260	.0630	.41	.42
53	1000	80	27	52	25	1	12.2			.0259	.103	.25	.28
54	1100	70	21	68	76	2½	19.5			.0335	.121	.28	.31
55	0500	80	27	67	25	1	19.5			--	--	--	--
56	0600	90	32	40	25	1	23.0			.0487	.213	.23	.26
57	0400	80	27	60	147	5	19.5			.0500	.183	.27	.31
58	0900	80	27	76	147	5	27.1			--	--	--	--
59	0800	90	32	42	147	5	27.1			.0746	.250	.30	.30
60	--												
2-surface													
61	1200	70	21	67	76	2½	--	.23		.0544	.409	.13	.16
62	0900	80	27	76	147	5				.0795	.1775	.45	.45
63	0300	90	32	63	122	4				.1141	.4025	.28	.33
64	1200	70	21	67	76	2½	--	.34		.0346	.159	.22	.25
65	0900	80	27	76	147	5				--	--	--	--
66	0300	90	32	63	122	4				.0715	.240	.30	.36
67	1200	70	21	67	76	2½	--	.44		.0265	.1125	.24	.27
68	0900	80	27	76	147	5				--	--	--	--
69	0300	90	32	63	122	4				.0549	.169	.33	.38

* cooled sample

** Experimental value at estimated critical time, θ_{cr}.

MICHIGAN STATE UNIV. LIBRARIES
31293010703241